Title

EVALUATION OF WELL-TO-WELL TRACERS FOR GEOTHERMAL RESERVOIRS. PART I: LITERATURE SURVEY. PART 2: LABORATORY WORK

Authors

Vetter, O.J.
Zinnow, K.P.

Publication Date

1981-08-01

LBL-11500
GREMP-14
UC-66a

Evaluation of Well-to-Well Tracers for Geothermal Reservoirs

Part 1: Literature Survey
Part 2: Laboratory Work

O. J. Vetter and K. P. Zinnow
Vetter Research

August 1981

Geothermal Reservoir Engineering Management Program

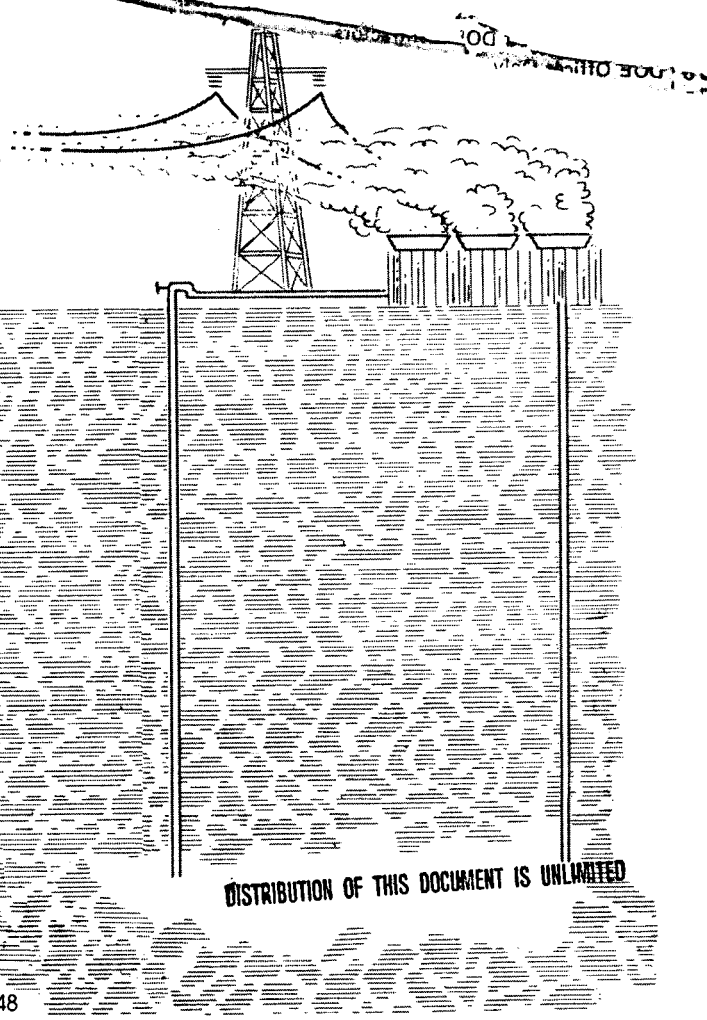

Earth Sciences Division
Lawrence Berkeley Laboratory
University of California

Prepared for U.S. Department of Energy under Contract W-7405-ENG-48

DISCLAIMER

Printed in the United States of America
Available from
National Technical Information Service
U.S. Department of Commerce
5285 Port Royal Road
Springfield, VA 22161
Price Code: A05

LBL-11500

EVALUATION OF WELL-TO-WELL TRACERS FOR GEOTHERMAL RESERVOIRS
Part 1: Literature Survey
Part 2: Laboratory Work

O. J. Vetter and K. P. Zinnow
Vetter Research
Costa Mesa, California 92626

Prepared for:
Lawrence Berkeley Laboratory
University of California
Berkeley, California 94720
Purchase Order No. 4501210

This work was supported by the Assistant Secretary for Resource Applications, Office of Industrial and Utility Applications and Operations Division of Geothermal Energy of the U. S. Department of Energy under Contract No. W-7405-ENG-48, through LBL under the Geothermal Reservoir Engineering Program (GREMP).

ACKNOWLEDGMENTS

This report was prepared by Vetter Research of Costa Mesa, California, and was supported by the Assistant Secretary for Resource Applications, Office of Industrial and Utility Applications and Operation, Division of Geothermal Energy of the U.S. Department of Energy under Contract W-7405-ENG-48, and through the Lawrence Berkeley Laboratory under the Geothermal Reservoir Engineering Management Program (GREMP), Purchase Order No. 4501210. The authors express their gratitude to the program's technical monitors, Alex Graf, Jack Howard, and Werner Schwarz, and to the contract administrator, Rich Arriaga, of the Lawrence Berkeley Laboratory (LBL) for their advice, consideration, and review of this study.

EVALUATION OF WELL-TO-WELL TRACERS FOR GEOTHERMAL RESERVOIRS

Contents

EVALUATION OF WELL-TO-WELL TRACERS FOR GEOTHERMAL RESERVOIRS
PART 1: LITERATURE SURVEY

O. J. Vetter and K. P. Zinnow
Vetter Research, Costa Mesa, California

SUMMARY

Published literature on tracers in underground reservoirs is reviewed. Emphasis was placed (a) on current use of radiotracers, (b) on interwell applications, (c) on the processes involving tracers flowing between wells, and (d) on geothermal applications of tracers. The major portion of this report is concerned with the concepts of tracer flow. Basic models for tracer dispersion and adsorption are discussed. The models can be put to test in a laboratory environment. Based on these models, flow in five-spot geometry has been modeled for field conditions. A generalized modification of these models can be used in field tests to predict produced tracer concentrations at the surface. This is the basis of a tracer program design to be discussed in Part 2 of these reports.

CONCLUSIONS

1. Tracers are a convenient tool for many jobs to verify or investigate critical characteristics of subterranean reservoirs.

2. Well-to-well tracers should not replace conventional pressure and rate measurements used for reservoir characterizations. Both investigation methods compliment each other.

3. Radioactive tracers require very small amounts compared to other chemical tracers. This may offer the only economical means for tracer jobs in geothermal operations because of the extremely large amounts of fluids to be traced.

4. Tracers have become an accepted tool in many applications in wells and reservoirs.

5. They are, in particular, used to determine the path and rate of travel of reservoir fluids.

6. When added to injected fluids, they disperse within the reservoir. This dispersion causes considerable problems in evaluating the tracer flow paths through analyzing of production well fluids.

7. In order to understand the produced tracer concentrations as a function of time, flow models have been developed.

8. The basic models predict symmetrical elution curves because they have only one adjustable parameter, for example the dispersion coefficient, which can be related to a standard deviation.

9. Elution curves produced in the laboratory even under most idealized conditions are normally not symmetrical but skewed.

10. Skewed elution curves need more elaborate models with more adjustable parameters.

11. "Capacitance" models have been developed with two more parameters. The volume fraction of a non-flowing region the pore space and a constant describing the exchange rate between the flowing and the non-flowing regions must be considered.

12. Three adjustable parameters are sufficient to fit the experimental elution curves in one-dimensional flow. There are many causes for the skewness of elution curves, for example, the geometry of the porous medium: it has to be sufficiently wide and long in order to be able to produce a symmetrical elution curve.

13. The interaction of the tracer with the rock material is also seen as influencing the elution characteristics.

14. A model involving Langmuir adsorption can account for many of the rock/tracer interactions. This model has more adjustable parameters than the capacitance models.

15. The many-parameter models have not been

transferred to field conditions. They do not appear to be applicable because of their complexity.

16. One of the flow models can give the tracer dispersion in a five-spot geometry.

17. This model has been modified for multifluid, multiwell situations and layered reservoirs. It has been used to predict, for example, peak concentrations of eluting tracers.

18. This flow model has been used as a basis for the design of many tracer programs in oil and gas fields. It seems also to be applicable for geothermal reservoirs.

19. Reports of application of tracers in geothermal operations are scarce. Field experiences as well as laboratory experiments under simulated conditions seem to be necessary.

20. Well-to-well tracer applications may become a critical requirement for the reinjection of heat-depleted brines into geothermal reservoirs. Only properly chosen tracers will allow a constant and quantitative reservoir verification to recognize the detrimental channeling from injection to production wells.

21. Without early recognition of injection water breakthrough in a quantitative fashion long lasting reservoir damage will be experienced. Tracers are a perfect and economical means to immediately detect and quantify this detrimental breakthrough.

1.0 INTRODUCTION

A tracer is, according to the American Heritage Dictionary, "An identifiable substance...that can be followed through the course of a...process, providing information on the pattern of events in the process or on the redistribution of the parts or elements involved". The substances are usually chemical elements (ions, isotopes) or compounds (complexes, molecules). They are identified through some detectable property or reaction such as mass, color, absorption or emission of radiation, etc. The properties of tracers will be the contents of sections 2.0 and 3.0 of this report. Sections 4.0 to 4.2 will deal with the information which can be provided by tracers used in the process of interest here: the movement of fluids in underground reservoirs. The introduction of tracers into this fluid flow process, however, can modify the processes adding some effects on its own. These non-equilibrium processes are discussed in section 5.0. They provide the basis for models and measurements reported in sections 6.0 to 9.0. Actual field tests and experiences are reflected in section 10.0. Sections 11.0 to 11.3 finally, will present the possibilities and difficulties of applying tracers in geothermal reservoirs.

2.0 TRACER PROPERTIES

A tracer is a simulator. It must be very similar to the substance which it has to trace, in every respect that is of importance in the process through which it is tracing. It must, on the other hand, be very different so as to be identifiable. These are two contradictory conditions. The selection of a tracer is thus the search for a compromise. For the tracer not to influence the process itself it must be used in quantities as small as possible.

By the amounts necessary for a given job, tracers can be divided into two groups: chemical tracers and radioactive tracers. Chemical tracers are those which have to be identified by general analytical methods such as conductivity, refractive index, elemental spectrometry, etc., while radiotracers are detected by their emitted radiation, usually beta or gamma. The amounts of tracer which have to be used are determined by the detection limits of these methods. Liquid scintillation counters for beta-radiation and gamma-spectrometers are by many orders of magnitude more sensitive than other and more conventional determination methods and instruments. Thus, minute quantities of radioactive tracers are required compared with chemical tracers. This makes handling them comparatively easy, too, although the radioactivity demands that certain precautionary measures be taken. The arrival of the tracer at some predetermined site is usually monitored over some length of time. The change of tracer concentration over this time span can give a wealth of information on how the tracer got there. This, in turn, allows to draw conclusions on the process (or processes) it was involved in.

3.0 RADIOACTIVE VERSUS CHEMICAL TRACERS

Radioactive tracers have mainly two advantages over chemical tracers:

1. Radioisotopes of elements can be used which are part of the system to be traced. Thus, radioisotopes can have a large amount of carrier which is identical in every respect but radioactivity. Any chemical reaction and all physical processes not influenced by radioactivity, especially adsorption, dispersion and flow characteristics which are of interest in this investigation, are identical for carrier and radioisotope. Except for isotope effects, a radioisotope can be an ideal tracer. It is involved in a physico-chemical reaction such as adsorption not according to its total concentration but only to the fraction

it represents in the carrier. The losses of these radiotracers are, thus, minimal. In aqueous systems, tritiated water is a tracer of this kind. For this reason, tritium has been found "excellent and may be the only practical tracer" in water flood projects (Burwell [1]).

2. The detection limit for radioisotopes is usually one in 1.0E19 to 1.0E22 parts. One tritium atom can be detected in 1.0E19 hydrogen atoms (Bolivar and Farouq Ali [2]). Detection limits for chemical tracers, on the other hand, are normally in the ppm to ppb range.

Both these advantages have the common result that very minute amounts of radiotracers are necessary compared to the quantities of chemical tracers previously required.

4.0 APPLICATION OF TRACERS IN WELLS AND UNDERGROUND RESERVOIRS

There are many features and processes which determine the progress of tracer concentration. Thus, many conclusions can be drawn, from a produced tracer, with respect to an otherwise inaccessible underground fluid reservoir. The kinds of questions a tracer is asked to answer are: What is the remaining oil saturation in the reservoir? What is the sweep efficiency of a water flood? What is the rate of flow between wells? Can a bad situation be remedied? The answers to all of these questions require knowledge about reservoir features which are normally too far from a well, and sometimes very localized, to be gained in any other feasible way. Depending on the problem at hand, tracers can be specially selected to provide just the information desired. We come here across a slightly different meaning of the term "tracer" from the one used so far. The tracer is not only used for following the path of the host fluid as unobtrusively as possible but also for getting involved in some special processes of its own in which the host fluid takes no part. Strictly, this would not be desirable of a tracer, yet it is sometimes fortunate and can be used to great advantage. The new meaning of "tracer" then is that it is present only in traces, that is in minute quantities. We will see more about the special processes involving tracers in section 5.0.

The next section will first deal with single well operations. Applications related to the flow between wells is left to section 4.2.

4.1 SINGLE-WELL APPLICATIONS

Mott and Dempsey [3] give a review of radiotracer applications in petroleum industry operations. The tracers used are gamma-emitters, detected by gamma-ray logging. In fluids, most commonly I-131 is applied. Others such as Co-60 and Sc-46 are also frequently used but have the disadvantage of longer half-life (5.3 years and 84 days, respectively, versus 8 days). Gaseous tracers are ethyl bromide tagged with tritium, Kr-85, Xe-133, or Br-82, and I-131 - tagged ethyl iodide. Particulate tracers, such as glass or plastic beads, fracturing sand, or ion exchange resins, are used after tagging with Sc-46, Ir-192, and Zr-95/Nb-95. The main areas of application are:

4.1.1 WELL DRILLING

Radiotracers are occasionally used to identify high-permeability zones into which drilling fluid is lost (Edison [4]). When too much fluid is returned, a radio-activation technique inducing a short-lived activity in the fluid allows to control or to avoid potentially hazardous conditions, e.g., a blowout (Rickard [5]). Another technique, reported by Millar and Buckles [6], and tested in the Mackenzie Delta, is to add tritiated water to the drilling mud to determine the amount of mud filtrate which has invaded the formation water. The radial extent of the invasion is also indicated. In a similar way, the invasion of core samples can be determined by comparing the pore water with the drilling fluid (Muskat and Coggeshall [7]; Armstrong and Lovelace [8]).

4.1.2 WELL COMPLETION

Tracers are used for orientation and depth correlation of perforators in multiple-string completions. Channels and casing leaks can be located after pumping a fluid with tracer through the suspected wellbore region. A radiotracer injector-detector sonde used for this purpose permits ejection of up to 100 separate downhole tracer slugs without surfacing. The cement top behind the casing can be located by introducing a radioisotope into the first portion of the cement slurry (Howell and Frosch [9]). When a particulate tracer is mixed throughout the cement, thief zones taking large quantities of cement can be located (Norelius [10]). Tagged depth markers are used for example, in salt wells to indicate the size of cavities created by the circulating water.

4.1.3 WELL TREATMENT

In hydraulic fracturing, some radioactive particles mixed with the propping agent give information on location, type, and orientation of fractures. The information is, however, accurate only from tracers within a few inches from the borehole. Radioactive fluids have been applied to locate fractures, in hydraulic fracturing as well as in acidizing in carbonate rocks. In acidizing, tracers are also used to control the extent of formation exposed to the acid. With tagged water, information on the zones that will take fluid under pressure can be obtained before starting the acidizing process. Production profiles which give the zones of fluid entry and determine the rate of entry are frequently measured with a radiotracer injector-detector probe. For more accurate flow velocity measurements, the probe sometimes contains two detectors. the oil producing and

water producing zones can be delineated by injecting radioactive oil. This oil will be produced, because of the different miscibility, in shorter time from an oil producing zone than from a water producing zone. The water saturation, thus can be estimated from the time it takes to produce the injected oil. Another method of profiling uses the interface between a radioactive and a non-radioactive fluid. One of the fluids is injected through the bottom of the well. By adjusting the pumping pressure, the interface can be moved upwards or down.

Formation squeeze causes corrosion problems in water producing wells. Corrosion inhibitors have been tagged with tritium to determine the amounts of inhibitor actively protecting, and remaining in the formation. Another method utilizes a strip of radioactive steel placed downhole for tagging the corrosion products and determining the corrosion rates. Scale inhibitors have been labeled with tritium and phosphorous-32 to determine the behavior of scale inhibitors under downhole conditions [11]. Critical adsorption/desorption characteristics as well as inhibitor compositions and hydrothermal stability of the inhibitors can be determined under actual field conditions [11].

4.1.4 ENHANCED RECOVERY

One of the more important applications of chemical as well as radioactive tracers in oilfield operations is in the secondary and tertiary recovery of oil. There, tracers are mainly used for three purposes:

1. Measuring the residual oil saturation;
2. Establishing the injection profiles for water flooding operations;
3. Determining the rate and path of travel between injection and production well.

4.1.4.1 MEASURING THE RESIDUAL OIL SATURATION

Dalton et al [12] describe a single-well tracer method to measure residual oil saturation which is an advanced development of the above mentioned method of measuring production profiles by injecting radioactive oil slugs. The method, based on the theory of chromatographic separations, makes an in-situ measurement using trace chemicals (not radioactive!) dissolved in formation water. With this technique, averages over large volumes are measured. The injected primary tracer, methyl or ethyl acetate, partially hydrolyzes in the reservoir to form the secondary tracer, methanol or ethanol. While methyl and ethyl acetate are soluble in both oil and water, methanol and ethanol are soluble only water. This separation of one tracer into two allows us to apply the principle of partition chromatography. The acetate will partition between oil and water, whereas the alcohol will not. Consequently, methanol or ethanol travel at higher velocity and return to the wellbore faster than the unreacted methyl or ethyl acetate. The residual oil saturation is determined from the difference in arrival times: the greater the difference in arrival times, the greater the oil saturation. This method was proven successful in four field applications. With computer simulation programs accounting for all aspects of the theory (such as drift, dispersion, reaction and others), a precision of 2 to 3 pore volume percent has been attained. Field experience has been obtained over a wide range of temperatures, salinities, and oil saturations.

Sheely [13] describes further field tests in five different wells at three locations using this method. Three of these tests are covered in detail. Ethyl acetate was used for the higher temperatures, n-propyl formate for the cooler reservoirs. The partition coefficients were determined and the test data were analyzed by using computer models.

While the original method considered only the water phase as flowing, a generalization to fractional flow of both the water and oil phases is given by Deans [14]. The theory of tracer movement is combined with the Buckley-Leverett theory of two-phase flow to establish the conditions under which chemical tracers, flowing with oil and brine, follow a characteristic oil saturation. Two potential uses of this result are given: The first, in laboratory core flood experiments, provides a means of detecting and correcting for permeability stratification in non-homogeneous samples. The second application is an extension of the single-well oil saturation test. Using multiple tracers, the new method gives points on the fractional flow versus saturation function.

Two further variations of measuring the single-well method oil saturation in petroleum reservoirs, again using chemical tracers, were patented to Keller [15,16]. Both methods are based on partition and use at least two tracers, one of them for comparison. The first method needs a mobile fluid phase in the formation, and a carrier fluid miscible with it. The comparison tracer is nonreactive in the formation, the other tracer is formed in the formation, away from the well, by the reaction of an injection precursor substance. This tracer and the precursor have to partition differently between the immiscible fluid phases. The other method uses the temperature dependence of the partition between the carrier fluid (injected at substantially different temperature than the reservoir has) and one of the fluid phases in the reservoir: One of the tracers must have a partition coefficient varying with temperature, the other must have one independent of temperature. After shut-in periods sufficient for the precursor to react, or for temperature equilibrium to be established, respectively, the produced fluids are analyzed for the presence of the tracer materials, and the fluid saturations are determined by applying the principles of chromatography.

4.1.4.2 INJECTION PROFILES

The efficiency of water flooding operations depends on the successful introduction of waters into the productive zones. There are non-nuclear methods, but radiotracer surveys are applied routinely. Logging methods include the interface (between radioactive and non-radioactive fluid) method and the plating (plating-out of tagged plastic particles) method. The flow-rate method is similar to that used in production wells except that the positions of ejector and detector are reversed. The radiotracer commonly used is I-131. The problems encountered are similar to those in production wells (Mott and Dempsey [3]). Recently, a new quantitative technique was presented by Wiley and Cocanower [17]. It utilizes the intensity of the radioactivity as a function of depth. The observed gamma ray count rate is corrected for system resolving time. Integration of the count rate while the tool moves through the radioactive material provides the relation to intensity. The integral of each run is then normalized to the intensity before any losses. Several field applications demonstrate improved accuracy over a manual geometric approximation technique.

4.1.4.3 DETERMINING THE RATE AND PATH OF TRAVEL

The rate and path of travel between wells is the object of the following, second section dealing with the flow of tracers through a reservoir.

4.2 INTERWELL FLOW APPLICATIONS

Tracer movement between wells relates information on the movement of traced fluids in the reservoir, indigenous or injected. Primary information concerns the flow rate: how much fluid moves at what velocity? This question needs to be answered for injected fluids such as water floods and high pressure gas, and most importantly in future geothermal applications for naturally or forcibly flowing reservoir fluids. Thus, sweep efficiencies and fluid loss into non-producing regions can be determined. If more than one production well is operated, flow directions and the communication between the injection well and the production wells can be tested. Flow rate and direction depend on the permeability of the reservoir rock. Permeability is due to natural porosity, for example of sandstones, and/or flow channels caused, e.g., by dissolving action of water in limestone. High permeability flow channels are mostly the consequence of natural or man-made fractures. Their cross section and orientation is obviously of great influence on the flow and production of the fluids. An opposed influence is exercised by impermeable barriers caused, e.g., by geological faults or volcanic intrusions. Tracers are an almost perfect means to quantitively determine the flow distribution between the flow channels of varying permeability.

Methods of measuring liquid and gas flow in turbulent motion using radioactive isotopes are reviewed by Clayton [18]. The paper discusses the principles, limitations, and performance of techniques based on both a constant-rate and a sudden injection of tracer. Measurement in closed conduits and in open channels and streams is considered, and attention is drawn to the differences. In constant-rate injection method, the product of flow rate and concentration beyond a distance sufficient for adequate mixing equals the product of injection rate and concentration. In sudden injection, the total injected activity is equal to the product of the flow rate and the time integral of the concentration. This time integral can be measured by continuously sampling, by collecting samples at equal time intervals and averaging the concentration, or by taking the total count in the flow (and considering the detector efficiency) at the sampling point. Alternatively, the linear flow velocity can be measured between two points which, multiplied by the cross-sectional area, yields the volumetric flow. Radioisotopes in sealed sources can produce ionization in a gas which can also be used to measure gas flow. The continuous-ionizaton method providing a means of measuring mass flow is compared with the mean-velocity method. Both methods are used as basis of instruments.

Hydrological applications of tracers, mostly dyes and salts, are common. Studies in soils and plants use radiotracers. Tests with radioisotopes tracing groundwater are also reported. Wiebenga et al [19], for example, used I-131 and tritium to determine the specific yield and permeability in an aquifer near a pumping borehole. In a free flow test, the direction and rate of flow of natural groundwater were also established.

In petroleum reservoirs, chemical and radioactive tracers are frequently used. Among others, dextrose, boron ammonia, fluorescein, rhodamine B, boron, I-131, Ir-192, Co-60, Kr-85, and He have been tested (Burwell [1], Bolivar and Farouq Ali [2]). Recently, the use of a stable free radical, or spin label, as a tracer for petroleum has been patented (Riedel [20]). A spin label is detected by electron spin resonance spectroscopy, with a detection limit about 1 million times lower than standard chemical tracers. For tracing water floods in sandstone, tritium may be the only practical tracer in Burwell's [1] judgment. If, however, a fracture system is present, a suitable dye would be used just as conveniently and more economically. In the meantime, this opinion, however, seems to have shifted in favor of radiotracers.

D'Hooge et al [21] report the successful use of four different radiotracers (C-14, Co-57, Co-60, and tritium) simultaneously in a sequence of Pennsylvanian age sandstone benches (West Sumatra Unit, northern half, in Rosebud County, Montana). These tracers offered an effective evaluation tool which can be used in pattern waterfloods. The diagnosis of the movement of the injected fluid in this multi-pay, discontinuous reservoir led to revisions of

injection and withdrawal rates in order to maximize volumetric sweep efficiency and reduce water cycling. The authors of this report have serious doubts about the applicability of the radioactive cobalt tracers in this type of a tracer study. Recent multiple tracer injections of three cobalt isotopes (Co-57, Co-58 and Co-60) in a Southern California Oil reservoir indicated extremely large adsorption rates of these tracers. Simultaneously injected tracers (e.g., various alcohols and tritiated water) traveled through the reservoir, whereas the cobalt isotopes (in form of hexacyanocobaltates) were retained by the reservoir rock.

Examples where tracer surveys were run and properly analyzed, resulting in thoughtful remedial work, are given by Ford [22] in five case histories. What actual results this remedial work had on production is also shown, when available. Among the tracers used in these instances are fluorescein dye, sodium bromide, ammonium thiocyanate, sodium metaborate, potassium nitrate, and tritiated water.

Injection of several tracers in different wells (more than one tracer into each injection well) simultaneously can be done to evaluate the areal flow patterns in subterranean reservoirs [23]. A case history where multiple tracers were injected at a single source, and the sweeping was performed with high pressure gas injection, is reported by Calhoun and Hurford [24]. Kr-85 and tritiated hydrogen and methane were used as tracers in the Fairway alternate gas-water miscible recovery project and were proven to be reliable. Among the results can be listed that (a) the source of breakthrough can be inferred, (b) the configuration of the gas displacement fronts, variations in sweep patterns, and fluid movements in general can be determined and (c) indications whether injected gas is going into solution or is miscible with the oil can be detected. Multiple tracer injections at a single source allow measurement of the relative velocities of the injected fluids behind the flood fronts. This could be used to determine the optimum gas-water injection ratio. The authors [24] conclude that radiotracer techniques may help to improve knowledge of flow conditions when two displacement mechanisms are operating simultaneously.

5.0 PROCESSES INVOLVING EQUILIBRATING TRACERS

Much of the information about a reservoir which a tracer can provide is gained by the fact that a tracer cannot be similar to its host in every respect. We can thus distinguish tracers of different quality. For tracing fluid flow in underground reservoirs, they can roughly be divided into two classes: those that can be made part of the natural system and those which cannot. Examples of the first class are radioisotopes of constituent elements of the fluids: tritium in water and petroleum, C in petroleum, or Na in brine. These tracers only have to achieve equilibrium with their own, non-radioactive kind. Tracers of the second class have to establish equilibrium, in principle, with every other kind present in the system. Depending on the type and amount of tracer as well as solvent, the non-equilibrium processes between tracer and rock can range in severity from dissolution of the rock material over leaching and ion exchange to adsorption. These processes take place not only in the field but are of importance also in laboratory experiments which invariably start out with non-equilibrium conditions. The most significant process is, however, the mixing of the tracer with the fluid it is to trace. At low flow rate, molecular diffusion plays a role here too, as it does under static conditions. At higher rates, the tracer is dispersed in the fluid to be traced.

The ability to trace a flowing fluid depends on the fact that the tracer is being perfectly mixed with the fluid, that is, especially with liquids. Since the tracer is normally injected into the reservoir or the water flood, the mixing takes some time and distance along the flow channels. For this reason, some minimal length is usually allowed for sufficient mixing, and tracer information is only gathered beyond this empirical length. Other than mixing, an ideal flow tracer should not get involved in any reaction outside the traced fluid. Tracer applications other than flow, however, often depend on such reactions, for example, partition between two liquids for saturation measurement. One such reaction cannot be avoided in a reservoir: adsorption on the rock material. This is an effect often regretted for flow tracing. But for special applications, one can again take advantage of it. An application immediately obvious is fracturing. In normal flow tracing, adsorption is considered detrimental, and otherwise unaccountable losses of tracer are blamed on it. In order to gain a quantitative understanding of information of reservoir tracer behavior, these equilibrating processes of mixing and adsorption/desorption have to be investigated.

Adsorption/desorption effects can also be used to their advantage like any other sorption effects which govern the dispersion of tracers within the reservoir. The principles of tracer adsorption chromatography [23] can be applied to determine critical reservoir parameters through tracer studies. Tracer partition chromatography [12 through 16] concerns itself only with the liquid and gas phases in the reservoir, whereas tracer adsorption chromatography [23] considers also the tracer interactions with the reservoir rock. Thus, tracer adsorption chromatography allows the determination of such variables as number, size and conductivity of fractures and other permeability streaks.

6.0 MODELS USED FOR DESCRIBING THE TRACER FLOW

Between injection and production the tracer is influenced by the traced fluid and the reservoir. How the different possible factors can modify the final appearance cannot be anticipated or analyzed in detail in an easy way. In order to predict the performance of a tracer and interpret the results obtained it is necessary to develop models and measure the

input data in laboratory experiments. The models put forward are mostly based on the dispersion equation. They regard different flow geometries, linear and areal (two-dimensional). The rock properties are considered isotropic, permeability due to porosity or fractures the same in all directions laterally. Deviations from the expected result can then be used to make inferences about the actual flow in the reservoir, as will be shown in the following sections.

6.1 BASIC MODELS

Tracer mixing and transport phenomena are handled in a number of ways. The most common of these is a generalization of diffusion and is called dispersion. This macroscopic diffusion should not be confused with a microscopic diffusion of molecules or ions. Dispersion contains both macroscopic and microscopic diffusion. Mathematical handling of these phenomena involves a partial differential equation which can be solved when certain boundary-value conditions are assumed. A simpler model consists of a series of perfectly mixed cells. This model requires only the solution of a series of ordinary differential equations. More complex generalized theories explain dispersion in terms of the actual properties of the media. For example, Bear and Bachmat [25] present a macroscopic theory based (a) on the hydrodynamics of the microflow through a porous medium model and (b) on statistical averaging procedures.

6.1.1 MIXING CELL

This model divides the porous medium into a series of cells in which perfect mixing occurs. The material balance of the nth cell is described by equation (1). The Nth (last) cell will produce a concentration versus time curve which can be interpreted by properly choosing the dispersion modulus. The dispersion modulus, multiplied by the mean interstitial flow velocity and the length of a mixing cell, produces the effective longitudinal dispersion coefficient.

6.1.2 DIFFUSION AND DISPERSION

Diffusion is a non-equilibrium, or unsteady, state. Mathematically it is represented by a partial differential equation of second order, which is commonly known (and used) as heat conduction equation (2), where the proportionality factor D is the diffusion coefficient. When a flow, of velocity v, is introduced in direction x, x becomes a moving coordinate. The diffusion equation is now (3). D is now generally a "dispersion" coefficient and a function of v: for laminar flow, D is proportional v, otherwise D is proportional to some power of v greater than 1. The proportionality constant for laminar flow in a porous medium is related to the grain, or pore, size distribution. If directions other than that of the flow are considered, D no longer is a constant but a tensor of rank 2 like, for example, conductivity. This means, that in an isotropic medium, there are two dispersion coefficients to consider, a longitudinal (or axial) one along the flow direction, and a lateral one perpendicular to it. The latter, of course, is smaller and may only represent molecular (i.e., microscopic) diffusion.

It is generally assumed, that a single dispersion coefficient can describe both the diffusive and dispersive effects. At zero velocity, the coefficient represents the effective molecular diffusion of the tracer in water (or other solvent) corrected for the effect of the porous medium. At high velocities, diffusion can be neglected, and the coefficient represents hydrodynamic dispersion. For intermediate situations, additivity of the two has been claimed and assumed over a wide range. However, if it is not important to depict either effect singly, a single coefficient is sufficient to use.

The dispersion equation governs longitudinal dispersion according to many theories forwarded, such as Taylor's [24] theory of displacement in capillary tubes, Scheidegger's [27] statistical theory of porous media, Keuleman's [28] "eddy diffusion" theory and Frankel's [29] "stagnant pockets" theory (Brigham [30]).

6.2 CAPACITANCE MODELS

The models discussed so far cannot match the experimental results in two important features:

1. While gas flow systems produced the predicted diffusion coefficients, liquid flow systems could not do so.

2. A slug of tracer injected at constant concentration should produce a symmetrical concentration vs time curve after traveling through the porous medium. The experimental results, however, normally show a long "tail" of the concentration curve.

The discrepancies between gas and liquid systems were interpreted as a capacitive effect on the liquid. It was suggested that this effect was caused by stagnant regions. These stagnant regions comprise a fraction of the pore volume which does not participate in the flow mixing (dispersion) of the tracer. They can be modeled as a film or as dead-end pores.

The basic models contain only one parameter (or two, if the flow velocity is also counted): the dispersion coefficient, or the length of a mixing cell. The "capacitance" models introduce two more parameters: the stagnant volume fraction and a constant which determines the rate of exchange of the tracer between the flow and the stagnant regions. With three parameters the models are flexible enough to adapt to experimental curves.

1. The volume fractions of the flow and stagnant regions can be expressed as f and (1-f), respectively. f is

sometimes called "effective porosity". It has to be kept in mind, however, that this usually designates the total interconnected pore volume in relation to the total volume while, here, it means the pore space with flow in relation to the total interconnected pore space. The tracer distribution between the two regions is now given by (4) and (5) for the two models respectively.

2. For the exchange between the two regions, two different mechanisms are considered: diffusion and first order mass transport. If the transfer of tracer from the flow to the stagnant region occurs by diffusion (Turner [31]), the equation for the concentration at a point in the stagnant region is given by (6). The effective molecular diffusion coefficient is much smaller for liquids than for gases. This can account for the observed discrepancies.

   If the transfer of tracer from the flow zone to the stagnant region occurs by first order mass transport, it is determined by equations (8) and (9) for mixing cells and dispersion, respectively.

Both mixing cell and dispersion models have been modified to include capacitance effects. They are usually based on the concept of first order mass transfer.

6.2.1 MIXING CELLS

The first model based on this concept was developed by Deans [30] as an extension of the mixing cell model. This model is now based on two equations, the material balance (8) in cell n and the mass transport (10) for cell n. For a large number of cells, an approximated differential form of this model is given by (11) and (12).

Deans passes, at too early a stage, from a description of the porous medium in discrete terms to one in continuous terms according to Levich et al [33]. These authors develop the mixing cell model further.

The transfer of a fluid element can be described by the following equations:

1. From cell to cell: (13)
2. From flowing zone to stagnant zone: (14)
3. From stagnant zone to flowing zone: (15)

The material balance is then given by equations (16) and (17).

6.2.2 DIFFUSION AND DISPERSION

The first extension of the dispersion model to include capacitance was published by Coats and Smith [34]. The basic equations are (18) and (19).

7.0 BOUNDARY CONDITIONS IN TRACER MODELS AND SOLUTIONS

In order to solve the model equations, initial and boundary conditions have to be stated. The tracer is usually injected at time t=0 as a spike, or beginning at that time (step, slug, constant rate) at a constant concentration. The porous medium is treated as an infinite (all x), semi-infinite ($x \geq 0$) or finite ($0 \leq x \leq L$) one-dimensional system.

7.1 BASIC MODELS

The effluent concentration (versus time) for a spike input of the tracer has a bell-shaped distribution curve. The basic models match this behavior with a normal distribution.

7.1.1 MIXING CELL

This model yields (Deans [32]), for a spike input, a concentration versus time curve produced by the Nth cell which is closely approximated by (20) if the dispersion modulus is chosen properly, and the flow path length N is not too small. All quantities are dimensionless if they are taken relative to the length of one mixing cell, (see (21), (22), (23)).

7.1.2 DIFFUSION

The diffusion equation (2) can be solved if the boundary conditions are stated. For the one-dimensional case, it is easiest to assume a cylinder of unit cross-section with its axis parallel to the x-axis. The diffusion of the tracer is then given, under the following initial conditions, first as a spike (delta function), second as a step, and third as a slug input:

1. At t=0, the tracer, of amount s, is placed in the plane x=0. In an infinite cylinder, the tracer concentration as a function of distance and time, is given by (24). If the cylinder is semi-infinite ($x \geq 0$), the tracer for $x < 0$ can be considered reflected at an impermeable plane x=o. Thus, the concentration is twice of the above (25).
2. A step input of tracer follows the boundary conditions given in (26). The tracer concentration can be derived from the above delta-function input (spike) by considering the superposition of small volume sources (27) at x=o. The sum is replaced by the integral (28). With substitution (29), this integral can be written (30)

in the form of a Gauss' error function (31). Thus, the concentration can be expressed in terms of the error function (32). This is usually written as (34) with the error function compliment (33).

3. A slug of finite length with initial conditions (35) diffuses through the infinite cylinder according to equation (36).

7.1.3 DISPERSION

In the presence of flow along the x-direction, the differential equation (3) is easily reduced to the case (2) without flow by substituting x' for x-vt (Danckwerts [40]). Here, x is the distance from the midpoint of the flood front, while x' is the distance from the inlet end of the porous medium. The solution for step-input is now (37).

This solution which defines the "S" shaped curve of the error function integral was, for example, used by Brigham et al [30] in experiments of miscible displacement in various porous media. Of interest are mainly solutions for finite lengths L of the porous medium. Calculations, for example, Brigham [35], are often found starting out with an infinitely long medium and the boundary conditions (38), where x stands now for x'. However, if one sets x=L in order to make the equation (37) applicable to experiments, the result (39), according to Brigham [35], does not correctly describe the curves obtained in core experiments where the mixing zone is usually appreciably long compared with the core length. If the "S"-shaped curve of the effluent concentration (versus pore volumes injected) were symmetrical, it would reach half of the injected concentration at one pore volume. However, in core experiments as well as in field studies, it usually first rises sharply, then tails out. It thus has to reach a value greater than 1/2 in order to balance the integrated values at smaller, and larger, than one pore volume. To make the calculations consistent with the equation and the boundary conditions, it has to be considered that the concentration gradient makes the displacing fluid (i.e., tracer) flow faster than the displaced fluid. Thus, the average concentration c' flowing across a plane as defined by (40) is always greater than the in-situ concentration in this plane because the concentration gradient (41) is negative. To obtain the concentration gradient, the equation for the concentration has to be differentiated (42). With this, the effluent concentration c' now is, for x=L, given by equation (43). At one pore volume eluted the tracer concentration is higher than half the injected concentration (44).

The difficulties encountered were due to the adaptation of a medium of infinite length to a core of finite length. A stricter treatment of the porous medium of finite length L is given by Coats and Smith [34]:

The most general treatment of the step-input as given by Bishoff and Levenspiel [36] considers a system composed of a packed bed preceded by an entrance section (denoted by subscript "a") and followed by an exit chamber (denoted by subscript "b"). The initial and boundary conditions are given by (45). The conditions are specialized and simplified to a semi-infinite system (x≥o) in three different ways:

1. Lapidus and Amundson [37] give conditions (46).

2. Aris and Amundson [38] corrected the first of these conditions, considering diffusion at the inlet (47), with the second condition unchanged.

3. With the same first condition as in 2 the second condition was changed (by Brenner [39], after Danckwerts [40]) to (48).

It can be concluded that the most realistic conditions for core experiments must contain a finite system of length L with diffusion at the inlet face but comparatively little mixing after exiting the core (49).

The solutions of the dispersion equation for these three sets of boundary conditions for step-input into a porous medium of finite length L are, in dimensionless form:

1. (50)

2. asymptotic solution (51), Brenner [39], and

3. even more complicated.

Approximations with less than 0.5% error for condition (52) are given as:

1. (53)

2. (54)

3. (55)

A table listing concentrations as a function of injected pore volumes for a range of dispersion values, computed from the approximate solutions, is given in the paper [34].

With these solutions, the effluent concentrations at one pore volume injected, are:

1. (56)

2. (57)

3. (58).

For the given numerical example, equations (56) and (58), give values 6% and 14% larger, respectively, than equation (57).

The second set of boundary conditions again leads to the incorrect result (57) of 1/2 because the condition (47) again defines in-situ concentrations while the respective flowing concentration is used in the first set: Calculated values are tabulated in several papers, e.g., Brigham [35], Fukui and Katsurayama [41].

7.2 CAPACITANCE MODELS

Two capacitance models have been presented: in section 6.2.1 the mixing cell model by Deans [32], and in section 6.2.2 the differential model by Coats and Smith [34]. Some solutions to these models will be presented in the next two sections.

7.2.1 MIXING CELLS CAPACITANCE MODEL (DEANS [32])

Deans gives a solution of his model for pulse (spike) conditions (59). This solution (60) can for large arguments z, and with an expansion of the square root into a series, be reduced to equation (61) predicted by the diffusion model for the diffusion modulus according to (62). A solution for step-input is presented by Coats and Smith [34]. With abbreviations (63) Deans' [32] equations read (64) to which the solution (Thomas [42]) is given by (65). This solution can again be approximated by the dispersion model. Levich et al [33] find that the contribution to the effective coefficient of longitudinal diffusion due to mixing in the flowing zone was lost by Deans' [32] approach. These authors, again using a delta-input function, arrive at a different solution:

The boundary conditions are given by (66). The system of equations for the mass balance (see 6.2.1) and boundary conditions is solved through a Laplace transformation.

The residence time distribution h(T), summed over N cells, approaches normal distribution for large N, and so does the concentration (67) leaving the last cell. The diffusion model has the same result for sufficiently large length L of the medium. By comparing the parameters of the two models the effective diffusion coefficient D is found (68). It is obvious that a small exchange rate p leads to large values of D. If the length L is not large enough a normal distribution is thus not established. The resulting curves rather show the familiar "tail" which can be described by two distributions: Solving the system of material balance and boundary condition equations through Laplace transformation for a small L (69) and p (70) results in a residence time distribution (71). Thus, the exiting concentration having two additive terms can be calculated. The first term relates a normal distribution, the other an exponentially decaying one. This is a 3-parameter model. The parameters l,f, and p/q, can be determined from experiments (72).

7.2.2 DIFFERENTIAL CAPACITANCE MODEL (COATS AND SMITH) [32])

This model is in dimensionless form given as (73) and (74). In special cases, this model reduces to the dispersion model for both sufficiently small and sufficiently large velocities:

1. For a small velocity, the rate group will be large and the mass transfer process essentially instantaneous.
2. For large velocity, the rate group will be negligibly small.

In both cases, the solution is the same as for the dispersion model, except that in the second case the (dimensionless) time must be multiplied by a factor of 1/f. For boundary conditions set 2 (47) the solution for the dispersion model is given above (51). The equations can be solved generally in the (complex) frequency domain by taking the Laplace transforms and combining the resulting (ordinary) differential equations (see Coats and Smith's [34] Appendix C).

The solution for the Laplace transform of the concentration can then be inverted to the time domain using the Cauchy integral theorem (for details see Churchill [43]). For the boundary conditions given above (set 2), the solution, as given by Coats and Smith [34], is (75) for x=L. For any x, the solution looks very similar, with substitutions (76) (Brigham [35]).

Brigham subjects this equation to the same critique as the dispersion model solutions by Coats and Smith [34]: again, a flowing concentration should be considered, and not the in-situ concentration. Brigham's equation to match laboratory effluent data to the dead-end pore model gives the flowing concentration c. c' is obtained by substitutions (77) in the above equation (75). Baker [44] describes a simpler way to determine the effluent concentrations: Again, the model equations are the same, whether they describe the in-situ or the flowing concentration. In each case, there are two concentrations to be considered, one in the flowing region and one in the stagnant region. Thus, four concentrations appear in the equations. The relations between the flowing and in-situ concentrations are the same (42) as in the dispersion model but there are now two such equations, one each for the flowing region and the stagnant region. "The flowing concentration in the stagnant region" may sound like a contradiction. Baker [44] points out that the model equations for flowing concentration are the equivalent of a wave equation: they predict the motion of a concentration waveform, not that of individual fluid elements. In order to solve these equations for the flowing concentrations the proper boundary conditions to be used are the same as those used in the dispersion model,

especially (78). After obtaining the solution in the complex frequency domain, Baker [44] suggests that rather than inverting it to the time domain, the data, instead, could be transformed to the frequency domain. An algebraic curve fitting procedure could then be used rather than the computer-time consuming and relatively inaccurate numerical integration in an iterative process. A method of transforming data to the frequency domain (as described by Clements and Schnelle [45]) and of fitting the model to the data is outlined in Baker's [44] Appendix B.

8.0 ADSORPTION

Adsorption from dilute aqueous solutions on reservoir rocks is generally considered in terms of the Langmuir isotherm. Two limiting cases can be distinguished: instantaneous adsorption (equilibrium system), and time-dependent, or rate-controlled adsorption (non-equilibrium system).

A basic discussion of the problem is found in a paper by Gershon and Nir [46]. Tracer transport is here based on the dispersion equation.

In the case of chemical equilibrium the tracer concentration in the solid phase (amount adsorbed per unit volume of porous medium) is proportional to the concentration in the liquid phase (proportionality constant k). Adsorption changes at the rate (79). Considering radioactive decay (80) an ideal adsorbable tracer changes according to (81) and, thus, follows the dispersion equation (82).

In steady state, this reduces to the ordinary differential equation (83). The general solution (Alexeev et al [47]) has the form (84). For non-equilibrium a first-order mass reaction (85) is often assumed (Lapidus and Amundson [37]). The last term in (85) is generally not known and thus neglected. For a radioactive tracer, this gives (86), and the differential equation is (87). This is formally identical with the above equation (82) for equilibrium. Two different situations should be considered: The steady state conditions using a radioactive tracer and the non-steady state conditions using a stable tracer. The latter is already discussed by Coats and Smith [34] (see section 7.2.2) for several sets (46) to (48) of boundary conditions. For the third of these sets, the solution is given (Bastian and Lapidus [48], as (88).

For the steady state, a radioactive tracer is considered. Solutions to the ordinary differential equation are given for several systems:

1. A tracer is injected into a porous medium of infinite length (system INF2) through the plane x=0 at a steady rate. The general solution (84) reduces to (89).

2. A semi-infinite medium is dealt with under the two conditions of cases 1 (46) and 2 (47) for finite length by Coats and Smith [34] discussed above. The solution can now be written as (90) with the constants of different value in the two cases SINF1 (91) and SINF2 (92).

3. The finite system of length L (FINT) is considered under the third set of boundary conditions (48) of Coats and Smith [35] leading to equations (93) and (94).

A useful approximation of the general solution is (95). A comparison of these solutions in approximations linear in 1/F reveals that the differences, for F>100 , are smaller than 1%. Only for high precision experiments (0.5%) should boundary conditions be taken into account. The non-steady state conditions, on the other hand, yield the following differences: for produced concentration of approximately 50% of the input concentration, the effects are of the order of 5% for G=100.

A more accurate approach to dealing with adsorption has been taken by Satter et al [49]. This model is based on dispersion (96) and Langmuir adsorption in the form (97).

At equilibrium, the adsorption rate is zero and the adsorption equation reduces to the isotherm (98). The linear relation (99) used by Lapidus and Amundson [37] and discussed by Gershon and Nir [46] (see above) is a special case with b=o. The solution for production of half the input concentration given here is identical to the one (55) given above in case 3 of Coats and Smith [34] if replacement (100) is made. This replacement can also be made in the other two cases (53) and (54). Gershon and Nir [46] discussed an approximation only.

At equilibrium, the dispersion and adsorption equations can be combined to (101). For a system of finite length L the transport equations are solved for condition (102) and set 3 (48) of the boundary conditions of Coats and Smith [34]. With the dimensionless variables the model equations for rate-controlled adsorption are (103) and (104), for equilibrium adsorption (105). The second term in the brackets in (105) is zero for negligible adsorption.

These equations contain five (5) dimensionless groups controlling dispersion and adsorption:

1. Dispersion group: (106)

2. For rate-controlled adsorption:
   a) adsorptive capacity group (107)
   b) flow rate group (108)
   c) kinetic rate group (109)

3. For equilibrium adsorption:

adsorptive capacity group (110).

Numerical solutions were obtained using the Barakat-Clark [50] finite difference method. The influence of the different groups was evaluated with the help of a computer. Normalized adsorption and effluent concentration histories were developed which are useful for designing and interpreting laboratory core floods. The authors conclude that data obtained at times much shorter than reservoir residence times should not be applied directly to estimate chemical loss in a reservoir when adsorption (or any other mechanism) is rate-controlled or time-dependent.

9.0 FLOW MODEL FOR FIELD EXPERIMENTS

Field tests differ from laboratory experiments by employing a different, more complicated, geometry. The models described above were geared to the simple linear case. But reservoirs, at least the common sandstone type, represent two-dimensional settings. Wells are sometimes arranged in a fairly regular pattern, where injection and production wells each form an (approximate) square grid. The offset is such that each well of one type is located in the center of a square formed by four wells of the other type. These so-called five-spots provide a relatively simple and highly symmetrical geometry for measuring and modeling.

Brigham and Smith [51] developed a model for the five-spot geometry. The dispersion equation for radial flow is identical to that for linear flow if the distance x is interpreted as radial distance r, and the linear flow velocity v is replaced by a quotient according to (111). This quotient is the volumetric injection rate (per unit height) Q divided by perimeter and porosity. This is equivalent to (112) for linear flow. The dispersion equation is, by approximation and substitution of variables, again (as in the linear case) reduced to a diffusion-type equation. The solution (Raimondi et al [52]) for step-input is given by the error function as (113). The difference of the argument to the linear case is due to the different dependence of the velocity on the distance. The solution in terms of the average distance traveled by the front is derived by Baldwin [53]. In the linear case the average traveled distance is described by (114) and the concentration by (115). This is a normal distribution with a standard deviation (116) which is a measure for the width of the dispersed front. Assuming two (additive) contributions to the standard deviation, one by the distance traveled (117) and one by the radial geometry (118) (required by keeping the volume constant), relation (119) is obtained for radial flow. With the boundary condition (120) Baldwin [53] obtains the solution (121), for sufficiently large r (122). Thus, the concentration (123) is analogous to the linear case. By modifying the argument of the error function with (124) the concentration (125) is identical to the above solution (113).

Baldwin [51] also considers converging flow at the producing well. If r is measured from there, then (because distance traveled is now negative) condition (119) is changed to (126) for converging flow. (127) now is the boundary condition for diverging-converging flow. Thus, the standard deviation is given by (128) and the concentration at distance r by (129) which, at (130) , is equal to the divergent concentration (125).

Brigham and Smith [51] do not consider convergent flow. They argue, instead, that a radial model can approximate the 5-spot geometry as far as the length of the front is concerned.

A finite slug is described by two error functions, one for the front and one (negative) for the back of the slug. At the midpoint (131) the peak concentration is given by (132). Introducing the undiluted "width" W (133) of the slug, equation (132) can be written in form (134). This compares to linear flow for a distance L (135) with the difference only in a numerical factor (square root of 3).

In tracer work, the desired output concentration is almost always less than one tenth of the input concentration. When the argument of the error function is less than about 0.1, the function can be approximated by a linear function (136). The mass of tracer (in lbs) injected is equal to the product of the perimeter times the width, the height, the porosity of the rock, the water saturation, the tracer injection concentration and the density (62.4). Thus, in order to produce a certain peak concentration at a well in the distance r=L, the mass of tracer to be injected can be calculated through (137). Using published breakthrough data (Dyes, Caudle and Erickson [56], Caudle and Witte [55], Fay and Prats [54]), Brigham and Smith [51] then arrive at an empirical formula for actually produced peak concentrations (138). Combining these two equations (136) and (137) gives a working equation (139) for the mass of a tracer to be injected.

Baldwin [53] compares the two prediction methods for peak producing concentrations and finds, for the same mixing coefficient, Brigham and Smith's [51] solution (by combining (133) and (137)) low by a factor of 1.4 because convergent flow is not considered.

In order to account for inhomogeneities of the reservoir, a layer-cake model was constructed (Brigham and Smith [51]): The peak producing concentration of the nth layer compared to that of the homogeneous reservoir are given by (140). The times to breakthrough are represented by (141). Predictions of both models (Brigham and Smith [51]: 3 layers, Baldwin [53]: 20 layers) were used to match the produced concentration curves in an inverted five-spot (2 1/2 acre) field test (Smith and Brigham [57]) successfully. In this test, 200 pounds of ammonium thiocyanate and 150 pounds of potassium iodide were injected as a slug, and about 40% and 45%, respectively, recovered by the end of

the test. No adsorption was indicated but a lagging of the ammonium ion.

10.0 MODEL APPLICATIONS IN FIELD TESTS

Experiences, in the field, with tracers are of a mixed nature. When tracers have been carefully and properly selected, they have yielded valuable information. This information is mostly relative, and qualitative in nature. A large number of chemical and radioactive tracers have been used in various applications.

Wagner et al [58] discuss, for the first time, basic tracer program design methods. Their design is based on the model equations developed by Brigham and Smith [51] discussed in the last section (which do not consider adsorption). This idealized five-spot model is modified for multifluid, multiwell and layered reservoir situations. A generalized formula (142) is derived for the tracer concentration produced at the surface. The factors P (dependent on the ratio of injection to production wells and the fraction of producing area for which breakthrough has occurred) and E (accounts for thermodynamic effects when the gas is expanded to atmospheric conditions) account for the dilution of a gas tracer. The factor P normally ranges from 1 to 4. Waterflood tracers can be treated with the same formula when the GOR is replaced by WOR and E equals one. The model is used to predict safe, detectable tracer concentrations and peak concentrations, and to determine the required analytical sensitivities. The field test (hydrocarbon miscible flood) was conducted in the South Swan Hills Unit, South Swan Hills Field, Alberta, Canada. Fourteen injection wells each were used for hydrocarbon solvent and for water. Multiple tracer (chemical and radioactive) were employed, tritium, tritiated ethane, and Kr-85 with the solvent, tritiated water, ammonium nitrate, and isopropyl alcohol with the water. Design criteria considered are: different tracers should be used for each injection well in fluids injected in adjacent well patterns; the injected amount of tracer (particularly radioactive) should produce safe levels of concentration yet well above detection limits; dilution factors for water tracers (besides adsorption) are dispersion and well pattern; for gases, dilution by co-produced gas in the separators and reduction in specific radioactivity due to expansion must be considered.

The usefulness of the prediction model was further proven in five programs reported by Wagner [59]. In addition to the tracers used in the South Swan Hills Unit (see above) other tracers were chosen from a list of preferred materials containing also: ammonium thiocyanate, sodium or potassium bromide and iodide, sodium chloride, fluorescent dyes, and water soluble alcohols as water tracers, and tritiated methane as gas tracer. Tracers were employed and proved for tracing interwell flow and to identify sweep problems: volumetric sweep efficiencies, identification of problem injection wells, directional flow trends, delineation of flow barriers, relative velocities of injected fluids, and evaluation of sweep improvement treatments. Results of the following field programs are discussed:

1. Levelland Unit (West Texas) tertiary miscible pilot
2. Salt Creek Field (Wyoming) potential micellar pilot
3. Little Buffalo Basin (Wyoming) waterflood
4. South Swan Hills Unit (Alberta, Canada) hydrocarbon miscible flood.

In the West Texas project, reservoir stratification was known from prior waterflood history. Thus, the model prediction could be compared to the actual tracer performance. It is shown to be in qualitative agreement.

The tracer information obtained will be especially useful to the design, control, and interpretation of a potential tertiary recovery process in the areas where the tests have been conducted.

11.0 TRACERS IN GEOTHERMAL APPLICATIONS

Fundamentally, application in geothermal reservoirs is not very different from that in oilfields. The basic differences, higher flow rates and temperatures, have to be reckoned with (see section 11.2). In section 11.3 the few reported geothermal applications are presented.

11.1 NEED FOR TRACERS IN GEOTHERMAL RESERVOIRS

The purpose of a tracer injection into a geothermal reservoir may drastically differ from that into an oil or gas reservoir. Reinjection of heat-depleted brines into geothermal reservoirs may be required for pressure maintenance and heat-mining operations. This reinjection poses an inherent danger to the life-span of a geothermal reservoir.

Assuming the reinjected and relatively cold brine channels through a system of fractures from the injection to the production wells, a potentially detrimental situation is generated. The front of the cold fluids will be heated and mixed with original and native reservoir fluids. This hydraulic front is preceding a temperature front. Unfortunately, this hydraulic front is masked and may not be recognizable at its early stages. Thus, the detrimental temperature front will approach the production wells without giving the operator a prewarning. As soon as the temperature front arrives at the production wells, a large and critically important portion of the geothermal reservoir is cooled down and lost for power production. A temperature drop of even a few degrees will have detrimental effects upon the value of a production well. One must not only consider the loss of enthalpy

(which may be minor) but also the change in entropy caused by this temperature drop. The overall effect upon the power plant efficiency may become of major concern.

Only tracers will allow a constant reservoir verification which is required to recognize the hydraulic fronts as early as possible. Furthermore, quantifying the appearance of reinjected brine in the production wells is absolutely required (a) to calculate the damage caused by cooling of the reservoir, (b) to predict the location of the temperature front and (c) to start remedial procedures by shutting down injection wells or to relocate these injectors. Failure to conduct these tracer studies may result in large financial penalties for the operator.

Routine injections of tracers into geothermal reservoirs may become a necessity not only to determine the location of a temperature front but also to determine the natural flow patterns within the reservoir. This could be achieved by injecting of various tracers into different injection wells and constantly monitoring the produced fluids from all production wells for their tracer content.

11.2 DIFFERENCES TO OILFIELD

Most subterranean application of tracers are related to oil reservoirs or ground water. Geothermal reservoirs are distinguished from oilfields in that they contain only an aqueous fluid which normally moves at much higher rates than oilfield fluids.

The lack of organic fluids in all known geothermal reservoirs eliminates all tracer problems related to a tracer partition between the two immiscible phases. The common absence of a gas phase in liquid-dominated reservoirs eliminates further tracer problems. Thus, tracer applications in geothermal reservoirs should be plagued by less problems than those in oil and gas fields. On the other hand, geothermal reservoirs may offer problems for tracer studies which are not normally encountered in oil and gas fields.

The main difference between hydrocarbon and geothermal reservoirs lies naturally in the high temperatures encountered in geothermal formations. Flashing of gases (i.e., mainly steam) during producton of geothermal fluids offers serious problems. For example, a flash of 20% steam will vaporize 20% of the produced liquids, thus having a concentrating effect upon the remaining liquids. Naturally, one must know precisely this flash to determine the produced quantity of the tracers. Another problem caused by this flashing may be the need to sample for tracers in a two phase mixture. This problem could be partially overcome by utilizing multiple tracers, some of which would partition between liquid and steam phase (e.g., tritiated water) and some of which would stay in the liquid phase.

The high temperatures may also offer problems related to the hydrothermal stability of some tracers. Molecules or complex ions may not be sufficiently stable under geothermal reservoir conditions. Unfortunately, the literature contains only very few hints about this hydrothermal stability, thus creating the need for some fundamental research. Physical reactions such as adsorption/desorption and ion exchange are temperature dependent. Again, the literature contains no references to these high temperature reactions.

The type of rock in the reservoir also has a major impact on the tracer behavior in a subterranean reservoir.

Oil reservoirs are related to porous rocks of sedimentary origin or a limited number of carbonate rocks, geothermal reservoirs and flow systems can exist in any kind of rock. Thus, production cannot rely only on natural rock porosity but has to utilize natural and/or induced fractures. Ground water is usually traced through soil and rocks at shallow depths, not through underground reservoirs.

The fractures and high permeability streaks in geothermal reservoirs must be recognized and described in detail (see section 11.1). This should offer only minor problems. The rock on the fracture faces or within the high permeability streaks exposes relatively small surface areas to the tracers as opposed to low permeability rock. Therefore, sorption reactions play a much smaller role in a fractured reservoir compared to a reservoir which relies on production through matrix permeability.

11.3 REPORTED APPLICATIONS

Reports on geothermal applications are rare so far. The first use of a radiotracer in a geothermal environment was performed by one of the authors and reported in 1978, by Gulati, Lipman, and Strobel [60]. A tracer survey was run, at the Geysers, in Sulfur Bank #1 in 1975. The immediate objective was tracing the reinjected steam condensate: did any of it vaporize, and how much reappears as steam at the production wells? Because of the phase change involved, tritium was selected as the tracer. 20 curies were injected in the form of tritiated water over a 24-hour period into one well, SB-1, using a precision injection pump at the wellhead. The first tritium was measured just seven (7) days after injection. Later it was observed in a total of 20 wells. The last tritium appeared 28 months later bringing the total amount recovered to 18% of the injected tracer. The regional flow pattern of the reservoir fluid seems to be radial. The injection well, however, is located in the southwest corner of the Geysers with all production wells within an angle of about 80°. This limits the observation of the flow pattern severely. The authors also conclude that the rate of heat transfer from rock to fluid can only be found with a tritium tracer survey. The time involved to recover a certain amount of heat cannot be predicted for a fractured system

because it is a function of the fracture intensity which is not known. This test has, for the first time, provided direct physical evidence that the rock heat is being mined over real time and not geological time.

Tester and Potter [61], in 1973, report on field experiments of a prototype, two wellbore, hot dry rock reservoir at the Fenton Hill site in New Mexico. The tests to characterize the hot, low-matrix permeability hydraulically-fractured granitic reservoir use fluorescent dye and radioactive tracers Br-82 and I-131. The radiotracers were used to diagnose injection and production zone flow paths near the wellbores, the dye was applied to measure fracture volume, residence time distributions and the degree of fluid mixing within the fractured region. The radiotracer experiments were originally done with I-131, introduced into the flow system with a conventional injector system gamma-ray detector logging tool. Several disadvantages became apparent: failure of the tool at high temperature, high I-131 backgrounds in consecutive experiments due to relatively long half-life (8 days), relatively high exposure during sample loading, and use of an isotope which has a very low concentration limit for surface storage because of health hazards.

A new tracer dispenser/gamma detector package was designed for Br-82 to be generated by neutron activation in a nuclear reactor. From the standpoint of half-life (36 hours), biologic sensitivity and gamma ray energy (1.5 MeV maximum), Br-82 appears almost ideal for this type of study. Ammonium bromide, encapsulated in a quartz vial, was irradiated and then loaded into a heavy metal shielded container in a hot cell. At the wellhead the logging probe containing the gamma counter (standard Geiger detector employing high temperature electronics) was connected to the shield containing the capsule. At the desired depth, an explosively activated ram broke the capsule mechanically and moved a piston to release trapped water which flushed the broken capsule. A total of six (6) radiotracer surveys were performed, the first four with I-131, the last two with Br-82.

Two surveys (with 20 mCi and 10 mCi I-131, respectively) were made to find the extent of damage done by thermal cycling to the cement behind the casing in the injection borehole, and to locate flow sinks, especially in one growing major anomalous region. These tests confirmed the existence of a major flow path behind the casing and gave evidence that natural fractures might provide openings for a flow system.

The next two surveys were performed after separate efforts to reduce the system impedance, the first by leaching with sodium carbonate, the other by redrilling the lower portion of the production well. The tracer surveys showed new flow sinks and multiple production zones and suggested that the new borehole is connected in parallel to a main flow system. The first survey using Br-82 was also made at high flow rate and high back pressure. It, thus, provided more useful results in interpreting data from the major flow tests. The flow rate of the tracer upwards behind the casing of the injection well could be estimated. In the production well, the positions of the main connecting fractures and the arrival times of the tracer at each fracture were measured (again). The last tracer test allowed to measure the fluid path after the casing was recemented. It indicated that the recementing was performed successfully.

For residence time distribution measurements, a pulse of concentrated sodium fluorescein dye (typically about 400 liters of a 200 to 300 ppm aqueous solution) was injected, pumped through the fractured region, and recovered in the production well. The residence times are under 10 hours. No decomposition or adsorption could be measured for 24 hour exposures at 200°C. The detection limit was approximately 0.05 ppm, the overall accuracy, in terms of volumes, ca 800 liters. Four (4) experiments during the 75-day flow test are summarized in statistical terms as well as graphically. The data show that the flow was well mixed without major short circuits. The observed shape of the residence time distribution is caused by dispersion within individual flow paths, and their superposition. The more circuitous routes in the rock probably account for the tail towards larger volumes. The experiments showed that the flow system grew considerably in size during the test and developed additional flow paths.

By the use of conventional and the tracer methods, a model of the present fracture system has been developed. The flow modeling was based on the dispersion equation. A single zone one-dimensional fit shows reasonable agreement. A more realistic multizone model and a two-dimensional model provide satisfactory curve matches because they have more adjustable parameters. However, due to the complex geometric relationships, simplifications are inherent to all the models. Thus, a unique model was not determined.

REFERENCES

1. BURWELL, E. L., "Multiple Tracers Establish Waterflood Flow Behavior", Oil & Gas J., pp. 76-79 November 28, 1966.

2. BOLIVAR, P.J., and FAROUQ ALI, S.M., "Flow of Radioactive Fluids in Porous Media", Producers Monthly, pp. 2-7, July 1967.

3. MOTT, W.E., and Dempsey, J.C., "Review of Radiotracer Applications in Geophysics in the United States of America", Proceedings of the Symposium on Radioisotope Tracers in Industry and Geophysics held by the International Atomic Energy Agency in Prague, November 21-25, 1966, International Atomic Energy Agency, Vienna 1967.

4. EDISON, J.E., "Radioactive Tracers Used

to Locate Lost Circulation", World Oil 138, 7, pp 197-199, 204, 1954.

5. RICKARD, J.A., "Method of Controlling Well Fluid Circulation by Radioactivation of Fluid Elements", U.S. Patent 3,115,576, December 1963.

6. MILLAR, R.H.G., and BUCKLES, R.S., "Tritiated Water as a Drilling Mud Tracer in Beaufort Exploration Wells", paper to be presented at the 25th Annual Technical Meeting of the Petroleum Society of CIM, Calgary, May 1974.

7. MUSKAT, M., and COGGESHALL, N.D., "Method of Determining The Fluid Content of Well Cores", U.S. Patent 2,458,093, January 1949.

8. ARMSTRONG, F.E., and LOVELACE, K., "A Study of Core Invasion by Waterbase Mud Filtrate Using Tracer Techniques", API Drilling and Production Practice-1961, New York: American Petroleum Institute, 1962, p. 104.

9. HOWELL, L.G., and FROSCH, A., "Detection of Radioctive Cement in Cased Wells", Trans. AIME 136, pp. 71-78, 1940.

10. NORELIUS, R.G., "Radioactive Tracer Logging With Oil Well Cementing", Pet. Eng. 29, pp. B-95, 96, 121-124, November 1957.

11. VETTER, O.J., "The Chemical Squeeze Process - Some New Information on Some Old Misconceptions", J. Pet. Tech., pp. 339-353, March 1973.

12. DALTON, R.L., DEANS, H.A., SHALLENBERGER, L.K., and TOMICH, J.F., "Single-Well Tracer Method to Measure Residual Oil Saturation", SPE paper 3792 prepared for the Improved Oil Recovery Symposium, Society of Petroleum Engineers of AIME, Tulsa, Oklahoma, April 1972.

13. SHEELY, C.Q., "Description of Field Tests to Determine Residual Oil Saturation by Single Well Tracer Method", J. Pet. Tech., 30, pp. 194-202, 1978.

14. DEANS, H.A., "Using Chemical Tracers to Measure Fractional Flow and Saturation In-Situ", SPE paper 7076 presented at the Fifth Symposium on Improved Methods for Oil Recovery, Society of Petroleum Engineers of AIME, Tulsa, Oklahoma, April 1978.

15. KELLER, T.E., "Method for Determining Fluid Saturations in Petroleum Reservoirs", US Patent 3,856,468, December 1974.

16. KELLER, T.E., "Dual Temperature Tracer Method for Determing Fluid Saturations in Petroleum Reservoirs", U.S. Patent 3,847,548, November 1974.

17. WILEY, R., and COCANOWER, R.D., "A Quantitativve Technique for Determining Injectivity Profiles Using Radioactive Tracers", SPE paper 5513, prepared for the 50th Annual Fall Meeting, Society of Petroleum Engineers of AIME, Dallas, Texas, September 1975.

18. CLAYTON, C.G., "Measurement of Flow of Liquids and Gases Using Radioactive Isotopes", Isotopes and Radiation Technology 4, pp. 93-108, Winter 1966-1967.

19. WIEBENGA, W.A., ELLIS, W.R., SEATONBERRY, B.W., and ANDREW, J.T.G., "Radioisotopes as Ground Water Tracers", JGR 72, pp. 4081-4091, 1967.

20. RIEDEL, E.F., "Tracing Flow of Petroleum in Underground Reservoirs", US Patent 3,993,131, November 1976.

21. D'HOOGE, J.A., SHEELY, C.Q., and WILLIAMS, B.J., "Interwell Radioactive Tracers - An Effective Reservoir Evaluation Tool: West Sumatra Field Results", SPE paper 8434, presented at the 54th Annual Fall Technical Conference and Exhibition, Society of Petroleum Engineers of AIME, Las Vegas, Nevada, September 1979.

22. FORD, W.O., JR., "Some Case Histories of Remedial Work Resulting from Water Tracer Surveys", J. Pet. Tech., 18, pp. 791-797, 1966.

23. VETTER, O.J., and CRICHLOW, H.B., "Radioactive Tracer Adsorption Chromatography In Geothermal Reservoirs", SPE paper 7960, presented at the 1979 California Regional Meeting of the Society of Petroleum Engineers of AIME, Ventura, California, April 1979.

24. CALHOUN, T.G., and HURFORD, G.T., "Case History of Radioactive Tracers and Techniques in Fairway Field", J. Pet. Tech., 22, pp. 1217-1224, 1970.

25. BEAR, J., and BACHMAT, Y., "A Generalized Theory on Hydroynamic Dispersion in Porous Media", Int. Ass. Sci. Hydrol. Symp. Haifa Publ. 72, pp. 7-16, March 1967.

26. TAYLOR, G.I., "Dispersion of Soluble Matter in Solvent Flowing Slowly Through a Tube", Proc. Royal Society 219 p. 186, 1953.

27. SCHEIDEGGER, A.E., "Statistical Hydrodynamics in Porous Media", J. Appl. Phys. 25, pp. 994-1001, 1954.

28. KEULEMANS, A.I.M., "Gas Chromatography", Reinhold Press, N.Y., 1957.

29. FRANKEL, S., "Mixing of Fluid Flowing in a Porous Medium", Conference on Theory of Fluid Flow in Porous Media, U. of Oklahoma, March 23-24, 1957.

30. BRIGHAM, W.E., REED, P.W. and DEW, J.N., "Experiments in Mixing During Miscible Displacement in Porous Media", SPEJ, pp. 1-8, March 1961.

31. TURNER, G.A., "The Flow Structure in Packed Beds", Chem. Eng. Sci. 7, pp. 156-165, 1958.

32. DEANS, H.A., "A Mathematical Model for Dispersion in the Direction of Flow in Porous Media", SPEJ, pp. 49-52, March 1963.

33. LEVICH, V.G., MARKIN, V.S., and CHISMADZHEV, Y.A., "On Hydrodynamic Mixing in a Model of a Porous Medium with Stagnant Zones", Chem. Eng. Sci. 22, pp. 1357-1367, 1967.

34. COATS, K.H., and SMITH, B.D., "Dead-End Pore Volume and Dispersion in Porous Media", SPEJ, pp. 73-84, March 1964.

35. BRIGHAM, W.E., "Mixing Equations in Short Laboratory Cores", SPEJ, pp. 91-99, February 1974.

36. BISCHOFF, K.B. and LEVENSPIEL, I., "Fluid Dispersion - Generalization and Comparison of Mathematical Models", Chem. Eng. Sci 17, pp. 245-255, 1962.

37. LAPIDUS, L., and AMUNDSON, N.R., "Mathematics of Adsorption in Beds, 6. The Effect of Longitudinal Diffusion in Ion Exchange and Chromatographic Columns", J. Phys. Chem.56, pp. 981-988, 1952.

38. ARIS, R., and AMUNDSON, N.R., "Some Remarks on Longitudinal Mixing or Diffusion in Mixed Beds", A.I.Ch.E.Journ. 3, pp. 280-282, 1957.

39. BRENNER, H., "The Diffusion Model of Longitudinal Mixing in Beds of Finite Length Numerical Values", Chem.Eng.Sci. 17, pp. 229-243, 1962.

40. DANCKWERTS, P.V., "Continuous Flow Systems: Distribution of Residence Times", Chem. Eng.Sci. 2, pp. 1-13, 1953.

41. FUKUI, M., and KATSURAYAMA, K., "Fundamental Study on Longitudinal Dispersion of Tritiated Water Through Saturated Porous Media", Health Physics 28, pp. 717-725, 1975.

42. THOMAS, H.C., "Heterogeneous Ion Exchange in a Flowing System", Journ. Am.Chem.Soc. 66, p. 1664, 1944.

43. CHURCHILL, R.V., "Complex Variables and Applications, McGraw-Hill Book Co.Inc., New York 1960.

44. BAKER, L.E., "Effects of Dispersion and Dead-End Pore Volume in Miscible Flooding", SPE paper 5632, prepared for the 50th Annual Fall Meeting, Society of Petroleum Engineers of AIME, Dallas, Texas, September 1975.

45. CLEMENTS, W.C., JR., and SCHNELLE, K.B., JR., "Pulse Testing for Dynamic Analysis", Industrial & Engineering Chemistry Process Design and Development, 2, pp. 94-102, 1963.

46. GERSHON, N.D., and NIR, A., "Effects of Boundary Conditions of Models on Tracer Distribution in Flow Through Porous Mediums", Water Resources Research 5, pp. 830-839, 1969.

47. ALEXSEEV, V.V., GRAMMAKOV, A.G., NIKONOV, A.I., and TABLEEV, G.P., "Radiometric Methods in the Prospecting and Extrapolation of Uranium Ores", translated from Russian edition, United States Atomic Energy Commission, AEC-tr-3738, 2, p. 434, 1957.

48. BASTIAN, W.C., and LAPIDUS, L., "Longitudinal Diffusion in Ion Exchange and Chromatographic Column, Finite Column", J. Phys.Chem., 60, pp. 816-817, 1956.

49. SATTER, A., SHUM, Y.M., ADAMS, W.T., and DAVIS, L.A., "Chemical Transport in Porous Media with Dispersion and Rate-Controlled Adsorption", SPEJ, pp. 129-138, June 1980.

50. BARAKAT, H.A., and CLARK, J.A., "On the Solution of the Diffusion Equations by Numerical Methos", J. Heat Transfer 88, No. 4, pp. 421-427, November 1966.

51. BRIGHAM, W.E., and SMITH, D.H., JR., "Prediction of Tracer Behavior in Five-Spot Flow", SPE paper 1130 prepared for the 40th Annual Fall Meeting, Society of Petroleum Engineers of AIME, Denver, Colorado, October 1965.

52. RAIMONDI. P., GARDNER, H.F., and PATRICK, C.B., "Effect of Pore Structure and Molecular Diffusion on the Mixing of Miscible Liquids Flowing in Porous Media", paper no. 43, AIChE-SPE Joint Symposium on Fundamental Concepts of Miscible Displacement, Part II, San Francisco, California, December 1959.

53. BALDWIN, D.E., JR., "Prediction of Tracer Performance in a Five-Spot Pattern", J. Pet. Tech., 18, pp. 513-517, 1966

54. DYES, A.B., CAUDLE, B.H., and ERICKSON, R.A., "Oil Production after Breakthrough as Influenced by Mobility Ratio", Trans. AIME 201, pp. 81-86, 1954.

55. CAUDLE, B.H., and WITTE, M.D., "Production Potential Changes During Sweep-Out in a Five-Spot System", Trans. AIME, 216, pp. 446-448, 1959.

56. FAY, C.H., and PRATS, M., "The Application of Numerical Methods to Cycling and Flooding Problems", Proceedings from Third World Petroleum Congress, Section II, p. 555, 1951.

57. SMITH, D.H., and BRIGHAM, W.E., "Field Evaluation of Waterflood Tracers in a Five-Spot", Producers Monthly, p.8-12, August 1965.

58. WAGNER, O.R., BAKER, L.E., and SCOTT, G.R., "The Design and Implementation of Multiple Tracer Program for Multifluid, Multiwell Injection Projects", SPE paper 5125 prepared for the 49th Annual Fall Meeting, Society of Petroleum Engineers of AIME, Houston, Texas, 1974.

59. WAGNER, O.R., "The Use of Tracers in Diagnosing Interwell Reservoir Heterogeneities - Field Results", SPE paper 6046, prepared for the 51st Annual Fall Technical Conference and Exhibition, Society of Petroleum Engineers of AIME, New Orleans, Louisiana, 1976.

60. GULATI, M.D., LIPMAN, S.C., and STROBEL, C.J., "Tritium Tracer Survey at the Geysers", Geothermal Resources Council, Transactions 2, pp. 237-239, 1978.

61. TESTER, J.W., and POTTER, R.M., "Interwell Tracer Analyses of a Hydraulically Fractured Granitic Geothermal Reservoir", SPE paper 8270, prepared for the 54th Annual Fall Technical Conference and Exhibition, Society of Petroleum Engineers of AIME, Las Vegas, Nevada, September 1979.

ACKNOWLEDGMENT

This study of tracers was funded by the United States Department of Energy, Division of Geothermal Energy (DOE/DGE) through Lawrence Berkeley Laboratory under Contract No. W7405-ENG-48 and subcontract No. 4501210.

APPENDIX

$$c_{n-1} - c_n = \frac{dc_n}{dt_d}, \quad n = 1, 2 \ldots N \qquad (1)$$

$$\frac{\partial c}{\partial t} = D \frac{\partial^2 c}{\partial x^2} \qquad (2)$$

$$\frac{\partial c}{\partial t} = D \frac{\partial^2 c}{\partial x^2} - v \frac{\partial c}{\partial x} \qquad (3)$$

$$f \frac{dc_n}{dt_d} + (1-f) \frac{dC_n}{dt_d} \qquad (4)$$

$$f \frac{\partial c}{\partial t} + (1-f) \frac{\partial c}{\partial t} \qquad (5)$$

$$\frac{\partial C_s}{\partial t} = D_m \frac{\partial^2 C_s}{\partial y^2} \qquad (6)$$

$$\frac{\partial c}{\partial t} = \frac{D_m}{\ell} \left(\frac{\partial C_s}{\partial y}\right)_{y=\ell_s} \qquad (7)$$

$$(1-f) \frac{dC_n}{dt_d} = k_d (c_n - C_n) \qquad (8)$$

$$(1-f) \frac{\partial C}{\partial t} = k (c-C) \qquad (9)$$

$$c_{n-1} - c_n = f \frac{dc_n}{dt_d} + (1-f) \frac{dC_n}{dt_d}, \quad n = 1, 2 \ldots N \qquad (10)$$

$$- \frac{\partial c}{\partial x_d} = f \frac{\partial c}{\partial t_d} + (1-f) \frac{\partial C}{\partial t_d}, \quad 0 \leq x_d \leq N \qquad (11)$$

$$(1-f) \frac{\partial c}{\partial t_d} = k_d (c-C) \qquad (12)$$

$$\mu = \frac{q}{fV} \qquad (13)$$

$$\nu = \frac{P}{fV} \qquad (14)$$

$$\gamma = \frac{P}{(1-f)V} \qquad (15)$$

$$\frac{dc}{dt} + (\mu+\nu)c - \nu C = 0 \qquad (16)$$

$$\frac{dC}{dt} + \gamma C - \gamma c = 0 \qquad (17)$$

$$f \frac{\partial c}{\partial t} + (1-f) \frac{\partial C}{\partial t} = D \frac{\partial^2 c}{\partial x^2} - v \frac{\partial c}{\partial x} \quad \ldots \quad (18)$$

$$(1-f) \frac{\partial C}{\partial t} = k\,(c-C) \quad \ldots \quad (19)$$

$$c(N,t_d) = \frac{1}{\sqrt{4\pi\psi t_d}}\, e^{-\frac{(N-t_d)^2}{4\psi t_d}} \quad \ldots \quad (20)$$

$$\psi = \frac{D_{eff}}{v\ell} \quad \ldots \quad (21)$$

$$N = \frac{L}{\ell} \quad \ldots \quad (22)$$

$$t_d = \frac{vt}{\ell} \quad \ldots \quad (23)$$

$$c = \frac{s}{2\sqrt{\pi Dt}}\, e^{-\frac{x^2}{4Dt}} \quad \ldots \quad (24)$$

$$c = \frac{s}{\sqrt{\pi Dt}}\, e^{-\frac{x^2}{4Dt}} \quad \ldots \quad (25)$$

Boundary conditions for step input: . . . . . (26)

$t = 0$: $c = c_o$ for $x < 0$

$c = 0$ for $x > 0$

$t > 0$: $c = c_o$ for $x \to -\infty$

$c = 0$ for $x \to \infty$

Length Δx of small volume source . . . . . (27)

$$c(x,t) = \frac{c''}{\sqrt{t}} \int_x^\infty e^{-\frac{\xi^2}{4Dt}}\, d\xi \quad \ldots \quad (28)$$

$$\eta = \frac{\xi}{2\sqrt{Dt}} \quad \ldots \quad (29)$$

$$c(x,t) = c''' \int_{\frac{x}{2\sqrt{Dt}}}^\infty e^{-\eta^2}\, d\eta \quad \ldots \quad (30)$$

$$\operatorname{erf} x = \frac{2}{\sqrt{\pi}} \int_0^x e^{-\eta^2}\, d\eta \; ; \quad \operatorname{erf}(\infty) = 1 \quad \ldots \quad (31)$$

$$c(x,t) = \frac{c_o}{2}\left[\text{erf}\,(\infty) - \text{erf}\,\left(\frac{x}{2\sqrt{Dt}}\right)\right] \quad \ldots\ldots\ldots\ldots\ldots\ldots \quad (32)$$

$$= \frac{c_o}{2}\left[1 - \text{erf}\,\left(\frac{x}{2\sqrt{Dt}}\right)\right]$$

$$\text{erfc}\ x \quad 1 - \text{erf}\ x \quad \ldots\ldots\ldots\ldots\ldots\ldots\ldots\ldots \quad (33)$$

$$c(x,t) = \frac{c_o}{2}\,\text{erfc}\,\left(\frac{x}{2\sqrt{Dt}}\right) \quad \ldots\ldots\ldots\ldots\ldots\ldots\ldots\ldots \quad (34)$$

Initial condition for slug . . . . . (35)

$t = 0 \;:\; c = c_o$ for $-H < x < +H$

$c = 0$ for $|x| > H$

$$c(x,t) = \frac{c_o}{2}\left[\text{erf}\,\left(\frac{H+x}{2\sqrt{Dt}}\right) + \text{erf}\,\left(\frac{H-x}{2\sqrt{Dt}}\right)\right] \quad \ldots\ldots\ldots\ldots\ldots \quad (36)$$

$$c(x,t) = \frac{c_o}{2}\,\text{erfc}\,\left(\frac{x-vt}{2\sqrt{Dt}}\right) \quad \ldots\ldots\ldots\ldots\ldots\ldots\ldots\ldots \quad (37)$$

Boundary conditions for step input . . . . . (38)

$c(x,t) \to 0$ for $x \to \infty$

$c(x,t) = \frac{c_o}{2}$ for $x = vt$

$$c = \frac{c_o}{2}\,\text{erfc}\,\left(\frac{1-t_d}{2\sqrt{t_{d/G_L}}}\right) \quad \ldots\ldots\ldots\ldots\ldots\ldots\ldots\ldots \quad (39)$$

$$c' = c - \frac{D}{v}\left(\frac{\partial c}{\partial x}\right) \quad \ldots\ldots\ldots\ldots\ldots\ldots\ldots\ldots\ldots\ldots \quad (40)$$

Concentration gradient $\frac{\partial c}{\partial x}$ . . . . . (41)

$$\frac{\partial c}{\partial x} = -\frac{c_o}{2}\,\frac{\partial}{\partial x}\left[\text{erf}\,\left(\frac{x-vt}{2\sqrt{Dt}}\right)\right] \quad \ldots\ldots\ldots\ldots\ldots\ldots\ldots \quad (42)$$

$$= -\frac{c_o}{2\sqrt{\pi Dt}}\,e^{\left(\frac{x-vt}{2\sqrt{Dt}}\right)^2}$$

$$c' = \frac{c_o}{2}\,\text{erfc}\,\left(\frac{1-t_d}{2\sqrt{t_d/G_L}}\right) + \frac{1}{2\sqrt{\pi t_d G_L}}\,e^{-\left(\frac{1-td}{2\sqrt{t_{d/G_L}}}\right)^2} \quad \ldots\ldots\ldots\ldots \quad (43)$$

$$c' = \frac{c_o}{2}\left[1 + \frac{1}{\sqrt{\pi G_L}}\right] \quad \ldots\ldots\ldots\ldots\ldots\ldots\ldots\ldots\ldots\ldots \quad (44)$$

Initial and boundary conditions for step input to a medium . . . . . (45)

of finite length L preceded by an entrance section (subscript a) and followed by an exit chamber (subscript b):

$t = 0$: $\quad c(x) = 0$

$t > 0$: $\quad c_a = c_o$ for $x = x_o$ where the concentration is step-changed

$$vc_a - D_a \frac{\partial c_a}{\partial x} = vc - D \frac{\partial c}{\partial x}, \quad \text{and } c_a = c \quad \text{for } x = 0, \text{ the inlet face of the medium}$$

$$vc - D \frac{\partial c}{\partial x} = vc_b - D_b \frac{\partial c_b}{\partial x}, \quad \text{and } c = c_b \quad \text{for } x = L, \text{ the outlet face of the medium}$$

Specializations of (45) for $x_o = 0$:

1) $\quad c = c_o \quad$ for $x = 0$ . . . . . (46)

$\quad c(x,t) \to 0 \quad$ for $x \to \infty$

2) $\quad vc_c = vc - D \frac{\partial c}{\partial x} \quad$ for $x = 0$ . . . . . (47)

$\quad c(x,t) \to 0 \quad$ for $x \to \infty$

3) $\quad vc_o = vc - D \frac{\partial c}{\partial x} \quad$ for $x = 0$ . . . . . (48)

$\quad \frac{\partial c}{\partial x} = 0 \quad$ for $x = L$

$D_b \ll D$ . . . . . (49)

$$\frac{c}{c_o} = \frac{1}{2}\left[\operatorname{erfc}\left(\frac{\sqrt{G_L}}{2} \cdot \frac{x_d - t_d}{\sqrt{t_d}}\right) + e^{G_L x_d} \operatorname{erfc}\left(\frac{\sqrt{G_L}}{2} \cdot \frac{x_d + t_d}{\sqrt{t_d}}\right)\right] \quad . . . . . \quad (50)$$

$$\frac{c}{c_o} = \frac{1}{2}\left[\operatorname{erfc}\left(\frac{\sqrt{G_L}}{2} \cdot \frac{x_d - t_d}{\sqrt{t_d}}\right) - e^{G_L x_d} \operatorname{erfc}\left(\frac{\sqrt{G_L}}{2} \cdot \frac{x_d + t_d}{\sqrt{t_d}}\right)\right] - \frac{G_L}{2}(x_d + t_d) \cdot$$

$$e^{G_L x_d} \operatorname{erfc}\left(\frac{\sqrt{G_L}}{2} \cdot \frac{x_d + t_d}{\sqrt{t_d}}\right) + \sqrt{\frac{G_L t_d}{\pi}}\, e^{-\frac{G_L}{4t_d}(x_d - t_d)^2} \quad . . . . . \quad (51)$$

$G_L > 50$ . . . . . (52)

$$\frac{c}{c_o} = \frac{1}{2} \operatorname{erfc}\left(\frac{\sqrt{G_L}}{2} \cdot \frac{x_d - t_d}{\sqrt{t_d}}\right) + \frac{\sqrt{t_d}}{\sqrt{\pi G_L}\,(x_d + t_d)}\, e^{-\frac{G_L}{4t_d}(x_d - t_d)^2} \quad . . . . . \quad (53)$$

$$\frac{c}{c_o} = \frac{1}{2} \operatorname{erfc}\left(\frac{\sqrt{G_L}}{2} \cdot \frac{x_d - t_d}{\sqrt{t_d}}\right) - \frac{\sqrt{t_d}}{\sqrt{\pi G_L}\,(x_d + t_d)}\, e^{-\frac{G_L}{4t_d}(x_d - t_d)^2} \cdot \left(1 - 2\frac{t_d}{1 + t_d}\right) \quad (54)$$

$$\frac{c}{c_o} = \frac{1}{2} \operatorname{erfc}\left(\frac{\sqrt{G_L}}{2} \cdot \frac{1 - t_d}{\sqrt{t_d}}\right) - \frac{\sqrt{t_d}}{\sqrt{\pi G_L}\,(1 + t_d)}\, e^{-\frac{G_L}{4t_d}(1 - t_d)^2} \quad . . . . . \quad (55)$$

$$\left(1 - 6\frac{t_d}{1 + t_d} - 2\frac{t_d^2}{(1 + t_d)^2}\right) \quad \text{for } x_d = 1, \text{ or } x = L$$

$$\frac{c}{c_o} = \frac{1}{2} + \frac{1}{2\sqrt{\pi G_L}} \quad ; \text{ for } G_L = 100 : \frac{c}{c_o} = 0.53 \quad \ldots\ldots\ldots\ldots \quad (56)$$

$$\frac{c}{c_o} = \frac{1}{2} \quad \ldots\ldots\ldots\ldots\ldots\ldots\ldots\ldots \quad (57)$$

$$\frac{c}{c_o} = \frac{1}{2} + \frac{5}{4}\frac{1}{\sqrt{\pi G_L}} \quad ; \text{ for } G_L = 100 : \frac{c}{c_o} = 0.57 \quad \ldots\ldots\ldots\ldots \quad (58)$$

Initial and boundary conditions for spike input . . . . . (59)

$t_d = 0$: $c(x) = C(x) = 0$

$t_d > 0$: $c(o) = \delta(0+)$

$$c(N,t_d) = e^{kN}\,\delta(t_d - Nf) + \frac{k^2 N}{1-f}\,e^{kN}\left[1 + \frac{t_d - N}{(1-f)N}\right] \cdot \frac{I_1\left(2kN\sqrt{1+\frac{t_d-N}{(1-f)N}}\right)}{kN\sqrt{1+\frac{t_d-N}{(1-f)N}}} \quad \ldots \quad (60)$$

with the unit impulse function $\delta(t_d - Nf)$ located at $t_d = Nf$.

$I_1(z) = J_1(iz)$ is the first order Bessel function of the first kind of imaginary argument.

$$c(N,t_d) = \frac{1}{\sqrt{4\pi\frac{(1-f)^2}{k}t_d}}\; e^{-\frac{(t_d-N)^2}{4\frac{(1-f)^2}{k}t_d}} \quad \ldots\ldots\ldots\ldots\ldots \quad (61)$$

$$\psi = \frac{(1-f)^2}{k} \quad \ldots\ldots\ldots\ldots\ldots\ldots\ldots\ldots \quad (62)$$

$$k_d = \frac{kL}{v} \; ; \; Y = k_d x_d \; ; \; x_d = \frac{x}{L} \; ; \; Z = \frac{k_d f}{1-f}\left(\frac{t_d}{f} - x_d\right) \quad \ldots\ldots\ldots\ldots \quad (63)$$

$$-\frac{\partial c}{\partial Y} = \frac{\partial C}{\partial Z} = c - C \quad \ldots\ldots\ldots\ldots\ldots\ldots\ldots\ldots \quad (64)$$

$$\frac{c}{c_o} = 1 - e^{-Z}\int_0^Y e^{-x}\, I_o(2\sqrt{xZ})\, dx, \text{ for } Z > 0, \text{ with } I_o \text{ a Bessel} \quad \ldots\ldots \quad (65)$$

function of first kind, zero order

Boundary conditions for spike input: $c(0) = \frac{1}{fV}$; $C(0) = 0$ . . . . . (66)

$$c(N,t) = \frac{h(T)}{q} \quad \ldots\ldots\ldots\ldots\ldots\ldots\ldots\ldots \quad (67)$$

$$D = \frac{vl}{2} + \frac{vl(1-f)^2 q}{p} \quad \ldots\ldots\ldots\ldots\ldots\ldots\ldots\ldots \quad (68)$$

$$1 << N << \frac{\mu}{\nu} \quad \ldots \quad (69)$$

$$\frac{\nu}{\mu} << 1 \ , \ \frac{\gamma}{\mu} << 1 \quad \ldots \quad (70)$$

$$n(\tau) = \left(1 - \frac{N\nu}{\mu}\right) \frac{\mu}{\sqrt{2\pi N}} e^{\frac{-(\mu\tau - N)^2}{2N}} + \frac{N\nu}{\mu} e^{-\nu\tau} \quad \ldots \quad (71)$$

Peak position of concentration curve is at $\frac{fL}{v}$ . . . . . (72)

$D = \frac{vl}{2\ell}$

the tail of the concentration curve gives $\gamma = \frac{pv}{q(1-f)\ell}$

$$\frac{1}{G_L}\frac{\partial^2 c}{\partial x_d} - \frac{\partial c}{\partial x_d} = f\frac{\partial c}{\partial t_d} + (1-f)\frac{\partial C}{\partial t_d} \quad \ldots \quad (73)$$

$$(1-f)\frac{\partial C}{\partial t_d} = k_d(c-C) \quad \ldots \quad (74)$$

$$\frac{c}{c_o} = \frac{2e}{\pi}\frac{t_d}{f}\int_0^\infty \frac{e^{\frac{G_L}{2}(1-\rho\cos\frac{\Theta}{2})}}{a_1^2+a_2^2}\left[a_1\cos\left(Z\frac{t_d}{f} - w\right) + a_2\sin\left(Z\frac{t_d}{f} - w\right)\right] dZ \quad \ldots \quad (75)$$

for $x_d = 1$ and $k_d = 1$

with $\rho = \sqrt{u_1^2 + u_2^2}$

$$\Theta = \tan^{-1}\frac{u_2}{u_1}$$

$$u_1 = 1 + \frac{4}{G_L}\left(1 + \frac{Bk_d + k_d(1+Z^2)}{(1+B)^2+Z^2}\right)$$

$$u_2 = \frac{4Z}{G_L}\left(1 + \frac{Bk_d}{(1+B)^2+Z^2}\right)$$

$$B = \frac{k_d f}{1-f}$$

$$w = \frac{G_L}{2}\sqrt{\rho}\sin\frac{\Theta}{2}$$

$$a_1 = 1 + \sqrt{\rho}\cos\frac{\Theta}{2} - Z\sqrt{\rho}\sin\frac{\Theta}{2}$$

$$a_2 = Z\left(1 + \sqrt{\rho}\cos\frac{\Theta}{2}\right) + \sqrt{\rho}\sin\frac{\Theta}{2}$$

Substitions wx_d for w . . . . . (76)

$$\frac{G_L x_d}{2}\left(1 - \frac{G_L v}{4w}\right) \text{ for } \frac{G_L}{2}\left(1 - \sqrt{\rho}\cos\frac{\Theta}{2}\right)$$

Substitutions . . . . . (77)

$$a_1 \text{ with } \frac{a_1}{2}\left(1 + \frac{G_L v}{4w}\right) + \frac{a_2 w}{G_L}$$

$$a_2 \text{ with } \frac{a_2}{2}\left(1 + \frac{G_L v}{4w}\right) - \frac{a_1 w}{G_L}$$

Boundary condition $c' = 1$ for $x = 0$, $t \geq 0$ . . . . . (78)

$$\frac{\partial c(\text{chem})}{\partial t} = \frac{1}{\phi}\frac{\partial c_r}{\partial t} = -\frac{k}{\phi}\frac{\partial c}{\partial t} \quad . . . . . (79)$$

where k is the equilibrium absorption constant, see (99).

$$\frac{\partial c(\text{rad})}{\partial t} = -\lambda c \quad . . . . . (80)$$

$$\frac{\partial c(\text{rad})}{\partial t} = -\lambda c\left(1 + \frac{k}{\phi}\right) = -\lambda\varepsilon c \quad . . . . . (81)$$

$$\frac{\partial c}{\partial t} = \frac{D}{\varepsilon}\cdot\frac{\partial^2 c}{\partial x^2} - \frac{v}{\varepsilon}\cdot\frac{\partial c}{\partial x} - \lambda c \quad . . . . . (82)$$

$$D\frac{d^2 c}{dx^2} - v\frac{dc}{dx} - \lambda\varepsilon c = 0 \quad . . . . . (83)$$

$$c(G) = k' e^{d_1 G} + k'' e^{d_2 G} \quad . . . . . (84)$$

with $G = \frac{vx}{D}$

and $d_1 = \frac{1}{2}\left(1 + \sqrt{1 + \frac{4}{F}}\right)$

$d_2 = \frac{1}{2}\left(1 - \sqrt{1 + \frac{4}{F}}\right)$

$F = \frac{v^2}{\lambda\varepsilon D}$

$$\frac{\partial c(\text{chem})}{\partial t} = -k_1 c + k_2 c_r \quad . . . . . (85)$$

$$\frac{\partial c(\text{chem + rad})}{\partial t} = -(k_1 + \lambda)c = -\lambda_e c \quad . . . . . (86)$$

$$\frac{\partial c}{\partial t} = D\frac{\partial^2 c}{x^2} - v\frac{\partial c}{\partial x} - \lambda_e c \quad . . . . . (87)$$

$$\frac{c(L,t)}{c_o} = 1 - 2\sum_{n=1}^{\infty} \frac{\alpha_n L \sin\alpha_n L}{(\alpha_n L)^2 + \frac{v^2 L^2}{4D^2} + \frac{vL}{D}} \cdot e^{\left[\frac{vL}{2D} - (\frac{v^2}{2D} + \frac{D}{\epsilon}\alpha_n^2)t\right]} \quad \ldots \quad (88)$$

where α_n are the roots of $\alpha_n L \cot\alpha_n L + \frac{vL}{4D} = \frac{(\alpha_n L)^2}{vL/D}$

$$\frac{c(x)}{c_o} = \frac{e^{d_2 G}}{d_1 - d_2} \quad \ldots \quad (89)$$

$$\frac{c(x)}{c_o} = k'' e^{d_2 G} \quad \ldots \quad (90)$$

$$k'' = c_o \text{ for SINF1, conditions (46)} \quad \ldots \quad (91)$$

$$k'' = \frac{c_o}{d_1} \text{ for SINF2, conditions (47)} \quad \ldots \quad (92)$$

$$k' = \frac{-d_2}{-d_2^2 + d_1^2 e^{(d_1 - d_2)^{vL/D}}} \quad \ldots \quad (93)$$

$$k'' = \frac{d_1}{d_1^2 - d_2^2 e^{(d_2 - d_1)^{vL/D}}} \quad \ldots \quad (94)$$

$$\frac{c(t)}{c_o} = e^{-\frac{G_L}{F}} \quad \ldots \quad (95)$$

$$D\frac{\partial^2 c}{\partial x^2} - \frac{q}{A\phi}\frac{\partial c}{\partial x} = \frac{\partial c}{\partial t} + \frac{1-\phi}{\phi}\rho_r \frac{\partial c_r}{\partial t} \quad \ldots \quad (96)$$

$$\frac{\partial c_r}{\partial t} = k_1 (1 - \frac{c_r}{c_{rs}})c - k_2 (\frac{c_r}{c_{rs}}) \quad \ldots \quad (97)$$

$$c_r = \frac{kc}{1+bc} \quad \ldots \quad (98)$$

with $b = \frac{k_1}{k_2}$ and $k = \frac{k_1}{k_2} c_{rs}$

$$c_r = kc \quad \ldots \quad (99)$$

Replacement: t_d by $\frac{t_d}{\theta}$ $\quad \ldots \quad (100)$

where $\theta = 1 + \frac{\rho_r(1-\phi)k}{\phi}$

$$D\frac{\partial^2 c}{\partial x^2} - \frac{q}{A\phi}\frac{\partial c}{\partial x} = \left[1 + \frac{(1-\phi)\rho_r k}{\phi(1+bc)^2}\right]\frac{\partial c}{\partial t} \quad \ldots \quad (101)$$

Condition $c_r = 0$ at $t = 0$ $\quad \ldots \quad (102)$

$$\frac{M}{L}\frac{\partial^2 c_d}{\partial x_d^2} - \frac{\partial c_d}{\partial x_d} = \frac{\partial c_d}{\partial t_d} + \rho_r \frac{(1-\phi)}{\phi c_o}\frac{c_{rs}\partial c_{rd}}{\partial t_d} \quad \ldots \quad (103)$$

$$\frac{\partial c_{rd}}{\partial t_d} = \left(\frac{c_o k_1 V_p}{q c_{rs}}\right)(1 - c_{rd})\, c_d - \left(\frac{k_2}{k_1 c_o}\right)\left(\frac{c_o k_1 V_p}{q c_{rs}}\right) c_{rd} \quad \ldots\ldots\ldots \quad (104)$$

$$\frac{M}{L}\frac{\partial^2 c_d}{\partial x_d^2} - \frac{\partial c_d}{\partial x_d} = \left(1 + \frac{1-\phi}{\phi}\rho_r \frac{k}{(1+bc_o c_d)^2}\right)\frac{\partial c_d}{\partial t_d} \quad \ldots\ldots\ldots\ldots\ldots \quad (105)$$

Dispersion group $N_D = \frac{M}{L}$ . . . . . (106)

Adsorptive capacity group $N_A = \frac{\rho_r (1-\phi) c_{rs}}{\phi c_o}$ . . . . . (107)

Flow rate group $N_q = \frac{c_o k_1 V_p}{q c_{rs}}$ . . . . . (108)

Kinetic rate group $N_k = \frac{k_2}{k_1 c_o}$ . . . . . (109)

Adsorptive capacity group for equilibrium adsorption: . . . . . (110)

$$N_{Ae} = 1 + \frac{(1-\phi)\rho_r}{\phi}\frac{k}{(1+bc_o c_d)^2}$$

Replacement velocity by $\frac{Q}{2\pi r \phi} = \frac{Q'}{r}$ . . . . . (111)

equivalent to $v = \frac{q}{A\phi}$ . . . . . (112)

$$\frac{c}{c_o} = \frac{1}{2}\,\mathrm{erfc}\left(\frac{Q't - \frac{r^2}{2}}{2\sqrt{\alpha \frac{r^3}{3}}}\right) \quad \ldots\ldots\ldots\ldots\ldots \quad (113)$$

with $\alpha = \frac{rD}{Q'}$

$\bar{x} = vt$ is the average traveled distance . . . . . (114)

$$\frac{c}{c_o} = \frac{1}{2}\,\mathrm{erfc}\left(\frac{x-\bar{x}}{\sqrt{4\alpha\bar{x}}}\right) \quad \ldots\ldots\ldots\ldots\ldots \quad (115)$$

Standard deviation $\sigma = \sqrt{2\alpha\bar{x}}$ . . . . . (116)

Distance traveled $\bar{x} = r$ . . . . . (117)

σr = constant . . . . . (118)

$d\sigma = \left(\frac{\alpha}{\sigma} - \frac{\sigma}{r}\right) dr$ . . . . . (119)

Boundary condition $\sigma = 0$ at the wellbore radius r_w . . . . . (120)

$$\sigma^2 = \frac{2}{3}\left[r - \frac{r_w^3}{r^2}\right] \quad \ldots\ldots\ldots\ldots\ldots \quad (121)$$

$$\sigma^2 = \frac{2}{3}\alpha r \quad \ldots\ldots\ldots\ldots\ldots\ldots\ldots\ldots\ldots\ldots\ldots\ldots \quad (122)$$

$$\frac{c}{c_o} = \frac{1}{2}\,\mathrm{erfc}\left(\frac{r-\bar{r}}{\sqrt{\frac{4}{3}\alpha r}}\right) \quad \ldots\ldots\ldots\ldots\ldots\ldots\ldots\ldots\ldots\ldots \quad (123)$$

$$\text{Multiplicator } \frac{r+\bar{r}}{2r} \quad \ldots\ldots\ldots\ldots\ldots\ldots\ldots\ldots\ldots\ldots\ldots\ldots \quad (124)$$

$$\frac{c}{c_o} = \frac{1}{2}\,\mathrm{erfc}\left(\frac{r^2-\bar{r}^2}{2\sqrt{\frac{4}{3}\alpha r^3}}\right) \text{ for r sufficiently near } \bar{r}. \quad \ldots\ldots\ldots\ldots\ldots \quad (125)$$

$$d\sigma = -\left(\frac{\alpha}{\sigma} + \frac{\sigma}{r}\right)dr \quad \ldots\ldots\ldots\ldots\ldots\ldots\ldots\ldots\ldots\ldots \quad (126)$$

$$\sigma^2 = \frac{2}{3}\alpha r \text{ at } r = r_e \quad \ldots\ldots\ldots\ldots\ldots\ldots\ldots\ldots\ldots\ldots\ldots \quad (127)$$

$$\sigma^2 = \frac{2}{3}\alpha\left[2\frac{r_e^3}{r^2} - r\right] \quad \ldots\ldots\ldots\ldots\ldots\ldots\ldots\ldots\ldots\ldots\ldots \quad (128)$$

$$\frac{c}{c_o} = \frac{1}{2}\,\mathrm{erfc}\left(\frac{r^2 - \bar{r}^2}{2\sqrt{\frac{4}{3}\alpha(2r_e^3 - r^3)}}\right) \quad \ldots\ldots\ldots\ldots\ldots\ldots\ldots\ldots \quad (129)$$

$$r = r_e \quad \ldots\ldots\ldots\ldots\ldots\ldots\ldots\ldots\ldots\ldots\ldots\ldots\ldots\ldots\ldots\ldots \quad (130)$$

$$Q't = \frac{r^2}{2} \quad \ldots\ldots\ldots\ldots\ldots\ldots\ldots\ldots\ldots\ldots\ldots\ldots\ldots\ldots\ldots \quad (131)$$

$$\frac{c_{mp}}{c_o} = \mathrm{erf}\left(\frac{Q't_1}{4\sqrt{\alpha\frac{r^3}{3}}}\right) \quad \ldots\ldots\ldots\ldots\ldots\ldots\ldots\ldots\ldots\ldots\ldots \quad (132)$$

where t_1 is the time over which the slug is injected.

$$rW = Q't_1 \quad \ldots\ldots\ldots\ldots\ldots\ldots\ldots\ldots\ldots\ldots\ldots\ldots\ldots\ldots\ldots\ldots \quad (133)$$

$$\frac{c_{mp}}{c_o} = \mathrm{erf}\left(\frac{W\sqrt{3}}{4\sqrt{\alpha r}}\right) \quad \ldots\ldots\ldots\ldots\ldots\ldots\ldots\ldots\ldots\ldots\ldots\ldots \quad (134)$$

$$\frac{c_{mp}}{c_o} = \mathrm{erf}\left(\frac{W}{4\sqrt{\alpha L}}\right) \quad \ldots\ldots\ldots\ldots\ldots\ldots\ldots\ldots\ldots\ldots\ldots\ldots \quad (135)$$

$$\frac{c_{mp}}{c_o} = \frac{1.13\sqrt{3}W}{4\sqrt{\alpha r}} \quad \ldots\ldots\ldots\ldots\ldots\ldots\ldots\ldots\ldots\ldots\ldots\ldots \quad (136)$$

$$m = 800\, h S_w c_{mp} L^{1.5} \alpha^{0.5} \quad \ldots\ldots\ldots\ldots\ldots\ldots\ldots\ldots\ldots\ldots\ldots \quad (137)$$

$$\frac{c_p}{c_{mp}} = 2.63\left(\frac{L}{\alpha}\right)^{-0.235} \quad \ldots\ldots\ldots\ldots\ldots\ldots\ldots\ldots\ldots\ldots\ldots \quad (138)$$

$$m = 304\, h_R \phi S_w c_p \alpha^{0.265} L^{1.735} \quad \ldots\ldots\ldots\ldots\ldots\ldots\ldots\ldots \quad (139)$$

$$c_n = c_p \frac{h_n}{h_R} \left(\frac{\kappa_n}{\kappa_{avg}}\right)^2 \quad \ldots\ldots\ldots\ldots\ldots\ldots\ldots\ldots\ldots\ldots \quad (140)$$

$$t_n = t_{avg} \frac{\kappa_{avg}}{\kappa_n} \quad \ldots\ldots\ldots\ldots\ldots\ldots\ldots\ldots\ldots\ldots\ldots \quad (141)$$

$$c_s = \frac{\Sigma \kappa_n h_n c_n}{\left(\frac{GOR}{RVF+WOR}\right)\left(P\Sigma \kappa_n h_n - \Sigma \kappa_n h_n f_n\right) + E\Sigma \kappa_n h_n f_n} \quad \ldots\ldots\ldots\ldots \quad (142)$$

NOMENCLATURE

A	Cross-sectional area
B	Abbreviation, in (75)
C	Concentration in stagnant region
C_n	Concentration in stagnant region of nth cell
C_s	Local concentration in stagnant pocket
D	Diffusion/dispersion coefficient
D_a	Dispersion coefficient in entrance chamber
D_b	Dispersion coefficient in exit chamber
D_{eff}	Effective diffusion/dispersion coefficient
D_m	Effective molecular diffusion coefficient
E	Factor allowing for thermodynamic effects when the gas is expanded to atmospheric conditions
F	Abbreviation, in (84)
G	Linear function of x, in (84)
G_L	G for x = L
H	Half the length of a slug
I_o	Bessel function of the first kind, zero order
I_1	Bessel function of the first kind
J_1	Bessel function of the first kind of imaginary argument
L	Finite length of porous medium
M	Abbreviation, M = D/v
N	Total number of mixing cells in finite medium, $N = L/\ell$
P	Number, in (140)
Q	Volumetric injection rate per unit hight
Q'	Normalized injection rate $Q' = Q/2\pi\phi$, see (111)
S_w	Water saturation
T	Residence time
V	Volume of a mixing cell
V_p	Pore volume
W	Width of slug in radial geometry, rW = Q't
Y	Function of x_d: $Y = k_d x_d$ (63)
Z	Function of x_d, see (63)
GOR	Gas/oil ratio, in STB/day
WOR	Water/oil ratio, in bbl water/STB oil
RVF	Reservoir volume factor
a_1, a_2	Functions in (75)
b	Abbreviations, defined in (98)
c	Concentration of tracer
c_o	Input concentration (step, slug, or constant rate)
c'	Flowing Concentration (vs. in-situ concentration), (40)
c''	Constant, in (28)
c'''	Constant, in (30)
c_a	Concentration in entrance chamber (45)
c_b	Concentration in exit chamber (45)
c_d	Dimensionless concentration $c_d = c/c_o$
c_{mp}	Peak, or midpoint, concentration of the slug
c_n	Concentration in the nth cell, or layer (bottom-hole)
c_p	Produced peak concentration
c_r	Concentration on rock phase (amount per unit volume)
c_{rd}	Dimensionless concentration on rock phase, $c_{rd} = c_r/c_{rs}$
c_{rs}	Saturation concentration on rock phase
c_s	Concentration produced at the surface (142)
d_1, d_2	Abbreviations, defined in (84)
f	Volume fraction of flowing region
f_n	Fraction of displacing fluid in the produced stream from nth layer (142)
h	Residence time distribution h(T)
h_n	Height of nth layer in reservoir (140)
h_r	Height of reservoir (137)
i	Imaginary unit
k	Mass transfer coefficient, kinetic rate constant or equilibrium adsorption constant
k_d	Dimensionless mass transfer coefficient, or rate group, based on cell length ℓ (8) or length of porous medium L (63)
k'	Constant (84)
k''	Constant (84)
k_1	Kinetic rate constant for adsorption (85)
k_2	Kinetic rate constant for desorption (85)
ℓ	Length of a mixing cell
ℓ_s	Length of stagnant pocket
m	Mass (lbs) of tracer injected
n	Numbers, n = 1, 2, ... N
p	Exchange rate between flowing and stagnant regions
q	Volume flow rate
r	Radial distance
r_e	Radius of a radial element
r_w	Welbore radius
$\bar{r}$	Average distance of the concentration front
s	Amount of tracer in spike (delta function)
t	Time
t_d	Dimensionless time, (based on length l (23) of cell or L of medium) or volume, $t_d = qt/V_p = V/V_p$

t_n	Time to break-through from nth layer
t_{avg}	Time to break-through averaged over all layers
t_1	Time for injecting a slug
u_1, u_2	Functions in (75)
v	Flow velocity
w	Function in (75)
x	Linear distance
$\bar{x}$	Average traveled distance vt
x'	Moving coordinate x-vt
$\|x\|$	Absolute amount of x
x_o	Position in entrance section where concentration is step-changed
x_d	Dimensionless distance, $x_d = x/\ell$
y	Distance, direction normal to x
z	Argument of Bessel function
Θ	Function, in (75)
ϕ	Porosity
α	Abbreviation, see (113)
α_n	(Used in (88))
γ	Quantity describing transfer of a fluid element from stagnant zone to flowing zone (15)
δ	Delta, or impulse, function
ε	Abbreviation, defined in (81)
η	Integration variable, see (29)
θ	Abbreviation, used in (100)
κ	Permeability
κ_n	Permeability of nth layer
κ_{avg}	Average permeability of the reservoir
λ	Radioactive decay constant, (80)
μ	Quantity describing transfer of a fluid element from cell to cell (13)
ν	Quantity describing transfer of a fluid element from flowing zone to stagnant zone (14)
ξ	Integration variable (28)
ρ	Function, in (75)
ρ_r	Density of rock material
σ	Standard deviation
ψ	dispersion modulus (21)
[ ]	Numbers in brackets are literature references
( )	Numbers in parentheses refer to the appendix

EVALUATION OF WELL-TO-WELL TRACERS FOR GEOTHERMAL RESERVOIRS
PART 2: LABORATORY WORK

O. J. Vetter and K. P. Zinnow
Vetter Research, Costa Mesa, California

PREAMBLE

The US Department of Energy/Division of Geothermal Energy (DOE/DGE) expressed interest in obtaining some background information related to the utilization of tracers for a better reservoir management in geothermal operations. Vetter Research (VR) was selected (a) to perform a critical literature search on tracers and (b) to conduct a laboratory study related to tracer selection and utilization in the field. Lawrence Berkeley Laboratory (LBL) was chosen by DOE/DGE as the contractor. LBL negotiated a contract with VR to perform this work. All laboratory work under this contract (No. 4501210) was started on January 15, 1980 and was finished on November 30, 1980. LBL's technical coordinator was Dr. O. Weres.

Part I of the final report contains a literature survey. In this part, Part II of the final report, the results and conclusions of the laboratory study are given.

1.0 ABSTRACT

Laboratory tests were conducted to determine the suitability of more than twenty chemicals as well-to-well tracers for geothermal reservoirs. Emphasis was placed on radioactive tracers. The tracer amount required for field jobs may be economically affordable if radioactive tracers are used, whereas the amount of more conventional chemicals may be prohibitive in common geothermal reservoirs.

Some of the critical elution characteristics of these tracers were measured in laboratory experiments. During the initial screening tests, nine of the tested tracers showed significantly better elution profiles than the remainder of the tested chemicals. Iodide showed the most suitable tracer behavior whereas hexacyanocobaltate showed the lowest recovery. These two tracers were subjected to numerous static tests.

Finally, the various tracers including tritiated water were then further examined in extensive flow tests to compare their interactions with different reservoir brines and reservoir rocks. The effects of reservoir brine composition on the retention times of the tracers were negligible. The clay content of the various rock materials has a pronounced effect on the elution characteristics of the tracers. In particular, the ion exchange rates of the clay minerals had the most overwhelming effect on the various tracer elution characteristics.

2.0 CONCLUSIONS

1. Of more than twenty tracers tested, a group of nine ionic and non-ionic tracers had significantly better elution characteristics than the rest which included all cations tested.

2. These anionic and non-ionic radioactive tracers needed no carrier in order to elute. However, the rest of the tested radioactive tracers needed a significant amount of non-radioactive carrier to elute at all. For these the carrier concentration must be larger by many orders of magnitude than that of any radioactive tracer.

3. Of the group of potentially suitable tracers, iodide had the best elution characteristics and hexacyanocobaltate had the worst. The best indication of suitability as a reservoir tracer is the amount of tracer recovered after a tracer slug passes through a sandpack.

4. In static tests no adsorption of iodide was observed under conditions which are considered the most favorable for adsorption that were employed in these tests. Thus, 5 x E-14 gram per square meter could be established as an upper adsorption limit.

5. In flow through sandpacks, iodide gave more consistent and predictable results than tritiated water. Hexacyanocobaltate results fluctuated badly and showed intolerable retention in the rock materials.

6. Sandpacks of five different silicate rocks gave some systematic differences in tracer elutions. These differences are, most likely, attributable to the

clay mineral composition of the rock.

7. According to the elutions of iodide and tritiated water, the rocks can be arranged in a sequence where longer retention times correspond to lower cation exchange rates of the clay minerals contained within each rock. Since anion and water exchange rates follow a similar scheme, the differing exchange rate among the rocks tested is a possible explanation for the series.

8. A slight influence of brine composition on the residence times of the tracers has been observed. The residence is shorter with deionized water than with highly saline brines.

9. The static test method permits an estimate of tracer loss due to microscopic effects as listed in Table 1. The sandpack flow tests allow a more direct comparison of the tracer interaction with different reservoir materials.

10. The simultaneous utilization of two or more tracers in tracer studies would aid in interpreting the microscopic effects.

11. More experimental work is required to ascertain some still obscure relationships for a number of tracer/liquid/rock interactions. Some complex relations were indicated by the experimental work but could not be conveyed with the required mathematical detail.

3.0 INTRODUCTION

Tracers are frequently used for studying the hydrology of subterranean reservoirs containing various types of fluids. As we mentioned in previous publications (1,2) tracers are not the only means to study the critical flow characteristics of subterranean reservoirs such as water, oil, gas and geothermal reservoirs. Pressure and flow test work (e.g., pulse testing and interference testing) is frequently applied to study these reservoirs between wells. However, in our opinion, tracers are a better means than pressure test work to evaluate the more critical reservoir characteristics between wells and at a larger distance from any of the wells. In other words, tracer techniques lend themselves to detailed investigations of the reservoir characteristics at locations further away from a wellbore. Tracers will allow a quantitative determination of the flow patterns within the reservoir.

Proper and sophisticated reservoir studies should include pressure and tracer test work. The two basically different reservoir evaluation and verification methods complement each other and should be used concurrently. Pressure test work gives more detailed and accurate information about reservoir locations close to the wellbore, whereas well-to-well tracers allows for a more detailed study in reservoir locations further away from the wellbores.

3.1 TRACERS IN SUBTERRANEAN RESERVOIRS

As shown in the previous report on this subject (Part 1: Literature Survey, see Preamble), the precise behavior of tracers in subterranean reservoirs is not well understood. The selection of any tracer and the evaluation of well-to-well tracer experiments will depend to a large degree on the various microscopic and macroscopic effects encountered or expected during tracer/fluid and tracer/rock interactions within the reservoir (see Part 1 of these reports). Numerous chemical and physical reactions between the tracer, the reservoir fluid and the reservoir rock can reduce the tracer concentration of the injected tracer slug, thus leading to unexpectedly low tracer concentrations (dispersion of the tracer in a large fluid volume), or to a partial or even entire loss of the injected tracers. The distinction between "microscopic" and "macroscopic" effects is rather artificial and is used only to describe the various interferences in well-to-well tracer jobs in a more orderly fashion. A thorough understanding of these microscopic and macroscopic effects is absolutely necessary to determine the usefulness and limitations of any attempted well-to-well tracer study in a subterranean reservoir.

3.1.1 ANTICIPATED MICROSCOPIC EFFECTS DURING WELL-TO-WELL TRACING

Chemical and physical interactions between all materials in a reservoir (tracers, fluids and solids) on a molecular level or within very small, confined and locally limited cells can be considered "microscopic" levels. For example, a cationic tracer can chemically interact with a clay on a "microscopic" level, thus leading to a scavenging of the tracer by a chemical reaction. Adsorption of the same tracer on the active adsorption sites of the rock material may be considered a physical interaction on a microscopic level. Even the distinction between chemical and physical reactions is rather superficial. For example, a tracer cation (e.g., NH_4^+) may be retained in the lattice of a clay by a combination of chemical and physical reactions. Often, this type of effect is called chemisorption. Ion exchange reactions are also typical examples of microscopic reactions, where the distinction between purely chemical and purely physical reactions becomes rather meaningless. Again, the rather superficial differentiation between chemical and physical interactions is used in this report for the sake of explaining the rather complex maze of possible reactions leading to interferences in a well-to-well tracer job.

Table 1 shows a listing of the various types of reactions leading to decreases of the tracer concentration as the tracer fluid travels from an injection well to a production well. Table 1 lists only the microscopic effects leading to an

undesired dispersion of various tracers in the reservoir. It contains both chemical and physical reactions contributing to a dispersion or loss of tracers in the reservoir.

3.1.2 ANTICIPATED MACROSCOPIC EFFECTS DURING WELL-TO-WELL TRACING

The "macroscopic" effects to be considered in tracing jobs are caused by numerous properties of the entire reservoir. Basically, we can differentiate between the macroscopic effects caused in a very homogeneous reservoir (considering the entire reservoir) and those caused by the heterogeneities in the same reservoir. Both types of macroscopic effects, caused by the fluid flow through the homogeneous and heterogeneous areas of a reservoir can lead to a considerable dispersion or losses of an injected tracer. Table 2 lists some of the macroscopic effects leading to the "undesired" dispersion of a tracer within a reservoir.

3.1.2.1 MACROSCOPIC EFFECTS LEADING TO TRACER DISPERSION IN A HOMOGENEOUS RESERVOIR

Assuming a subterranean reservoir consists of (a) an absolutely homogeneous rock matrix and (b) a very uniform fluid composition and (c) no microscopic reactions take place between the injected tracer fluids and the reservoir materials, we must still expect a rather large dispersion of the tracer in the produced fluids. Figure 1 shows the basic situation encountered during tracer movement between an injection and production well. Because one cannot expect linear flow patterns (see Figure 1), just the effect of varying arrival times of the tracer due to the macroscopic horizontal flow pattern within the reservoir will automatically lead to considerable tracer dispersion. If the producing well is not properly completed over the entire producing interval of the reservoir, a similar type of dispersion due to the lack of vertical linearity of the flow pattern must also be expected.

3.1.2.2 MACROSCOPIC EFFECTS LEADING TO TRACER DISPERSION IN A HETEROGENEOUS RESERVOIR

Homogeneous reservoirs are rare if they exist at all. More likely, a "real world" reservoir contains numerous heterogeneities such as fractures, high permeability streaks, pinch-outs, etc. These macroscopic heterogeneities have rather large effects on the tracer behavior in the reservoir. Figures 2 and 3 illustrate the effect of vertical and horizontal heterogeneities on the macroscopic behavior of a tracer. Any tracer reaching high permeability streaks (or fracture) containing fluids which will drain into a producing well, will also flow into a producing well at a rate depending upon the permeability (or conductivity) of the various permeabilities and the geometries of the varying permeability streaks present. Actually, many tracer injections are performed to determine the permeability and/or geometries of the varying flow channels (high permeability streaks and/or fractures).

3.2 TRACERS IN GEOTHERMAL RESERVOIRS

Basically, there is no fundamental difference between a tracer study in any subterranean reservoir and that in a geothermal reservoir. However, some severe problems must be expected within a geothermal reservoir in addition to the common problems due to the complexity of the flow mechanisms in any subterranean reservoir. These additional problems are mainly caused by the following facts:

1. Geothermal reservoirs are very large reservoirs and the well flow rates are generally much larger than in other operations such as oil, gas and leach mining fields. These sometimes huge flow rates may require extremely large amounts of tracers during well-to-well tracing or all tracer concentrations may have to be very small (to become economically affordable!), thus aggravating all microscopic problems (see later in this report).

2. The chemical (hydrothermal) stability of most tracers becomes extremely important due to the high temperatures in these reservoirs.

3. The chemical and physical interactions between tracer molecules and reservoir materials (fluids and solids) are often temperature dependent. More often than not, the pertinent reactions have not been studied at temperatures normally encountered in geothermal reservoirs. Consequently, very little information is available in the published literature on the topic at the present time.

4. Many (or most) geothermal fluids within the reservoir consist of single-phase aqueous fluids under fairly low pressures but extremely high temperatures. Fluid flashing within the wellbore or surface equipment is frequently encountered, and generates frequent problems regarding the partition of tracers into the liquid and gas phase under these high temperature conditions. Even if a chosen tracer is non-partitioning between the liquid and gas phases, the analytical problems may be severe or may even become unsurmountable unless a material balance between flashed liquid and gas phases are made prior to the evaluation of the tracer concentrations in the produced liquids.

4.0 OBJECTIVES OF THE PRESENT LABORATORY STUDY

The present study had three major objectives:

TABLE 1

MICROSCOPIC EFFECTS LEADING TO TRACER DISPERSION

(WELL-TO-WELL TRACING)

1. TRACER INJECTION METHOD:
   a. Tracer Concentration in Slug
   b. Chemical Properties of Tracer
   c. Composition of Injection Water
2. RESERVOIR CHARACTERISTICS:
   a. Micro-Tortuosity of Rock Matrix
   b. Temperature and Pressure
   c. Rock Materials
   d. Fluid Composition
   e. Linear Velocities
   f. Rock Surface Areas
3. DIFFUSION
4. CHEMICAL REACTIONS:
   a. Hydrothermal Stability of Chemical
   b. Interactions Between Tracer and Formation Materials
5. CHROMATOGRAPHY EFFECTS:
   a. Adsorption-Desorption
   b. Partition
   c. Isotope Exchange
   d. Ion Exchange
   e. Hydration Water Exchange

TABLE 2

MACROSCOPIC EFFECTS LEADING TO TRACER DISPERSION

(WELL-TO-WELL TRACING)

1. TRACER INJECTION METHOD:
   a. Duration of Tracer Injection
   b. Tracer Concentration in Slug
   c. Size of Slug
   d. Water Injection Rate
2. RESERVOIR CHARACTERISTICS:
   a. Heterogeneity of Reservoir (Fractures and High Permeability Streaks)
   b. Macro-Tortuosity of Rock Matrix
   c. Wellbore Entry Profiles
   d. Confinement of Reservoir (Vertical and Horizontal)
   e. Flow Patterns

1. Examine a number of chemicals or isotopes for their suitability as well-to-well tracers in geothermal reservoirs to provide operators with a basis for their selection of tracers for field jobs. This would allow operators of geothermal reservoirs to intelligently select from the commercially available materials.

2. Study some of the more pertinent microscopic effects leading to tracer dispersion and/or losses during a well-to-well tracer job.

3. Evaluate the methods used to examine the tracers in the laboratory for their suitability as well-to-well tracers in the field.

It is self-evident that macroscopic effects leading to tracer dispersions and/or losses in a geothermal reservoir cannot be evaluted in a laboratory study. No attempt was made in the present study to evaluate these macroscopic effects.

4.1 SELECTION OF TRACERS FOR FIELD JOBS

The selection of one or more tracers for any specific field application is a tough problem in most cases. The operator would like to choose from a number of alternatives for various reasons, depending upon the objectives of a field tracer job. The operator must have a detailed knowledge of the following characteristics of each tracer in consideration:

1. Hydrothermal stability.

2. Adsorption/desorption characteristics on the reservoir rock.

3. Chemical reactivity with other reservoir materials.

4. Analytical detectability.

5. Cost of tracer and tracer analyses.

6. Technical and legal requirements to handle the specific tracer or tracer mixture.

7. Availability of the tracer.

In reality, this list of properties comprises a "wish list". For example, sometimes, one would like to inject tracers having certain adsorption/desorption characteristics and, in other cases, it would be desirable to have tracers showing a radically different adsorption/desorption behavior.

Most ideally, one would like to have a catalog of tracers and tracer properties which would allow us to sensibly choose from all available tracers for the design of various tracer jobs in the field. Unfortunately, no such catalog exists. This present study could generate the first rudiments of such a desired tracer catalog.

4.2 STUDY OF MICROSCOPIC EFFECTS LEADING TO TRACER DISPERSION AND/OR LOSSES

The operator of a geothermal reservoir would like to know the pertinent details of tracer behavior contributing to the tracer dispersion and/or losses. However, only the microscopic effects can be evaluted in a laboratory study such as is described in this report.

The study of the miroscopic interactions between a tracer and all rock materials under simulated reservoir conditions, will not only allow the operator to select the most suitable tracers for his specific site, but will also allow him to evaluate the tracer elution profile in a more thorough and sophisticated fashion. Many of the otherwise unexplainable variations of the tracer concentrations in the produced fluids could be related to microscopic reactions, thus allowing the operator to extract the most critical macroscopic tracer behavior. In most cases, the macroscopic tracer behavior is directly related to the heterogeneities in the reservoir. These heterogeneities are of particular interest for accurate reservoir verifications and an acceptable reservoir management.

4.3 METHODS USED TO EVALUATE AND SCREEN POTENTIAL RESERVOIR TRACERS

The literature survey (Part 1 of this report, see also Preamble) indicates that there is no published reference regarding acceptable laboratory methods to evaluate tracers used for geothermal reservoirs. Whatever has been published on the overall behavior of tracers in geothermal reservoirs must be considered suspect because of the uncertainties related to the microscopic and macroscopic effects leading to tracer dispersions and/or losses in the reservoir. It appeared to us after examining the literature and discussing the subject of tracers in geothermal reservoirs with personnel from various operators that laboratory methods have not as yet been developed. A serious attempt was made in the present study to examine various prospective m 'ods to establish acceptable laboratory procedures for screening and evaluating potential tracers for their applicability in geothermal reservoirs.

5.0 SELECTION OF PARAMETERS FOR LABORATORY TESTS

In this chapter the parameters of the laboratory tests are discussed. The requested matrix of temperatures, rocks, brines and tracers (5.0) had to be modified (5.1). Our reasoning for the selection of rocks (5.1.1), and brines (5.1.2) is also outlined in this chapter.

The main objective of the laboratory tests was to characterize the influence of reservoir parameters on the adsorption/desorption characteristics of radioactive tracers. The

main parameters of concern are:

1. The type of reservoir rocks
2. The composition of the geothermal brines
3. The subterranean temperatures

The following test matrix was to be used during this contractual work on tracer evaluations:

1. Temperatures: 3 (170°C, 220°C, 260°C)
2. Brines: 5 (3 synthetic and 2 artificial)
3. Rocks: 5 (3 reservoir and 2 clean rocks)
4. Tracers: 5

Each rock and tracer was to be tested with three (3) brines (one synthetic and two artificial brines) at three different temperatures.

5.1 SELECTION OF ROCKS AND BRINES

Originally, it was planned to employ three (3) simulated geothermal brines, one each of (a) low, (b) moderate and (c) high salinity. These brines were to be formulated to resemble, respectively, the brines at (a) East Mesa, (b) Puna (Hawaii), Roosevelt Hot Springs, or Heber, and (c) Niland or Brawley. At least two additional aqueous fluids (called artificial brines) were to be used: (a) distilled water and (b) a pure NaCl solution having the same ionic strength as one of the naturally occurring brines. The overall number of different brines thus is seven.

The rock material was supposed to be of the type that was in contact with the naturally occurring brine. Four geothermal rock types were to be employed:

1. Sandstone from East Mesa
2. Granite from Roosevelt Hot Springs or Fenton Hill
3. Basalt from Hawaii, and
4. Franciscan Greywacke from the Geysers area.

In addition, clean quartz and calcite were also to be used. This proposed list of rocks is partially in contradiction with the list of brines. For example, no rock type typically in contact with the high salinity brines (Niland or Brawley) was available. Also, it was not clear what kind of brine to use with Fenton Hill granite for rather obvious reasons.

Consequently, a rock from a high salinity brine reservoir and Fenton Hill granite were not used in this study. The use of brines (synthetic and artificial) with the "clean" minerals quartz and calcite has been rather arbitrary. However, critical information was expected from these arbitrary experiments because of the wide-spread occurance of these two materials in numerous geothermal reservoirs.

5.1.1 ROCKS

For the actual tests only three different geothermal rocks were used. Since basalt and greywacke were not available, "greenstone" from Desert Peak, Nevada was used as a substitute material. Some tests were also run with Berea sandstone because this rock material represents a frequently used "reference rock". Thus, the following rocks and minerals were used in the tests:

1. Geothermal: Sandstone from East Mesa, Rhyolitic tuff from Roosevelt Hot Springs (Thermal Power) and Greenstone from Desert Peak
2. Non-Geothermal: Berea Sandstone, Quartz and Calcite

5.1.2 BRINES

The respective brines were made up by utilizing available analyses of natural brines. The synthetic brine was to be formulated to have the same major cation composition (Na, K, Li, Ca, Mg) as its natural counterpart, with the pH under reservoir conditions calculated or estimated. The artificial brines had the same ionic strength as the respective naturally occurring brines. The ionic strength of the Desert Peak brine is higher than that of the other two brines used (East Mesa and Roosevelt Hot Springs). The Desert Peak brine was also employed in the tests with the "clean" rock and minerals. The three brines have the following ionic strengths:

East Mesa:	0.037
Roosevelt Hot Springs:	0.103
Desert Peak	0.179

When the pH was available from analyses, it was given as 5. As a result, all the brines were used at a pH value of 5.

5.2 SELECTION OF TRACERS

The tracer candidates selected for the laboratory work should be those which are thought to have the greatest likelihood of success in geothermal reservoirs. It is, in the published literature, generally agreed upon that tritiated water is the most if not the only successful substance. Iodide and bromide have also been favorably mentioned. Radioactive bromide, however, can hardly be used as an interwell radioactive tracer because of the short half-life (35 hours) of the available

isotope Br-82. Aside from these two, there is no basis for comparing other radiotracers. For this reason it was decided to run pretests for about 20 different tracers under approximately the same conditions.

The following tracers were evaluated: I- (I-129), Br- (Br-82), Cl- (Cl-36), Na+ (Na-24), Rb+ (Rb-85), Cs+ (Cs-137), Ca++ (Ca-45), Sr++ (Sr-90), Fe+++ (Fe-57), H2SeO3 (Se-75), CrO4-- (Cr-51), PO4--- (P-32), SO4-- (S-35), [Co(CN)6]--- (Co-57), SCN- (C-14), formaldehyde HCOH (C-14), (Cr-51)-EDTA, (Sb-124)-EDTA, (In-114m)-EDTA, (Cr-51)-NTA and tritiated water.

6.0 EXPERIMENTAL SET-UP AND PROCEDURES

The different experimental setups are discussed for static (6.1) and flow experiments (6.2). For the flow tests (6.2.2.3) it was necessary to pretest some variable parameters (6.2.2.1). The procedure for selecting the radiotracers is described in (6.2.2.2).

6.1 STATIC TESTS

Room temperature tests were performed to obtain more accurate results related to the rock/tracer interactions. In these experiments, 5g of rock material in the 230 to 325 mesh grain size fraction is mixed with 25 milliliters of water and the tracer. This system is left on a shaker for 45 to 65 hours for reaction. After the rock material has sufficiently settled, about five milliliters of the solution is sampled and centrifuged for about 15 minutes. A one-milliliter sample is then analyzed.

Several experimental set-ups for the static adsorption tests at high temperatures have been considered. Limited by feasibility and availability, it was decided to use the following arrangement and procedure: Two cells similar to the flow cells used with the sandpacks are connected through a valve. Also, a filter is installed between the two cells. One cell initially contains rock sample, brine and tracer while the other cell is empty. With the valve between the two cells closed, the apparatus is heated in a pre-heated oven to the desired temperature and the tracer/rock interaction is performed. Then the empty cell is quickly chilled in cold water to create a lower pressure inside. Thus, when the valve is opened, the liquid is drawn through the rock material and a retaining filter into the second chamber and separated from the rock at the experimental temperature (or as close as possible to it). After the valve is closed the whole apparatus is cooled by submersion in water until it reaches room temperature. It is then opened to take a liquid sample for analysis.

In the case of the blank (no rock material was present), practically all liquid can be transferred from chamber to chamber. However, in the presence of rock material, the amount of transferred liquid is considerably less. Assuming that the liquid retained by the rock material in interstices has the same tracer concentration as the recovered portion, the amount of tracer absorbed on the rock sample of known weight and surface area can be determined from the difference of the input and recovery values of liquid volume and tracer concentration, and from the comparative values of a blank (without rock material).

6.2 FLOW TESTS

This chapter describes the flow apparatus (6.2.1) and the procedures (6.2.2) applied (a) to pretest the influence of some parameters, (6.2.2.1), to (b) select the tracers for the tests (6.2.2.2) and (c) to perform the actual tests (6.2.2.3).

6.2.1 SET-UP

A schematic of the flow apparatus is presented in Figure 4. An ISCO - (Instrumentation Specialties Company) syringe type pump (Model 314 2850 PSI Metering Pump) transfers hydraulic fluid (mineral oil) from one reservoir (R1) to another reservoir (R2) where it displaces the brine in the flow line. Pretests and tracer selection tests were conducted at higher flow rates than the actual tests. For the higher rates, an Altex Model 100A Solvent Metering System was used which more conveniently pumps the aqueous solution continuously and directly. The tracer is injected with the aid of an injection valve (IV) and a Rheodyne Model 7125 Syringe Loading Sample Injector. The brine containing the tracer is brought to the experimental temperature before entering the sandpack (or core) (SP) in an oil bath. All high temperature flow equipment is made of Hastelloy C. A pressure relief valve (PR) maintains a sufficiently high pressure in the high temperature section to keep the brine in a liquid state. The eluent is collected continuously, usually in one milliliter portions, with an Eldex Universal Fraction Collector. Two such systems are operated in parallel. They are interconnected, with three reservoirs (R2) and three sandpacks (SP) so that brine and rock material can be exchanged without interrupting the flow in either system.

6.2.2 PROCEDURES

Procedures were varied in the pretests (6.2.2.1) in order to establish the best way to conduct the tracer selection tests (6.2.2.2) and the actual tests (6.2.2.3).

6.2.2.1 PRETESTS

The influence of the flow rate on the elution was tested using the Altex pump. The lowest constant flow rate obtainable was measured as 0.028 milliliter per minute. An 8-inch sandpack was used to reasonably shorten the times necessary for these tests.

To investigate the effect of fines (including clays) on the elution curve, a series of elutions were obtained from differently prepared "sand". East Mesa sandstone was (a) ground, (b) then washed, stirred and decanted by hand, and,

finally, (c) stirred in a blender to remove as much of the fines as possible. Each pack was tested at three different flow rates: 2, 1, and 0.5 milliliter per minute. Nevada sand (100-140 mesh size fraction) was also tested for comparison.

The sandpacks were packed as a slurry and compressed under force. This gave the best reproduceable results.

With regard to temperature, two effects have to be considered: (a) temperature of the sandpack and (b) the equilibration of the brine/tracer at this temperature. It was considered necessary that the brine/tracer be brought up to the experimental temperature before it entered the sandpack in order to assure equilibrium conditions for measuring the adsorption/desorption reactions. For this purpose, a heating coil was installed in the oil bath. A cooling coil is designed to reduce the temperature of the eluent to ambient.

6.2.2.2 TRACER SELECTION

The tracers were injected as 100-microliter slugs of tracer in deionized water and pumped in succession through the same sandpack of ground-up East Mesa sandstone at a rate of 5 milliliters per hour corresponding to a velocity of about 4 feet per day. The sandpack is 8 inches long and contains an 80 to 140 mesh grain size fraction which has been washed by stirring and decanting before packing. Only the sandpack is kept at a temperature of 170°C in an oilbath, thus allowing the injection and sampling to be done at room temperature.

6.2.2.3 ACTUAL TESTS

The tests were conducted at 170°C. Both heating by coil and water cooling the effluent were found to be unnecessary at the flow rate used. Heating and cooling (in the oilbath or surrounding air) through the metal tubing of the flow lines was sufficient.

The flow tests were run at a linear velocity of 1 foot per day (0.021 ml/minute). A 24-inch sandpack thus takes two days to pass one pore volume. A short porous medium, on the other hand, tends to produce skewed tracer elution curves. This tendency is known from the literature and is evident in our elutions (Figures 5 and 6) from a 2.65-inch long Berea core. Therefore, it was decided that a porous medium with a length of 8 inches, a value between these two values, should be used.

The intention was to test the interaction of the rock materials with the tracers. For this reason, the different materials used had to be in a form allowing them to be as comparable as possible. Consolidated rock has some properties such as permeability, porosity, pore sizes, etc. which change from core to core and certainly vary from rock to rock. These properties influence the dispersion of a flowing tracer. To keep these parameters as constant as possible sandpacks were used. In order to make the packs as homogeneous as possible the rocks were ground to 80-140 mesh size and packed as a slurry. The porosity of these packs is 37-40%. The ground sand was not washed. Instead the pack was flushed before commencing the tests until the effluent water appeared clear (no particles). The retaining filters had an effective pore size of 10 micrometers.

The tracers, according to the experiments (7.2), fall into two main groups: those which eluted with a minimum amount injected, and those which needed a substantial amount of carrier to elute at all. The first group was judged to be a more suitable type of tracer. In this group, iodide had the best recovery, hexacyanocobaltate the lowest. These two tracers were chosen for further investigations.

Tracers are usually injected in either of two forms: as slugs or as spikes. The tracer dispersion in the porous medium causes the tracer to elute in a bell-shaped normal distribution curve (spike) with S-shaped elution curve in the front and back of the peak. Testing a series of slugs of increasing tracer concentration may yield the information to construct an adsorption isotherm. Satter et al (3) have developed a model based on Langmuir type, rate-controlled adsorption. To use such a model for determining the adsorption isotherms was, however, beyond the scope of this work. We also found no measurable adsorption in the static tests for the best tracers, i.e., iodide. The adsorption effects of these tracers were extremely small and not measurable with the employed test methods. Consequently, it was decided to go to a less time consuming (by an estimated factor of 10) route and use spike or slug inputs of constant amounts instead of slugs of varying concentrations.

In this way, a combination rock-brine-tracer can be tested for its interactions in a few days and qualitative comparisons can be made for all combinations with three tracers (iodide, tritiated water and hexacyanocobaltate) within the available time of several months. The evaluation was made chromatographically, that is, the elution curves can be compared for breakthrough time, peak position, and shape.

7.0 ATTEMPTED AND COMPLETED TEST MATRIX

The proposed test matrix for static adsorption tests and flowing adsorption/desorption tests with sandpacks and cores as mentioned above (4.0) calls for using 5 rocks (2 for core tests) with three (3) different brines at three (3) different temperatures for five (5) tracers. Time permitted us to run sandpack tests with three tracers and core tests with only one rock at one temperature, 170°C.

The lowest feasible temperature was chosen in the beginning because the highest tracer retaining effect can be anticipated at low temperatures. As the temperature is increased, the temperature coefficient is negative for all processes of interest, that is adsorption, ion exchange, and selective sorption. While

diffusion and dispersion (mixing) is increased with increasing temperature, there is less sorption. The swelling of expandable clays is diminished with increasing temperature. Simultaneously, the cation exchange capacity is reduced because the ions move into fixed lattice positions, especially in the octahedral layer, from where they cannot further exchange. This rock altering process as a function of temperature starts with the smallest ions at lower temperatures. Thus, the lyotropic series of cation exchange can be altered with increasing temperature. In fact, the solubility of the rock material may become a greater effect than all these processes combined.

Thus, experiments at comparatively low temperatures establish an upper limit for the adsorption/desorption effects.

The static tests were also attemped at 170°C. Because of inconsistent results and large experimental errors which could not be overcome, tests were later run at room temperature.

The attempted test matrix includes 6 rocks:

1. East Mesa sandstone
2. Desert Peak greenstone
3. Roosevelt Hot Springs rhyolitic tuff (Thermal Power)
4. Crystalline quartz
5. Crystalline calcite
6. Berea sandstone.

each with three (3) different brines:

1. Deionized water
2. Synthetic brine, formulated after natural brine
3. Artificial brine, (NaCl-solution of equal ionic strength)

Each rock-brine combination was to be tested with three (3) tracers:

1. Tritiated water (H-3)
2. Iodide (I-129)
3. Hexacyanocobaltate (Co-57)

Of this attempted test matrix the following tests have been completed:

1. Static tests: Static tests have been performed in deionized water. Room temperature experiments with hexacyanocobaltate have been run. Iodide has been used with Berea sandstone only.
2. Flow tests: Sandpack tests at 170°C have been completed. Some core tests with Berea sandstone have also been run (in deionized water). The other geothermal rocks listed are of insufficient permeability, except possibly graywacke. Graywacke, however, was not available and has been substituted by Berea sandstone although Berea sandstone is not a geothermal rock.

8.0 EXPERIMENTAL RESULTS

The results obtained in characterizing the rock material (8.1) selecting tracers (8.2), static adsorption tests (8.3), and flow tests: pretests (8.4), sandpack (8.5), and core experiments (8.6) follow.

8.1 CHARACTERIZATION OF ROCK MATERIAL

Four rocks were used: East Mesa sandstone, rhyolitic tuff from Roosevelt Hot Springs (Thermal Power), Desert Peak "greenstone", and non-geothermal Berea sandstone. The rocks contain quartz and feldspar and some accessory minerals (calcite, magnetite, apatite, zircon, pyrite, etc.). The major difference with respect to tracer interaction with aqueous fluids is made by the sheet silicates; namely, kaolinite in Berea sandstone, smectite in East Mesa sandstone, illite and mica in the tuff, and chlorite (and others) in the Desert Peak greenstone. These minerals have vastly different sorption qualities and ion exchange capacities.

Only the sandstone was available in larger pieces such that fresh cores could be obtained for each test. The other rock was available only in cuttings of mainly millimeter and smaller sizes. In order to compare all rock materials, SEM micrographs were taken (Figure 1). Ordinarily this is adequate only for the sandstone. However, it gives an impression of two important features: the clay or mica structure and the porosity.

1. East Mesa and Berea sandstones. The appearance of the two sandstones is very different. The East Mesa sandstone consists of irregularly shaped grains which seem mostly to be up to 100 micrometer in size (Figure 7) while the Berea sandstone shows much larger grains, mainly with smooth flat surfaces (Figure 8). These grains in Berea sandstone are quartz which have grown new surfaces obviously in situ (Figure 9). The next series of micrographs shows the major constituents - quartz, feldspar and clay minerals. The feldspars are not

easily detected in East Mesa sandstone though they are often somewhat more angular than the quartz grains. Microprobe analysis revealed several grains as feldspar (e.g., Figure 10 bottom center and right). Most of the surface is coated to make analysis of the grain itself impossible (e.g., angular grain top center-left in Figure 10 has the shape of feldspar). In Berea sandstone the appearance is almost the opposite. Here, quartz is regularly shaped and feldspar more in a state of seeming disintegration (Figure 11, center). The clays cover the East Mesa grains almost completely except for a few bare spots of contact between grains. The clays give the larger grains a sponge-like appearance. In Berea sandstone, on the other hand, the clays appear in clusters in recesses and pores between the larger grains (Figure 12). The following series of micrographs allows a closer look at some features. X-ray diffraction reveals that East Mesa sandstone contains calcite which is, however, only a minor constituent. Some small angular crystals (e.g., Figure 13, below center) have been identified as calcite. There are also some thick pore linings (Figure 14) which may be calcite or silica. They are, however, completely covered with clay minerals and identification was not possible. In Berea sandstone we found, as a curiosity, a small pyrite crystal (Figure 15), a cube slightly left of, and below, the center). Of more importance is visual evidence for a process of dissolving potassium feldspar (Figure 16, center: layered skeleton) and growing quartz (Figures 16 and 17) and kaolinite (Figure 17). As a chemical formula this process can be written as 4 units of feldspar plus 5 molecules of water resulting in one unit of kalolinite, 8 units of quartz, plus 2 molecules potassium hydroxide remaining in solution and washed out.

The remaining series of SEM micrograhs provides a close-up look at the two different clay minerals, the open honey-comb-like structure of the smectite in East Mesa sandstone (Figures 18 and 19) and the massive harmonica-like clusters of kaolinite in Berea sandstone (Figures 20 and 21). X-ray diffraction shows the East Mesa clay minerals to be smectite, smectite-illite mixed layers, and some chlorite.

2. Roosevelt Hot Springs - rhyolitic tuff (Thermal Power). Rhyolite is the volcanic equivalent of granite. It is thus comparatively fine grained and composed mainly of alkali felspar and quartz (which are hard to distinguish in SEM micrographs) and some mica apparent by its platy structure. The term "tuff" is applied to material that was ejected in fragments as volcanic ash rather than in the form of liquid lava.

   Tuff is composed of fine particles and may represent a transition between igneous and sedimentary rocks. The material from Roosevelt Hot Springs contains a number of accessory minerals such as magnetite (Figure 22 center and Figure 23 with back-scatter detector), sometimes in the form of perfectly shaped crystals (Figures 24 and 25 with back-scatter detector), titanite (Figure 26, lighter areas, with back-scatter detector), apatite (Figure 27, dark hexagonal shape left of center) and zircon (Figure 27, typical shape at right lower third). The clay fraction was analyzed by X-ray diffraction. It consists of kaolinite, illite and smectite-illite mixed layers, and chlorite.

3. Desert Peak "greenstone". This material was available (as the tuff from Roosevelt Hot Springs) only in cuttings taken from a long range of footage and later mixed up. The material obviously contains pieces of different rocks in unknown proportions. Some of the observed surface textures of selected pieces are shown in SEM micrographs Figures 20 through 31. X-ray diffraction of a separated clay fraction showed the presence of kaolinite, illite and chlorite.

8.2 TRACER ELUTION

All tracers were first applied as purchased or prepared in the laboratory (EDTA-, NTA-, and hexacyanocobaltate-tracers). A minimum amount of carrier-free radioactive material was used, only as was required for detection in the liquid scintillation counter or gamma spectrometer, typically to provide ten thousand to a hundred thousand counts per minute in the slug to be injected.

Tracers of the first group yielded an elution curve as shown Figures 32 through 39. This group includes: Tritiated water, I-, Br-, Cl-, Na+, H2Se03, SO4--, SCN-, formaldahyde HCOH, [Co(CN)6]---, Cr-EDTA, Sb-EDTA. The injected amounts varied from 2xE-13 g for SO4-- to 3xE-7 g for Na+ and formaldehyde. I-129 had to be used at an amount of 5xE-5 g because of its relatively low specific activity.

The tracers of the second group (see Figures 36, 37, 40 and 41) eluted only when considerable amounts, typically over 10 mg of non-radioactive carrier were added. The following tracers fall into this group: Rb+, Cs+, Ca2+, Sr2+, Fe3+, CrO4--, PO43-, In-EDTA, and Cr-NTA. The group includes both cations and anions. The ion exchange capacity of most clays is similar for both.

Three candidates showed no elution even at the highest amounts used. Injected were 1.4 mg In-EDTA and 9.5 mg Cr-NTA without apparent elution. These amounts cannot easily be increased without serious impacts on the economics of a tracer job in the field. Fe-59 was injected with 7xE+3 ppm carrier without elution. A nearly saturated FeCl3 solution proved so viscous that it plugged up the entire injection loop.

Thallium-204 being an unlikely choice for tracing was not further pursued after it initially failed to elute.

Due to the design of the experiments, several interactions of tracers were observed:

1. Between structurally similar anions: H2SeO3 eluted slowly with what appeared to be a long tail (see Figure 37). Subsequently injected chromate seems to have caused a second elution peak of H2SeO3 by pushing it out of the sandpack.

2. Between anions and cations: An expected PO4--- elution (beta-counting) turned out to be mostly if not all Cs+ (or Rb+) when analyzed in the gamma-spectrometer, (see Figure 40). This Cs+ and Rb+ was injected during earlier experiments but did not elute during the earlier tests.

3. Between chemically similar cations: Cs+ has a long elution tail carrying previously injected Rb+ which did not elute until Cs+ acted as a carrier.

8.3 STATIC TESTS

The results of the static adsorption tests are presented in Tables 3 and 4. These tables give the amount of tracer both in concentration (ppb) and weight (grams, in 25 ml) at the start of the experiments and the amounts recovered at the end as percentages of the starting values. The experimental errors are indicated by the variations of the amounts recovered in blanks where no rock material was present. These errors are estimated at around 15%, while the counting errors at a 95% confidence level are below 0.65% generally.

Wherever the recovered amount is more than 15% away from 100%, (i.e., the recovery is below 85% of the blank), sorption reactions are indicated. For example, if 80% of 2.5xE-8g tracer is recovered, the other 20% or about 5xE-9g are adsorbed on the rock material. This absorption, of course, depends upon the available surface area. For example, Berea sandstone with a BET-surface of 0.8 m2/g or 4 squaremeters of available surface area (5g rock) was used in some experiments. In this example the adsorption amounted to approximately 1xE-9g/m2 of tracer of an initial concentration of about 0.8 ppb or 2xE-8g in 25 ml. Plotting these adsorptions on a particular rock versus the remaining tracer concentration in the liquid produces adsorption isotherms. The method could provide a quick and rough check for an upper limit of how much of a given tracer may be adsorbed on a given rock.

Table 3 gives the results of adsorption on Berea sandstone at room temperature for two different tracers: hexacyanocobaltate (Co-57) and iodide (I-131). The data indicate that there may be adsorption of as much as 4xE-8g of the cobalt tracer on 4 square meters of rock surface. The iodine tracer, however, shows no measurable adsorption during experiments using traces as large as 2.5xE-12g. The iodide adsorption can, therefore, be considered to be below 10xE-14/square meter.

The adsorption of the cobalt tracer on the other rock materials is demonstrated in Table 4. It was measured in three different runs as indicated by the numbered columns. The deviation of the data obtained in run number 2 is obvious. There, the radioactive tracer additive was accidentally almost 200 times lower than in the other two runs. The recovery in the blanks is, with one exception, consistent but low.

Tests were also run in the Hastelloy-C apparatus at 170°C. The tracer used was iodide (I-129) and it was used within the same concentration range of the room temperature experiments. The experimental error with this set-up is about twice as high. However, measurable adsorption has not been found. This is not surprising because adsorption is probably less at higher temperatures.

8.4 PRETESTS FOR FLOW TESTS

In the pretests, the influence of experimental parameters on the elution of tritiated water was observed. In particular, changes with rate, content of fines, packing, and temperature were evaluated.

The influence of different flow rates on the elution curve is shown in Figure 42. Three different flow rates were chosen: 1.0, 0.3, and 0.028 milliliter per minute. The elution curve widens with decreasing flow rate causing the peak concentration to drop. It also seems to shift slightly to larger produced volume, or longer time. This indicates kinetic effects of the interaction between tritiated water and the rock matrix.

The content of fines, including clays, seems to play the major role in shaping the elution curve. To investigate this effect, a series of elutions were obtained from differently prepared "sand". Figure 43 shows the elution from the material as it is when ground. Figure 44 after it was washed (by hand), and Figure 45 after cleaning by stirring in a kitchen blender (this action, however, may also break up some of the harder particles). Each pack was tested at flow rates of 2, 1, and 0.5 milliliters per minute. Figure 46 shows the elutions at one milliliter per minute in comparison with elution from

TABLE 3

STATIC ADSORPTION ON BEREA SANDSTONE

CONCEN-TRATION[a.]	TRACER AMOUNT[b.]	HEXACYANOCOBALTATE		IODIDE	
		BLANK	BEREA SANDSTONE	BLANK	BEREA SANDSTONE
.0001	2.5 x E-12	-	-	93.9	99.7
.001	2.5 x E-11	-	-	97.6	103.8
.01	2.5 x E-10	-	-	101.1	94.7
.01	2.5 x E-10	101.3	80.2	97.2	99.4
.1	2.5 x E-9	105.8	73.8	94.2	105.0
1	2.5 x E-8	93.3	80.1	96.4	99.7
10	2.5 x E-7	105.7	85.7	98.1	106.6
100	2.5 x E-6	98.6	101.0	98.0	100.0
1000	2.5 x E-5	107.3	99.7	100.8	102.3
10000	2.5 x E-4	99.7	114.1	97.6	100.3
100000	2.5 x E-3	-	-	101.1	98.8
BET-SURFACE (m2/g)			0.8		0.8

a. Concentration expressed as ppb.

b. Tracer Amount expressed as gms/25 ml.

TABLE 4

STATIC ADSORPTION OF HEXACYANOCOBALTATE (CO-57)

CONCEN-TRATION[a.]	TRACER AMOUNT[b.]	BLANK			CALCITE			QUARTZ		EAST MESA SANDSTONE		DESERT PEAK GREENSTONE		THERMAL POWER RHYOLITIC TUFF		
		1	2	3	1	2	3	2	3	2	3	2	3	1	2	3
.01	2.5 x E-10	1	77.7	101.3	-	60.3	-	45.9	-	14.3	-	13.8	-	-	69.8	-
.1	2.5 x E-9	-	96.8	105.8	-	5.3	-	55.5	-	29.8	-	12.4	-	-	9.2	-
1	2.5 x E-8	-	76.0	93.3	86.2	-	3.8	19.6	-	18.8	-	4.5	-	67.9	9.5	-
10	2.5 x E-7	98.8	72.0	105.7	82.1	8.1	-	59.2	-	6.9	-	-	87.8	-	12.1	-
100	2.5 x E-6	92.8	76.8	98.6	80.8	13.2	-	61.6	-	9.6	-	-	79.5	74.6	-	96.8
1000	2.5 x E-5	98.2	78.5	107.3	96.2	11.8	-	44.1	-	18.2	-	-	98.8	-	-	35.4
10000	2.5 x E-4	-	-	99.7	-	-	88.9	-	111.2	-	106.6	-	-	-	-	103.5
100000	2.5 x E-3	-	-	105.7	-	-	109.6	114.8	114.8	-	114.2	-	-	-	-	-

BET-SURFACE (m2/g)

a. Concentration expressed as ppb.

b. Tracer Amount expressed as gms/25 ml.

relatively "clean", that is clay-free, Nevada sand (100-140 mesh size fraction). Removing the fines, mostly clays, obviously results in sharpening the elution peak.

Packing of the sandpacks was checked with the aid of elution curves. Figure 47 shows elutions under identical conditions as in Figure 44, but from a different pack. The elutions at one milliliter per minute from both packs are directly compared in Figure 48. The differences in packing are thought to be statistical.

The influence of the temperature of the sandpack is shown in Figure 49. The set-up at room temperature and its internal volume, is similar to the apparatus used at 170°C with the one-loop cooling coil. Higher temperature is found to sharpen the elution peak. Initially, a longer cooling coil was employed which increased the total volume of the apparatus by 5 milllilter (Figure 49). Water cooling, however, proved to be unnecessary at the low flow rates employed in the actual tests. Similarly, a heating coil which was used to guarantee the temperature equilibration upstream of the test equipment could be eliminated because tests showed that the test temperature was quickly reached in the short tubing immersed in the oil bath.

8.5 SANDPACK FLOW TESTS

The results of the sandpack tests are presented as elution curves in Figures 50 through 66. The amounts injected were constant for H-3 and I-129. They averaged 5472 counts per minute for H-3, and 4665 counts per minute for I-129. The amounts of tracers eluting are given, in the graphs, in counts per minute and per milliliter. 100 on the scale, thus, is equivalent to about 2% of the injected amounts, or more exactly 1.83% for H-3 and 2.19% for I-129. While the amounts recovered from these injected tracers were reasonably constant, the amounts of Co-57 recovered differed vastly and was not predictable. We had to change the amounts injected during the course of these experiments.

A value of 2.46 mg of "cold" carrier was finally agreed upon in order to reliably elute this tracer. Still, the amounts varied so much as not to be able to represent them on the same scale. However, it is obviously not practical to keep track of the tracer continuously after it has been injected for the first time. Thus, Co-57 is shown with a different scale on the right hand side of the graphs. This scale gives the amount eluting per milliliter as a percentage of the total amount recovered, considering only this particular injection. Since the elution tail must be terminated somewhere, the amount recovered is somewhat arbitrary. But this scale unifies the vastly differing elution curves.

At first injecting about 10xE-11 grams of hexacyanocobaltate into deionized water flowing through the East Mesa and Desert Peak sandpacks resulted with no elution. Therefore, the injected amount was increased by one to two orders of magnitude for the following experiments with brine and NaCl-solution. These experiments were repeated for quartz with all three aqueous solutions. The tracer eluted only from the East Mesa sandstone at 10xE-10g with brine and 10xE-9g with NaCl-solution, the elution with NaCl-solution being distorted by equipment malfunction. Subsequently, it was attempted several times to repeat the latter elution with injections varying from 10xE-11 to 10xE-9 grams. Amounts in the same range were also tried with quartz in deionized water. None of these injections resulted in elution.

The elution curves are summarized in Table 5. The most important properties are shown: the position and height of the elution peak and the recovered amount of tracer in percent of an injection aliquot. The highest count was not necessarily identified with the elution peak if it could be considered a fluke or if several counts around the peak position strayed from a smooth curve. The peak position was then estimated and may be different from a centroid presentation of the peak count in the table. The recovery was not complete in every case for time reasons. The produced volume is 30 ml per day (24 hours). The volume of the apparatus is about 25 ml. Thus, the tracer starts eluting (break-through) about one day after injection and most of it has eluted about one day later. During this second day, another tracer could be introduced following the previous one at about one "pore" volume and eluted during the following day. With this procedure, however, one elution can sit on the tail of a previous one. In order to make the different elutions comparable, each curve was cut off at 50 ml after injection. There are now two numbers by which the recovery can be evaluated, both listed in Table 5. The first one is the count in the last milliliter recovered, which when compared to the peak count can give an estimate of the tail. The other number is the total count recovered up to this point, and its percentage of the injection aliquot. The difference from one hundred percent is obviously the amount eluting in the tail plus the amount not being recovered. The latter can thus be estimated in principle. As can be seen in Table 5 the recovery determined in this way is generally close to 100% for iodine tracer, but lower for tritiated water which presents a special problem due to evaporation. Such evaporation losses are unfortunately not avoidable under the experimental conditions. The loss is sometimes severe and obvious, for example, as shown in the elution curves with brine and NaCl-solution from Desert Peak greenstone and with deionized water from quartz. The losses were measured and estimated in several cases, however, the data presented has not been corrected for evaporation losses.

Recovery of the cobalt tracer is, as expected, much lower than that of the other two tracers. In order to minimize interferences, the tracers were always injected in the same sequence (tritium - iodine - cobalt) into each rock-brine system. Thus, the sequence as presented in Table 5 is the sequence in time of the elutions unless repetitions were necessary.

TABLE 5

SANDPACK ELUTIONS OF INJECTED TRACERS

ROCK	BRINE	TRACER	INJECTION ALIQUOT	PEAK POSITION	PEAK COUNT	50 ml PRODUCED VOLUME COUNT	AMOUNT RECOVERED	
			cpm	ml	cpm/ml	cpm/ml	cpm	% of Aliquot
East Mesa Sandstone	Water	H-3	5472	34.5	388	4.6	4371	79.9
		I-129	4660	34.0	406	10.3	4480	96.1
		Co-57	46550	30.0	2068	35.0	21744	46.7
	Brine	H-3	5472	37.5	348	41.6	4745	86.7
		I-129	4660	37.0	374	29.5	4448	95.5
		Co-57	30412	34.5	319	37.0	3846	12.6
	NaCl Solution	H-3	5472	36.5	329	59.0	4684	85.6
		I-129	4660	37.5	364	60.0	4548	97.6
		Co-57	395000	28.0	11839	119.0	150640	38.1
	Water	H-3	5472	30.0	580	10.4	4985	91.1
Desert Peak	Water	H-3	5472	42.0	241	130.0	3616	66.1
		I-129	4660	39.0	375	58.4	4102	91.5
		Co-57	44653	34.5	2311	78.0	21838	48.9
	Brine	H-3	5472	32.0	253	36.2	4061	74.2
		I-129	4660	40.0	294	76.6	3736	80.2
		Co-57	44653	34.0	1706	47.0	15142	33.9
	NaCl Solution	H-3	5472	39.0	279	98.7	4197	76.7
		I-129	4660	37.0	338	64.0	4188	89.9
		Co-57	44653	32.0	1507	14.0	12561	28.1
	Water	H-3	5472	37.0	437	52.8	5052	92.3
Quartz	Water	H-3	5472	35.5	359	23.6	4099	74.9
		I-129	4660	33.0	332	6.0	3923	84.2
		Co-57	43691	34.0	340	49.0	6377	14.6
	Brine	H-3	5472	37.0	237	55.9	3373	61.6
		I-129	4660	34.0	279	48.3	4531	97.2
		Co-57	46820	30.0	95	6.0	753	1.6
	NaCl Solution	H-3	5472	34.0	260	36.4	4735	86.5
		I-129	4660	35.0	295	46.8	4362	93.4
		Co-57	45021	31.0	170	6.0	1761	3.9
	Water	H-3	5472	34.0	533	0.0	5128	93.7
Thermal Power	Water	H-3	5472	37.0	338	78.3	4642	84.8
		I-129	4660	36.0	358	52.5	4630	99.4
		Co-57	45000	36.0	3645	572.0	44463	98.8
	Brine	H-3	5472	35.0	377	42.1	4817	88.0
		I-129	4660	38.0	344	55.5	4673	100.0
		Co-57	53084	38.0	791	132.0	9767	22.7
	NaCl Solution	H-3	5472	37.0	316	73.4	4379	80.0
		I-129	4660	36.0	342	94.4	4524	97.1
		Co-57	50674	38.0	950	220.0	12073	31.7
	Water	H-3	5472	38.5	289	224.0	4686	85.6
Calcite	Water	H-3	5472	40.0	233	106.0	4365	79.8
		I-129	4800	36.0	254	61.0	4667	97.2
		Co-57	13860	31.0	70.5	6.2	1337	9.65
	Brine	H-3	5472	31.0	202	88.0	4114	75.2
		I-129	4800	29.0	284	91.0	4860	101.0
		Co-57	14330	20.0	663	--	8990	62.7
	NaCl Solution	H-3	5472	32.0	195	69.0	3890	71.1
		I-129	4800	43.0	246	170.0	3643	75.9
	Water	H-3	5472	30.0	216	38.0	4156	86.6
Berea	Water	H-3	5472	32.0	401	11.0	4657	85.1
		I-129	5809	28.0	559	20.0	5563	95.8
		Co-57	13600	35.0	457	37.0	3044	37.1
	NaCl Solution	H-3	5472	33.0	299	55.0	4690	85.7
		I-129	5809	33.0	488	72.0	5969	102.8
		Co-57	13277	33.0	454	33.0	6198	46.7
	Water	H-3	5472	28.0	426	4.6	4557	83.3

As a final check on the condition of each sandpack, a last elution of tritiated water (in deionized water) was always obtained (Figures 67 through 72). This elution normally has an earlier breakthrough than a first one obtained under the same circumstances. This result may be due to the fact that the sand has lost fines during the course of the experiments and/or the change in chemistry taking place by dissolution of rock material, adsorption, ion exchange, etc. During the tracer selection test, we also ran control experiments with tritiated water and found the breakthrough to be randomly distributed, not following a systematic pattern.

8.6 CORE TESTS

Core tests have been run on Berea sandstone which has a porosity of around 20%. The core is about 1 inch in diameter. Thus, the same flow rate that was used in the sandpack tests results in the same linear velocity of about 1 foot per day. Tests have been run in deionized water with all three tracers, and in sodium chloride solution with tritiated water.

The elution curves are shown in Figures 5 and 6. They are summarized in Table 6. Since the core is shorter than the sandpack (2.6 inches vs. 8 inches) the residence times are also shorter.

9.0 INTERPRETATION OF EXPERIMENTAL DATA

In the tracer selection tests nine tracers were found to require substantially lower input than the others in order to elute (9.1). Two of them were subjected to static tests (9.2). No adsorption of iodide on Berea sandstone was found. In the flow tests, however, small differences in residence times were encountered (9.3). These can be attributed to various factors, for example, total surface area. It was hoped that by using sandpacks the parameters could be made as equal as possible. It would, however, require many more experiments to ascertain some definite relations. Instead, here we discuss a possible contributing factor to adsorption. The different clay minerals can account for some systematic differences in residence times found in some experiments (9.3.2).

9.1 TRACER COMPARISON

The tracer comparison showed that the tracers can be divided into two groups, that is, those eluting with the minimal amount injected, and those requiring a substantial amount of carrier in order to elute. The two groups seem to undergo fundamentally different reactions in the system. Clearly, only tracers of the first group are desirable. When considering the properties of the elution curves, Na+, H_2SeO_4 and Sb-EDTA (see Figures 36,37 and 39) can also be eliminated. The remaining tracers (Figures 32 through 35, 38 and 39) in this group, tritiated water, I-, Br-, Cl-, SO_4^{--}, SCN-, formaldehyde HCOH, hexacyaocobaltate, and Cr-EDTA, showed the shortest residence times with the elution peak at 26 to 33 ml after injection and the highest peak counts relative to the recovered amounts (over 6% in the peak centroid of 1 milliliter) compared with all other tracers tested, see Table 7a,b. These nine tracers are the obvious candidates for further testing.

From the list of the nine tracers to be considered, radioactive Br- can be eliminated because its short half-life of 35 hours precludes its use in interwell tracing.

As has been said above, tritiated water and iodide are the prime choices for reservoir tests as evidenced by our laboratory experiments. These two tracers were among those with the highest recovery rate.

9.2 STATIC ADSORPTION

The significance of static adsorption is that a certain amount of tracer is retained on the rock surface. More important is the fact that the total adsorption involving rock material is probably more than an external surface effect. Adsorption may include phenomena like ion exchange and processes like dissolution and diffusion inside solids, that penetrates the normal surface. Thus, the tracer behavior may be in part time-dependent, irreversible, and not as strictly a function of the surface area. These aspects must be taken into account in interpreting the results of experiments.

In static experiments adsorption may occur, but nothing is known about possible ion exchange with the rock material for both iodide and cobaltate. In the tests, no evidence for either process was found for iodide in Berea sandstone. The results for the cobalt tracer, which was tried with all test rock materials, is not conclusive. This confirms the good results for iodide obtained during the initial tracer selection experiments and the ambiguity anticipated for hexacyanocobaltate.

9.3 FLOW TESTS

The experimental results can be interpreted in terms of "adsorption" (9.2.2) considering the theoretical results obtained by Satter et al. [3] and can be applied in a general way (9.2.1).

9.3.1 THEORETICAL CONSIDERATIONS

Elution curves for spike input are normal distributions, that is, symmetrical bell-shaped curves determined by one parameter, namely, the standard deviation. This is true, however, only if the dispersing medium is sufficiently long. If it is shorter, the elution curves are skewed. In models based, as usual, on the dispersion equation, this asymmetry is normally attributed to inhomogeneous flow of the tracer in the porous medium (capacitance effect). In the simplest way, the pore space is divided into two regions, one flowing, the other non-flowing due to dead-end pores. The volume fraction of this stagnant region and a constant describing the exchange rate between the two regions (or the molecular diffusion into the stagnant portion) provide two more parameters. The total of three

TABLE 6

BEREA CORE ELUTIONS

ROCK	BRINE	TRACER	INJECTION ALIQUOT cpm	PEAK POSITION ml	PEAK COUNT cpm/ml	50 ml PRODUCED VOLUME COUNT cpm/ml	AMOUNT RECOVERED cpm	AMOUNT RECOVERED % of Aliquot
Berea Sandstone	Water	H-3	5472	18	578	14	4400	80.4
		I-129	5809	19	971	22	5857	100.8
		Co-57	13209	18	1162	0	6098	46.2
	NaCl Solution	H-3	5479	18	511	25	4052	74.0

TABLE 7a.

ELUTION OF BETA-ACTIVE TRACERS

RADIOTRACER	ISOTOPE	AMT. INJ. g	ALIQUOT cpm	AMT. RECOVERED cpm	AMT. RECOVERED % of Aliquot	PEAK COUNT cpm/ml	PEAK COUNT % of Amt. Recovered	PEAK POSITION ml	PEAK HALF WIDTH ml
HTO	H-3		4,739	3,061	64.6	315.6	10.5	30	9.0
				5,031	106.2	412.6	8.2	28	12.0
				4,431	93.5	353.6	8.0	30	12.5
				4,714	99.5	506.2	10.7	29	8.0
				4,373	92.3	337.8	7.7	30	12.0
			6,926	4,785	69.1	439.8	9.2	34	13.0
			5,478	4,730	86.3	325.9	6.9	34	14.0
			5,606	4,148	74.0	308.4	7.4	33	13.0
Cl^-	Cl-36	2.5×10^{-7}	122,344	120,564	98.5	8789.0	7.3	31	13.0
I^-	I-129	4.86×10^{-5}	18,071	12,370	68.5	1207.0	9.8	28	10.0
Ca^{2+}	Ca-45	5×10^{-13}	5,385	0	0	0	0	-	-
		1×10^{-5}	22,074	0	0	0	0	-	-
		5×10^{-4}	24,391	0	0	0	0	-	-
		1.5×10^{-2}	19,024	75,573		>3750.0	>5.0	33	19.0
Sr^+	Sr-90	3.5×10^{-5}	38,465	0	0	0	0	-	-
		1×10^{-3}	52,291	0	0	0	0	-	-
		3×10^{-2}						32	>16.0
Tl^{3+}	Tl-204	9×10^{-10}	27,585	0	0	0	0	-	-
SO_4^{2-}	S-35	2×10^{-13}	49,556	24,556	49.4	1640.0	6.7	28	15.0
PO_4^{3-}	P-32	7×10^{-14}	30,427	0	0	0	0	-	-
		4.13×10^{-5}	26,928	0	0	0	0	-	-
		1.25×10^{-2}	26,204	0	0	0	0	-	-
		3.75×10^{-1}	not det.					33	29.0
SCN^-	C-14	7.4×10^{-8}	22,973	11,884	51.7	968.0	8.1	27	11.0
HCOH	C-14	3×10^{-7}	17.625	12,519	71.0	1011.0	8.1	31	14.0

TABLE 7b.

ELUTION OF GAMMA-ACTIVE TRACERS

RADIOTRACER	ISOTOPE	AMT. INJ. g	ALIQUOT cpm	AMT. RECOVERED cpm	% of Aliquot	PEAK COUNT cpm/ml	% of Amt. Recovered	PEAK POSITION ml	HALF WIDTH ml
$[Co(CN)_6]^{3-}$	Co-57	$8x10^{-11}$	61,124	>16,641	>27.2	1106.0	6.6	29	7.0
Na^+	Na-24	3.10^{-7}	8,041	6,796	84.5	346.0	5.1	50	36.0
Br^-	Br-82	$1.4x10^{-7}$	4,608	5,086	110.4	360.0	7.1	33	13.0
Cr-EDTA	Cr-51	$3.86x10^{-8}$	3,429	1,018	29.7	89.0	8.8	28	15.0
In-EDTA	In-114m	$2.14x10^{-6}$	84,538	0	0	0	0	-	-
		$1.57x10^{-1}$	80,616	0	0	0	0	-	-
		1.410	not det.	0	0	0	0	-	-
Sb-EDTA	Sb-125	$1.04x10^{-9}$	7,738	0	0	0	0	-	-
		$3.07x10^{-1}$	7,401	1,395	18.85	60.0	4.3	60	35.0
Cr-NTA	Cr-51	$2.73x10^{-9}$	42,564	0	0	0	0	-	-
		$5.0x10^{-4}$	3,840	0	0	0	0	-	-
		$9.5x10^{-3}$	not det.	0	0	0	0	-	-
CrO_4^{2-}	Cr-51	w/o carrier	not det.	0	0	0	0	-	-
		$4.96x10^{-5}$	not det.	0	0	0	0	-	-
		$1.5x10^{-4}$	30,419	0	0	0	0	-	-
		3.10^{-2}	30,339	33,750	111.2	893.0	2.6	50	42.0
H_2SeO_3	Se-75	$3.75x10^{-10}$	15,124	14,572	96.4	333.0	2.3	60	-
Rb^+	Rb-86	$3.8x10g^{-7}$	19,524	0	0	0	0	-	-
Cs^+	Cs-137	w/o carrier	21,435	0	0	0	0	-	-
		388ppm	29,268	0	0	0	0	-	-
		$1.7x10^{-4}$	30,071	0	0	0	0	-	-
		6x10-	30,603	26,076	85.2	1487.0	5.7	-	-
Fe^{++}	Fe-59	w/o carrier	1,492	0	0	0	0	-	-
		$4.3x10^{-5}$	4,682	0	0	0	0	-	-
		$7x10^{-4}$	4,470	0	0	0	0	-	-

parameters permits fitting the model to experimental curves. The capacitance model can thus account for the asymmetry of the elution curve which is manifest in a steeper rising in the beginning and a slower falling in the end and, as a result, an earlier peak (for spike input) or inflection point (for step input) as compared with the symmetrical distribution.

The deviations from symmetrical dispersion can be attributed to other effects, for example adsorption. The simpliest case of adsorption is the Langmuir type where the adsorption on the solid is proportional first to the concentration in the liquid, then reaches a saturation (assymptote). The region of proportionality is governed by the kinetic rate constants for adsorption and desorption, the saturation region by the saturation concentration on the rock phase. Thus, three additional constants are required to describe Langmuir adsorption. Other types of adsorption require even more constants. Satter, et al. have published a model and some computer derived solutions for Langmuir type adsorption on which interpretation of elution curves can be based.

Their model involves dispersion and Langmuir adsorption. Some numerical solutions are given graphically for step input. Consequently, the computer generated curves can be used to qualitatively explain trends of the elution curves presented here. To make these comparisons, two facts have to be kept in mind:

1. The step input can be considered as the integration of a number of spike input functions. Thus, a similar symmetry prevails, for input as well as for elution functions: the ideal elution curves are symmetrical around the point of inflection (step input) and the peak (spike input), respectively. These two points correspond in position as well as in breakthrough points on both curves.

2. The step elution involves only adsorption on the rock material while the desorption is shown with a separate and similar step. With spike input, however, adsorption and desorption are represented in the same elution curve which thus may be inherently less symmetrical because of the desorption "tail".

In summary, the experimental elution curves have comparable positions but possibly lower symmetry than the computer curves by Satter, et al. These authors investigate the influence of four different groups of constants (parameters) which appear in different places in their model equations (see part 1 of this report for details). By holding three of these groups constant and varying only one, the effect of this group can be separated. The findings can be summarized in the following way:

1. The dispersion group influences the shape but not the position of the elution curve.

2. The adsorption group affects the position of the elution curve through the saturation concentration on the rock phase: the higher it is the later the elution occurs.

3. The flow rate group involves the ratio of the kinetic rate constant for adsorption to the saturation concentration (on the rock material). The higher this ratio is the more the elution shifts to longer times. The shape of the elution curve can also be affected by this group.

4. The kinetic rate group is essentially the ratio of the kinetic rate constants for desorption and adsorption. The higher the desorption rate is, the earlier the elution appears.

In short, Langmuir adsorption causes the elution to be later, the higher the saturation concentration is, the larger the kinetic rate constant for adsorption is (in relation to the saturation concentration) and the smaller the rate constant for desorption is (relative to that for adsorption).

9.3.2 EXPERIMENTS

Satter et al. [3] showed that the position of the elution curve (breakthrough, peak) depends on the input concentration: the lower it is the later the elution appears. For spike input this relates to the total amount of tracer used. We have used different amounts for the three tracers but these amounts are constant for each tracer in all experiments (except the cobalt tracer in East Mesa sandstone).

Also the three tracers are different with respect to their dispersion coefficients which influences the shape of the elution curve, that is the width and the skewness. We have found that the rising slope of the tritium elution curve is generally not as steep as that of the other two tracers.

Thus, the position and the shape of the elution curve initially is arbitrary for each of the three tracers as far as our experiments are concerned. Each tracer, however, has eluted from the sandpacks with a certain sequence of residence times (see Figure 73).

Iodide eluted in the order of increasing breakthrough and peak concentration time first from Berea sandstone, then from quartz, East Mesa sandstone, Thermal Power tuff, and finally from Desert Peak greenstone. This is independent of the brine used except that the elution from East Mesa sandstone was sometimes retarded (breakthrough later than from the tuff in synthetic brine, peak later than other peaks in NaCl-solution).

Tritiated water was found to generally follow the same elution sequence as iodide, yet with more uncertainties. Again, East Mesa sandstone had the longest residence time when synthetic brine or NaCl-solution was used. In addition, the elutions from quartz were somewhat out of the order: earlier in NaCl-solution, later in the other carriers, when compared to the other elutions.

The cobalt tracer followed a different sequence of residence times. It eluted first from East Mesa sandstone, then from quartz, Desert Peak greenstone, Berea sandstone, and last from Thermal Power tuff. Exceptions were few: East Mesa sandstone again produced a late elution peak with synthetic brine; breakthrough from Berea sandstone was later in water but earlier in NaCl-solution than the sequence indicates.

The difference in residence times of the iodide and tritium tracer in various rocks can be interpreted in terms of adsorption. The rocks fall into the series Berea sandstone, quartz, East Mesa sandstone, Thermal Power tuff, and Desert Peak greenstone with increasing residence times. This sequence possibly relates to progressively slower "desorption", that is, slower interaction with the tracer. Since all factors influencing the elutions such as permeability, porosity, surface area, flow rate, etc., were made as equal as possible, the different interactions revealed should be attributable to the nature of the rock materials. Of the components of the rocks used here, the clay minerals are considered to be chemically, most active. In this series, the rocks contain the following clay minerals:

1. Berea sandstone: kaolinite
2. Quartz: none
3. East Mesa Sandstone: smectite, smectite/illite mixed layer, chlorite
4. Thermal Power tuff: illite, smectite/illite mixed layer, chlorite
5. Desert Peak greenstone: kaolinite, illite, chlorite.

Discounting quartz, this sequence of clay minerals can be generalized to: kaolinite/smectite, (montmorillonite)illite, and chlorite. This series is known (Grim [4]) to represent decreasing exchange rates for cations. For anions and water as used here nothing comparable is known. However, the reasons given for the reactions of cations also hold for anions or water. The main reaction sites for kaolinite are broken edges, for smectite interlayer sufaces, for illite and chlorite localized crystallization defects. The access to, and from, these sites in the series obviously is increasingly more difficult, quite independent of the chemical nature of the reactant.

The influence of the different brines is slight. Generally, the residence time is equal to or a little longer in synthetic brine and NaCl-solution than in deionized water.

For iodide, this is again more evident than for the other tracers. We had only two incidences where breakthrough of a synthetic brine (from quartz), or the concentraton peak of a NaCl-solution (from Desert Peak greenstone), occurred earlier than those of deionized water.

For tritiated water, however, this holds only for the two sandstones. The Thermal Power tuff shows no great difference, but quartz and Desert Peak greenstone seem to retain the tracer longest in deionized water.

For the cobalt tracer, the picture is more complicated. However, only in two cases did we find an elution in synthetic brine (from quartz) or NaCl-solution (from Berea sandstone) more than about two milliliters earlier than in deionized water.

The differences between the elutions in synthetic brine and NaCl-solution, both in concentration peak and breakthrough, are usually not more than one or two milliliters which is not considered significant. The two exceptions were the elutions of tritiated water from Desert Peak greenstone, and the cobalt tracers from East Mesa sandstone. The shift of the elution curve to longer residence times can possibly be explained by a higher "adsorption" rate in brine compared to deionized water.

10.0 TEST EVALUATION

In trying to apply the results of laboratory experiments to field work two points have to be discussed. How do the employed methods compare (10.1), and what can the data obtained in the laboratory predict with respect to actual performance in a reservoir (10.2)?

10.1 EVALUATION OF LABORATORY METHODS

Laboratory methods are usually not immediately relevant to field work. There are too many variables which govern the behavior of a tracer in a complex geothermal reservoir. Only a few of these variables can be investigated in laboratory experiments. Normally the results of these experiments are used to support fairly simple models (see Part 1 of this report) which give mass balances and transport equations for a one-dimensional geometry and a diffusion-dispersion-type propagation. Certain parameters or variables can be isolated and dealt with separately such as flow velocity, dispersion coefficient, length of the porous medium, porosity, permeability, etc. Application of these models to actual reservoirs, however, is not possible because all quantities are reduced to mean values or averages. The real-time aspects are lost and the models then acquire the appearance of arbitrariness. In essence, reservoirs cannot be modeled in the laboratory.

In the work undertaken here an attempt was made to help understand the "real world" of reservoir work rather than to establish or build some laboratory model. In the field, the many different factors influencing the flow of a tracer cannot be separated, they cannot even be identified. Only their collective interaction will determine the final result, that is, how much tracer arrives at the producer, and when.

The static tests described in Section 6.1 can provide an upper limit for the loss of tracer to the reservoir rock provided the total surface of contact between rock and tracer can be estimated. A pre-condition for accuracy is that the rock material used is representative for the reservoir, not just for the wellbore where it was taken.

At room temperature these tests are straightforward. At reservoir temperatures, however, the sampling for analysis is much more difficult.

The flow tests give indications for the actual flow of the tracer. A simulation of reservoir flow can not be achieved in the laboratory. The setup described in Section 6.2 can be used with cores or sandpacks. Cores represent the reservoir, in principle, better than sandpacks. In fact, however, the cores available for laboratory tests may not have the average geometrical and hydrological characteristics of the reservoir. In addition, cores must be long enough or they will distort the elution curve of the tracer. With sandpacks, different rock materials are easier to compare. We used the same modular cells as in the static tests and could thus subject comparatively much more rock material (surface area) to each test. The flexibility in applying the tracer is greater in flow than in static tests. The tracer can be injected in different ways. Two of these are particularly easy to relate to the elution curves; the one-time spike, and the slug of constant concentration. A slug input and elution is much more time consuming, but a succession of slugs could provide information similar to static testing. Flow-through monitoring of the tracer would be desirable. However, this in-line monitoring is not as sensitive as conventional counting. A spike input of the tracer comes closer to the conditions and circumstances encountered in interwell tracer work.

10.2 IMPLICATION FOR TRACER WORK IN THE FIELD

The tests have yielded a series of eight tracers (out of more than twenty) which can be considered good tracers. They eluted with no extra carrier necessary. Of these tracers, iodide is probably the best. No adsorption was found in static tests under conditions considered worse than those encountered in the reservoir. This establishes an upper limit of 5 x E-14 gram per square meter of rock suface for possible loss in the formation due to interaction with the reservoir rock. However, time-dependent interaction processes are an essential factor. Satter et al. [3] conclude in their computer study that "any rate controlled mechanism can affect significantly the way laboratory results should be translated to field applications. When adsorption of a chemical is rate-controlled or time-dependent, core flood data obtained at times much shorted than reservoir residence times should not be applied directly to estimate chemical loss in a reservoir". While we have no indication that adsorption of iodide is time-dependent, other tracers may very well show this effect.

Flow tests gave indications that residence times of tracers are influenced by reservoir rock and brine. This is important in deducing flow rates from breakthrough times of a tracer.

The type of clay minerals found in the reservoir is thought to play a major role in the flow of the tracer. The significant property is the exchange rate for the tracer.

The data obtained in our tests are insufficient for actual quantitative estimates mainly because of the short length of the porous medium and, thus, of the times of flow. The small differences encountered would render these estimates not accurate enough for comparison. Small fluctuations in experimental conditions have significant influence on the results. The accuracy of these data can, however, be vastly improved by using multitracer cocktails. As most field data are interpreted on a relative basis, the use of two or more tracers simultaneously will definitely aid in interpreting the interactions with reservoir rock due to microscopic effects [5].

REFERENCES

1. Vetter, O.J., "Tritium Tracer as a Means for Reservoir Verification in Geothermal Reservoirs", Proceedings, EPRI Annual Geothermal Project Review and Workshop, pp. 1714--1723, Kah-Nee-Ta, Oregon, July 1977.

2. Vetter, O.J., "Use of Tracers in Geothermal Systems", prepared for the Second Invitational Well Testing Symposium, University of California, Berkeley, October 25-27, 1978.

3. Satter, A., Shum, Y.M., Adams, W.T., and Davis, L.A., "Chemical Transport in Porous Media With Dispersion and Rate-Controlled Adsorption", SPEJ pp. 129-138, June 1980.

4. Grim, R.E., "Clay Mineralogy", McGraw-Hill Book Company, New York 1968.

5. Vetter, O.J. and Crichlow, H.B., "Radioactive Tracer Adsorption Chromatography in Geothermal Reservoir", SPE paper 7960, presented at the California Regional SPE Meeting, Ventura, California, April 18-20, 1979.

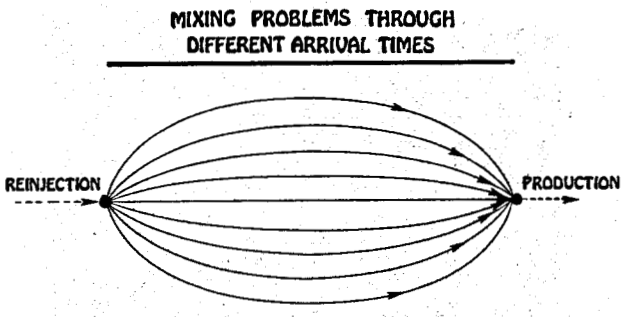

Fig. 1 Tracer Dispersion by Non-Linear Flow Pattern

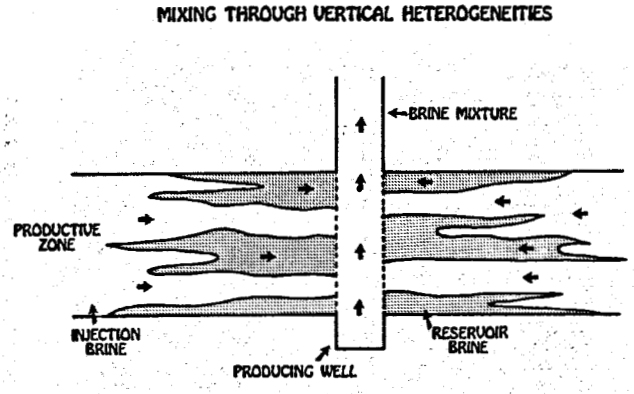

Fig. 2 Tracer Dispersion by Vertical Heterogeneities

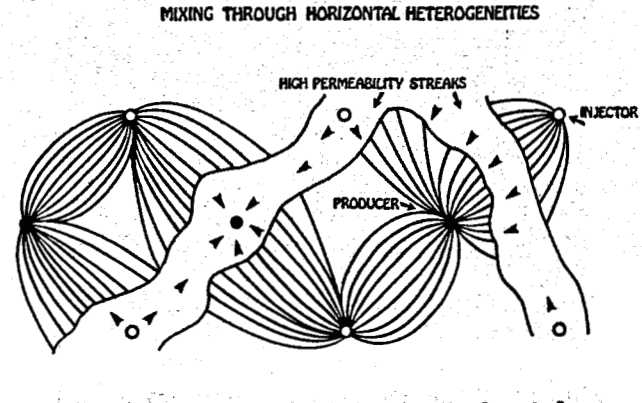

Fig. 3 Tracer Dispersion by Horizontal Heterogeneities.

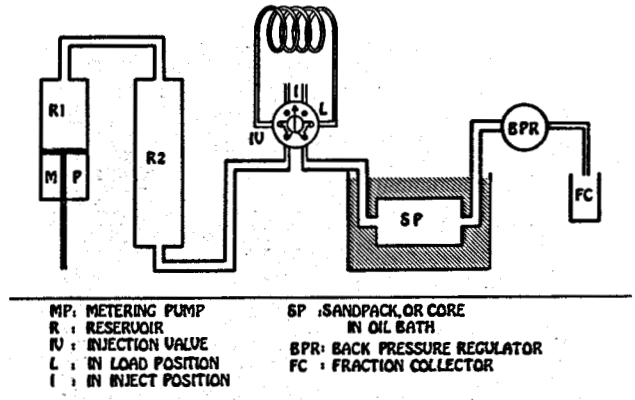

Fig. 4 Flow Apparatus

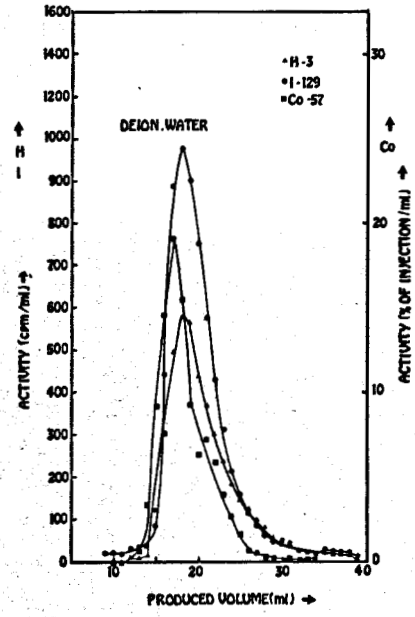

Fig. 5 Tracer Elutions from Berea Sandstone Core in Deionized Water

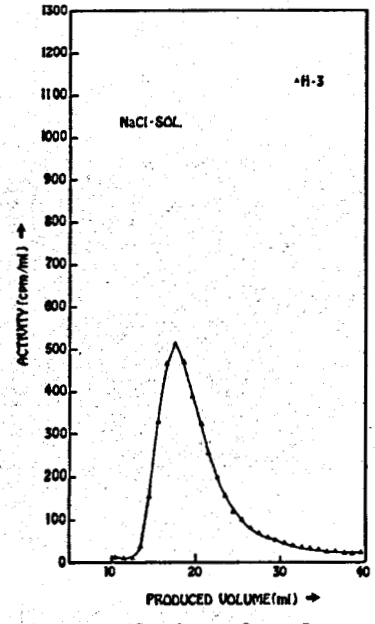

Fig. 6 Tracer Elutions from Berea Sandstone Core in NaCl-Solution

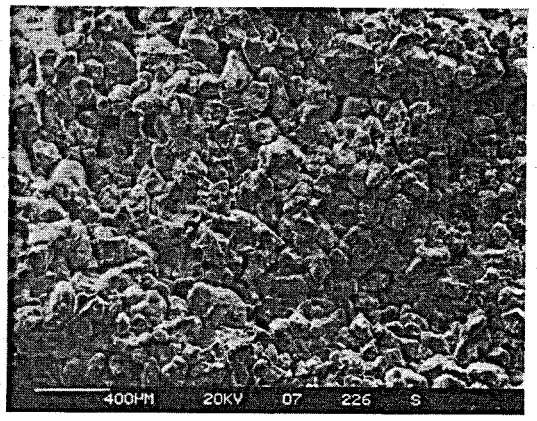

Fig. 7 East Mesa Sandstone

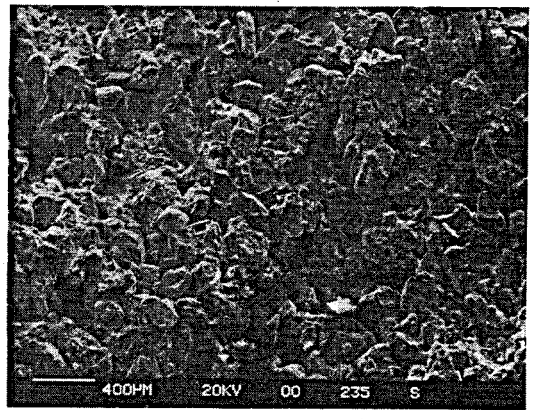

Fig. 8 Berea Sandstone

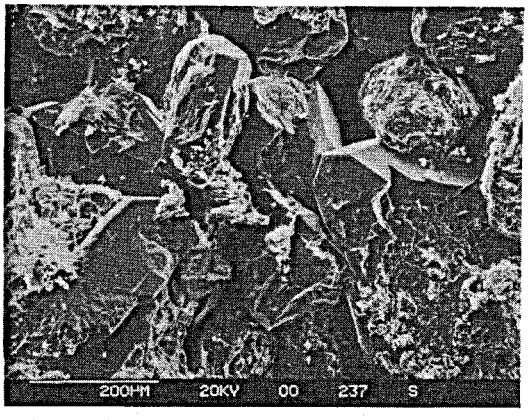

Fig. 9 Berea Sandstone. Fresh Quartz Surfaces

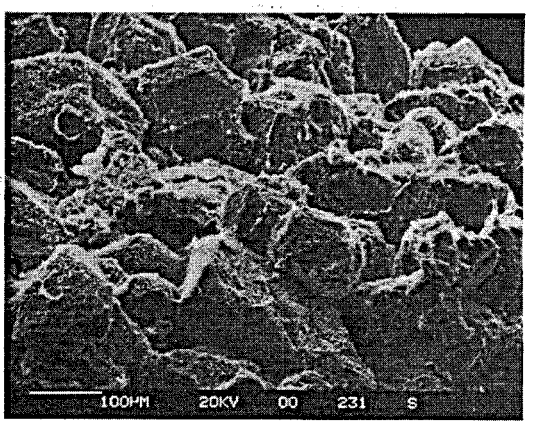

Fig. 10 East Mesa Sandstone. Feldspar Grains (Bottom Center and Right)

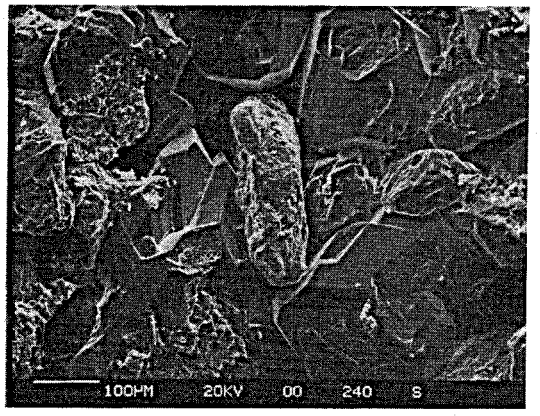

Fig. 11 Berea Sandstone. Disintegrating Feldspar (Center).

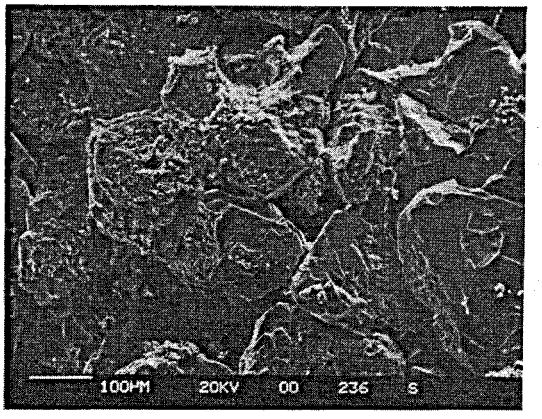

Fig. 12 Berea Sandstone. Large Grains and Clays

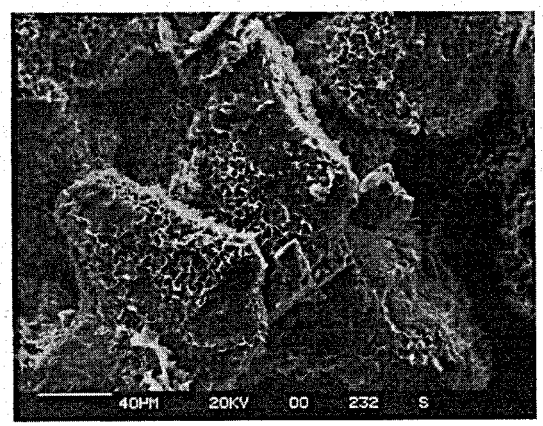

Fig. 13 East Mesa Sandstone. Calcite Crystal (Below, and to the Right of, Center).

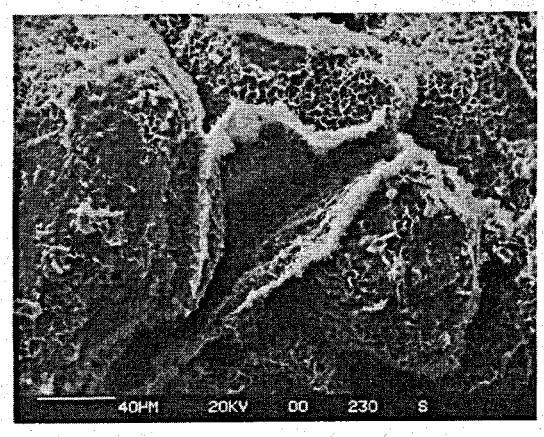

Fig. 14 East Mesa Sandstone. Pore Lining (Unidentified Material).

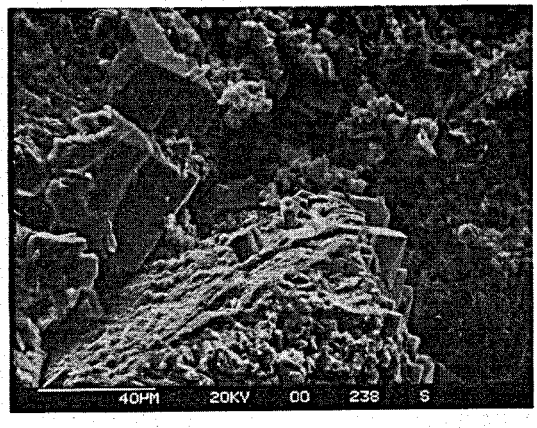

Fig. 15 Berea Sandstone. Pyrite Crystal (Below Center).

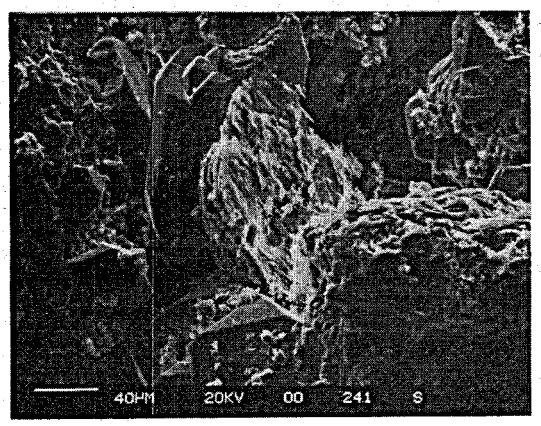

Fig. 16 Berea Sandstone. Dissolving Potassium Feldspar (Center) and Growing Quartz

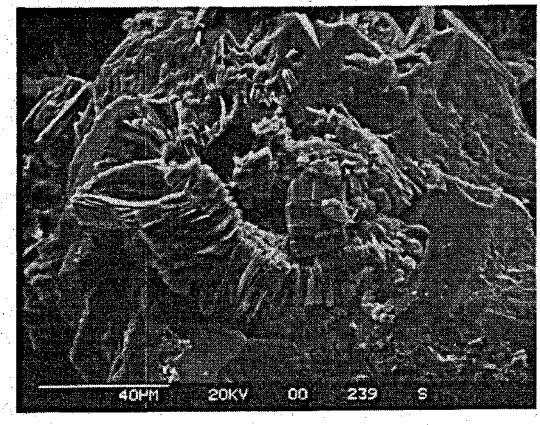

Fig. 17 Berea Sandstone. Quartz and Kaolinite

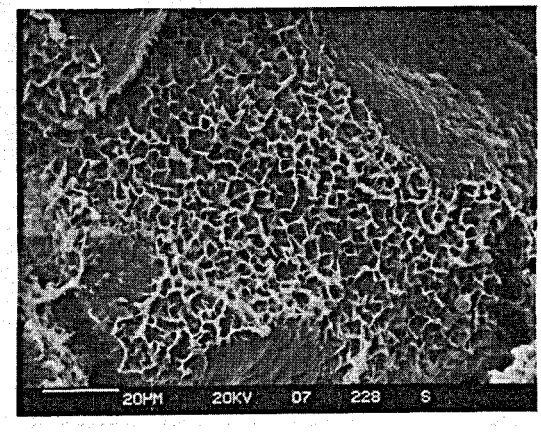

Fig. 18 East Mesa Sandstone. Smectite-Covered Surface

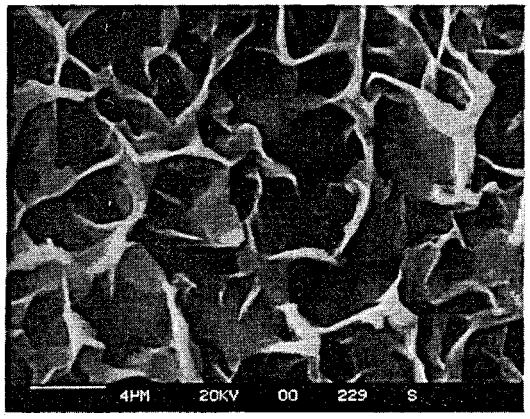

Fig. 19 East Mesa Sandstone. Smectite Close-Up

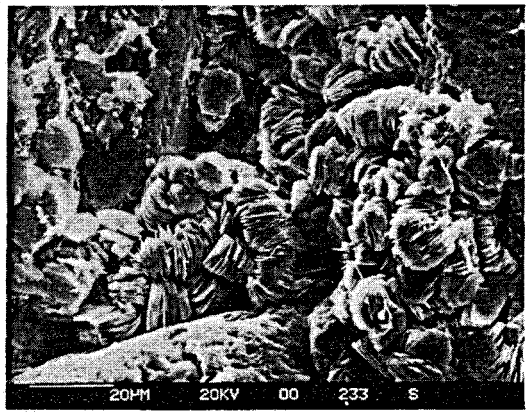

Fig. 20 Berea Sandstone. Kaolinite Cluster

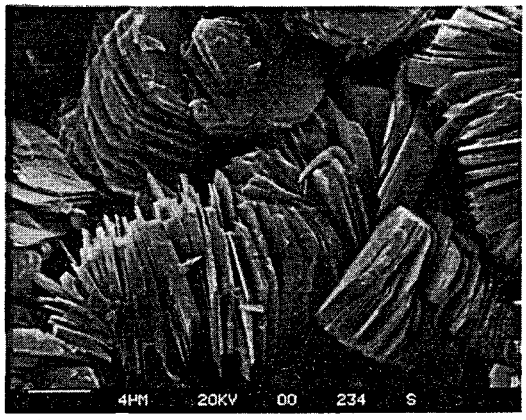

Fig. 21 Berea Sandstone. Kaolinite Close-Up

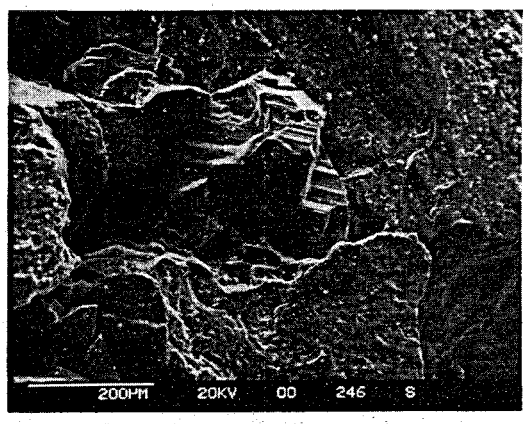

Fig. 22 Roosevelt Hot Springs Tuff (Thermal Power). Accessory Magnetite

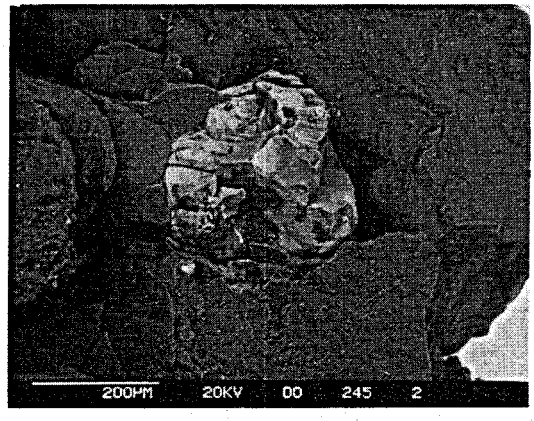

Fig. 23 Roosevelt Hot Springs Tuff (Thermal Power). Accessory Magnetite (Backscatter Detector)

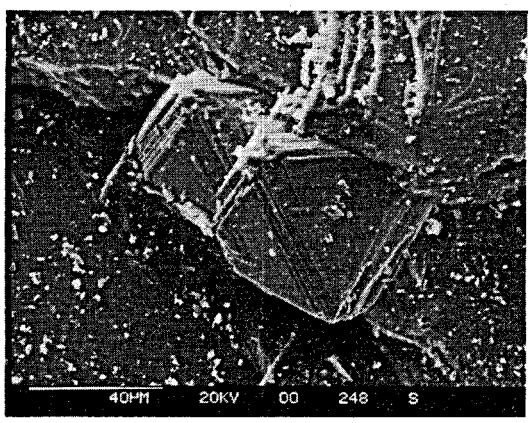

Fig. 24 Roosevelt Hot Springs Tuff (Thermal Power). Accessory Magnetite

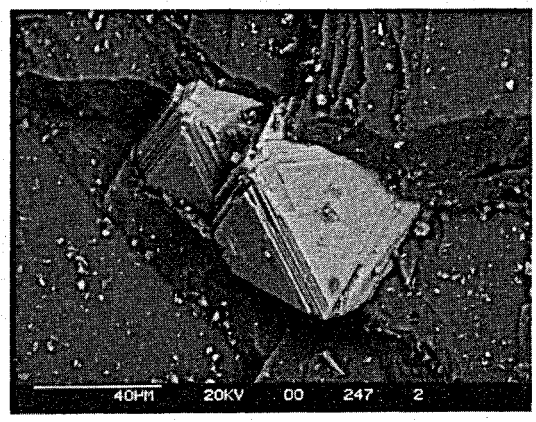

Fig. 25 Roosevelt Hot Springs Tuff (Thermal Power). Accessory Magnetite (Backscatter Detector)

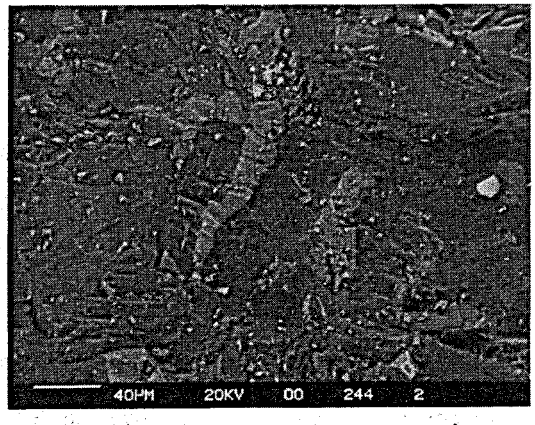

Fig. 26 Roosevelt Hot Springs Tuff (Thermal Power). Titanite (Lighter Areas, Backscatter Detector)

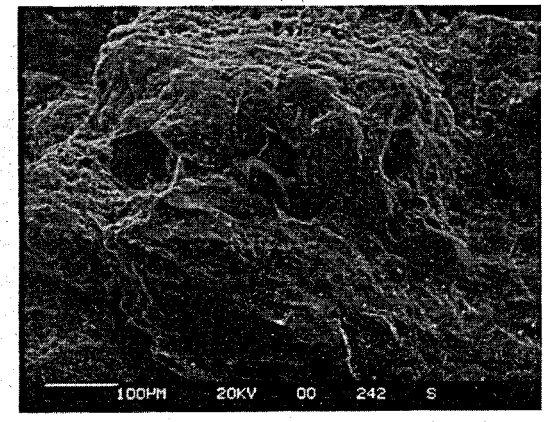

Fig. 27 Roosevelt Hot Springs Tuff (Thermal Power). Apatite, Hexagonal Crystal

Fig. 28 Desert Peak Greenstone. Chlorite

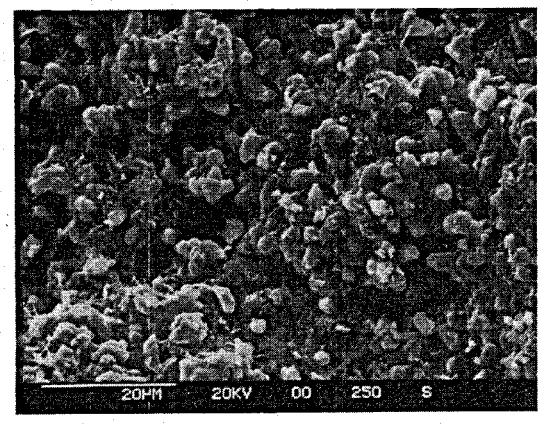

Fig. 29 Desert Peak Greenstone. Calcite Crystals

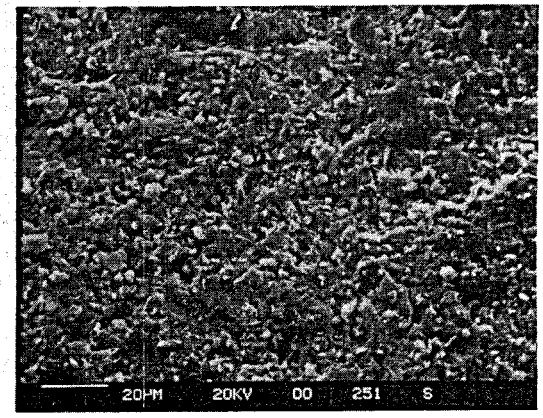

Fig. 30 Desert Peak Greenstone. Surface Structure

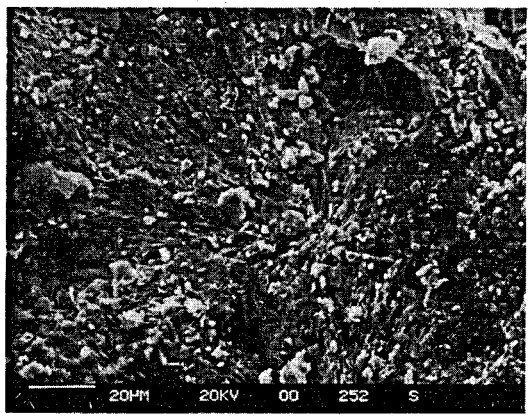

Fig. 31 Desert Peak Greenstone. Surface Structure

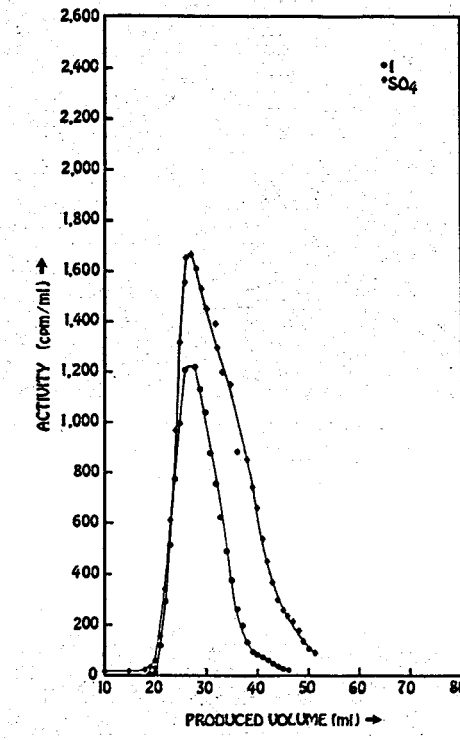

Fig. 33 Tracer Selection: Iodide and Sulfate Elutions

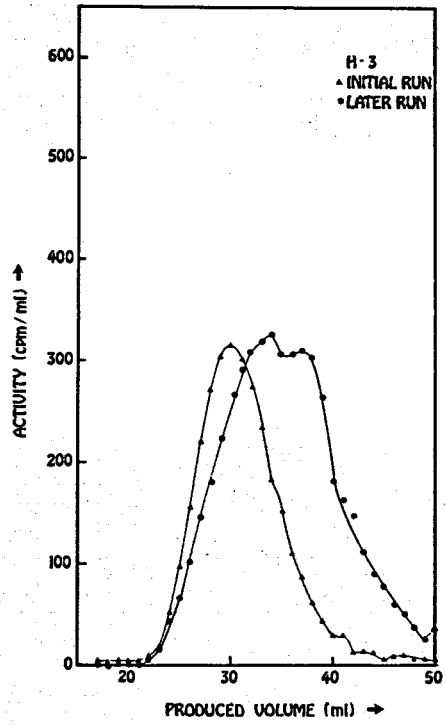

Fig. 32 Tracer Selection: Tritium Elutions

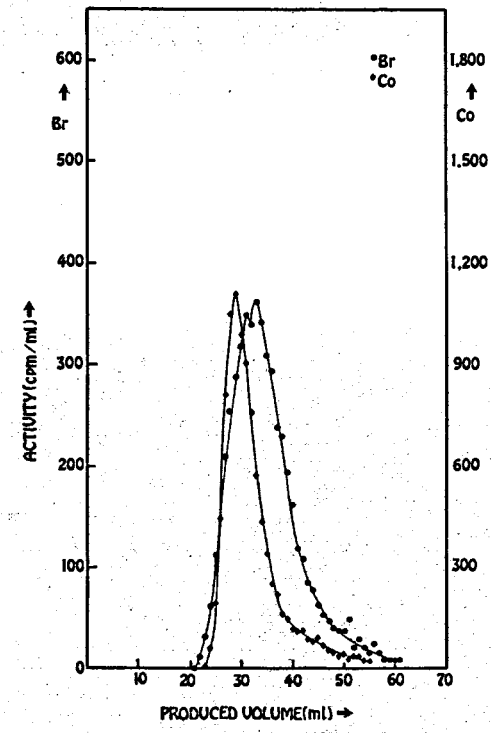

Fig. 34 Tracer Selection: Bromide and Hexacyanocobaltate Elutions

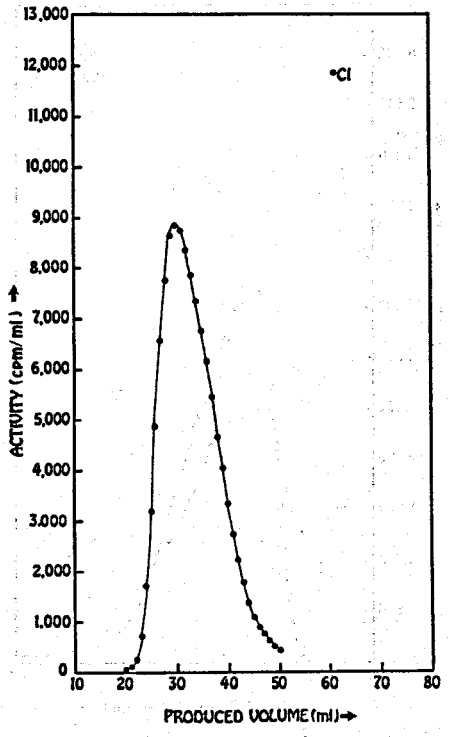

Fig. 35 Tracer Selection: Chloride Elution

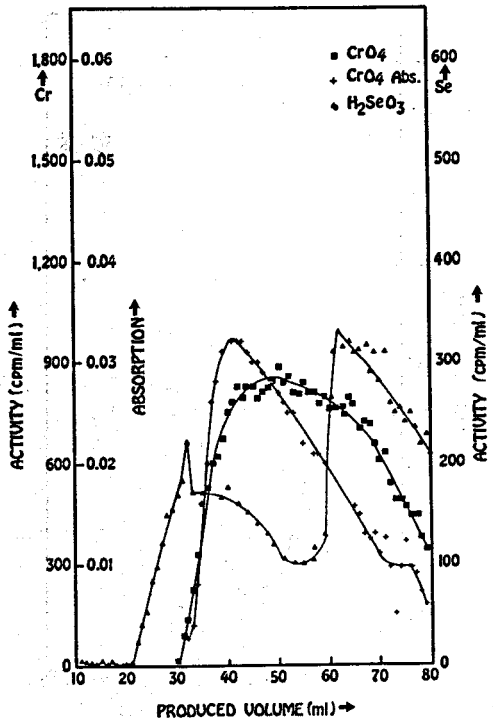

Fig. 37 Tracer Selection: Selenious Acid and Chromate Elutions; Chromate Visible Absorption

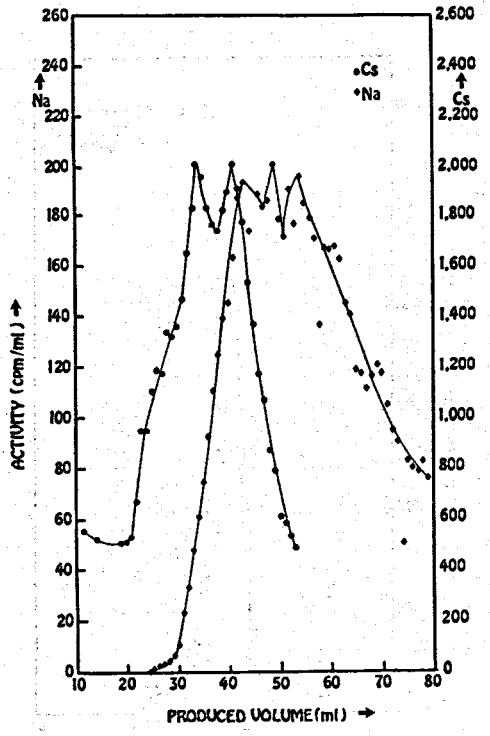

Fig. 36 Tracer Selection: Sodium and Cesium Elutions

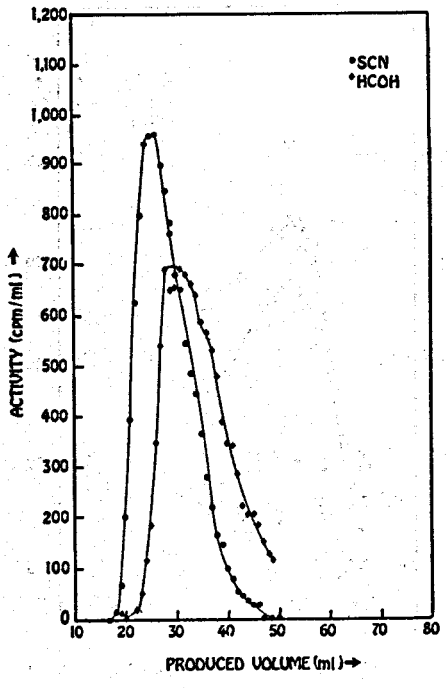

Fig. 38 Tracer Selection: Thiocyanate and Formaldehyde Elutions

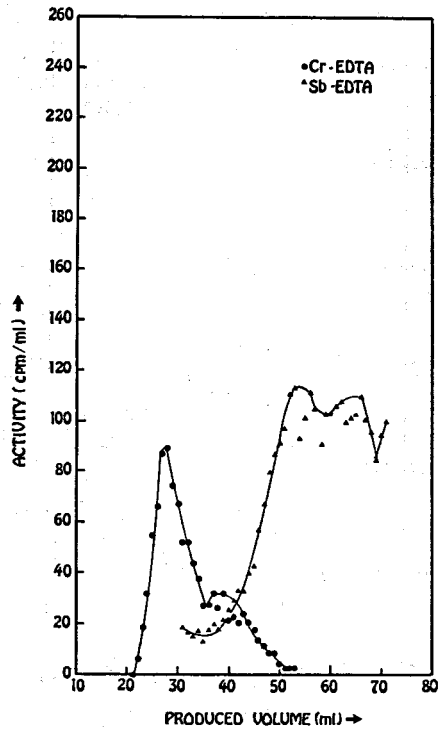

Fig. 39 Tracer Selection: Cr and Sb-EDTA Elutions

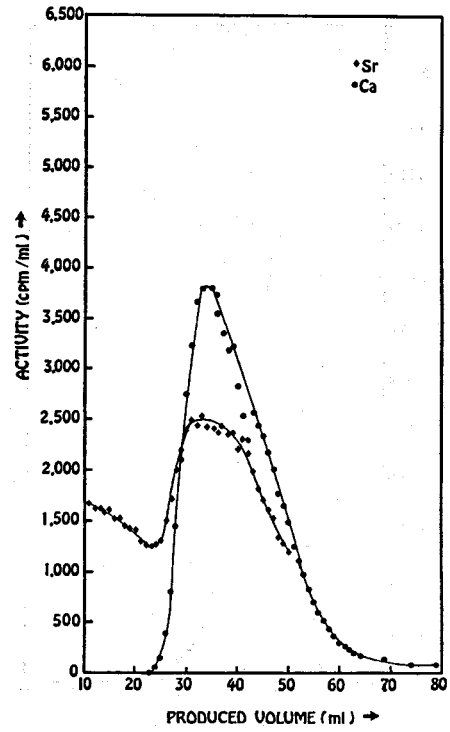

Fig. 41 Tracer Selection: Calcium and Strontium Elutions

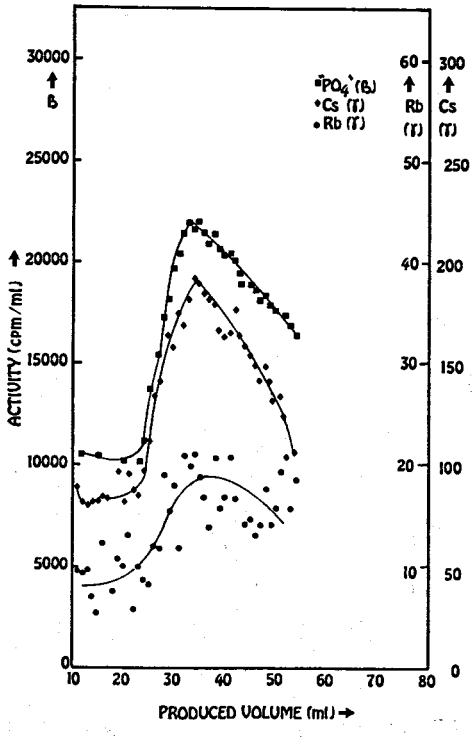

Fig. 40 Tracer Selection: Phosphate, Rubidium and Cesium Elutions

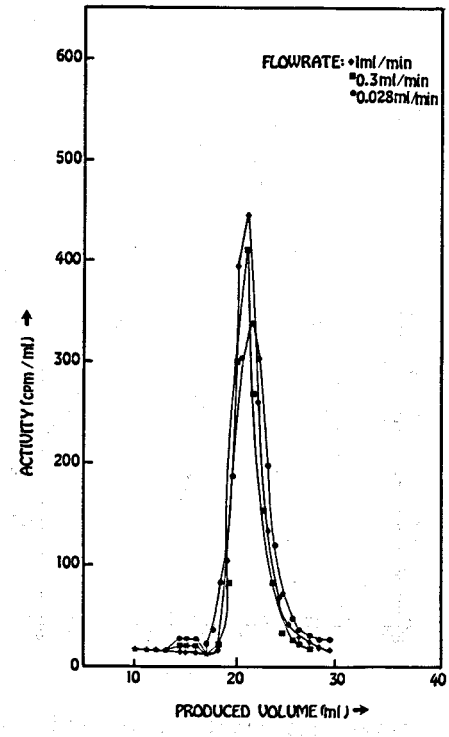

Fig. 42 Tritium Elutions, Influence of Flowrate

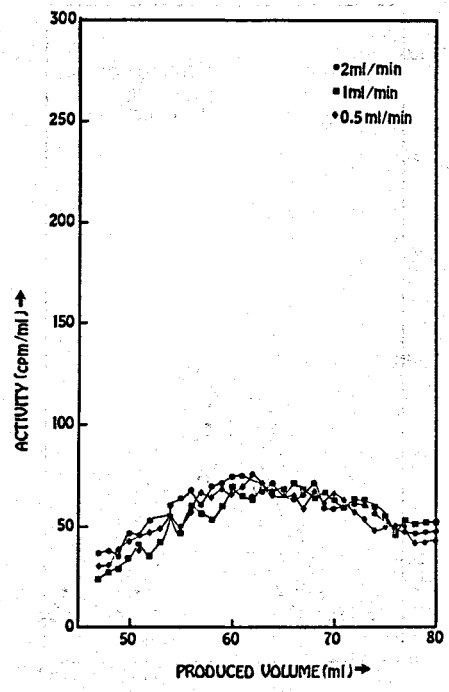

Fig. 43 Tritium Elutions from Ground-Up East Mesa Sandstone at Different Flowrates

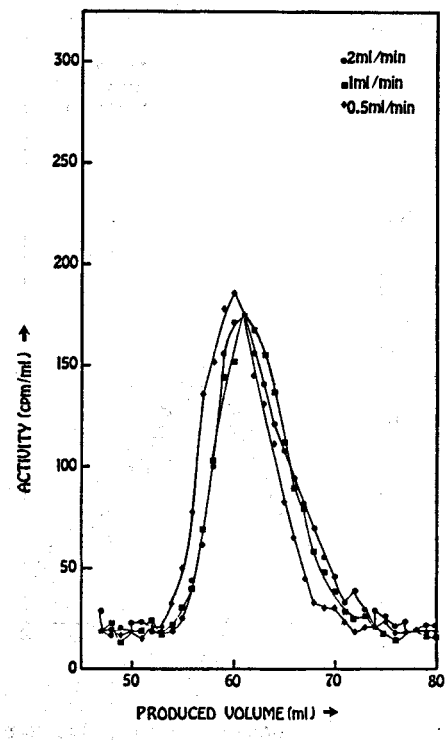

Fig. 45 Tritium Elutions from Ground-Up and Mechanically Cleaned East Mesa Sandstone at Different Flowrates

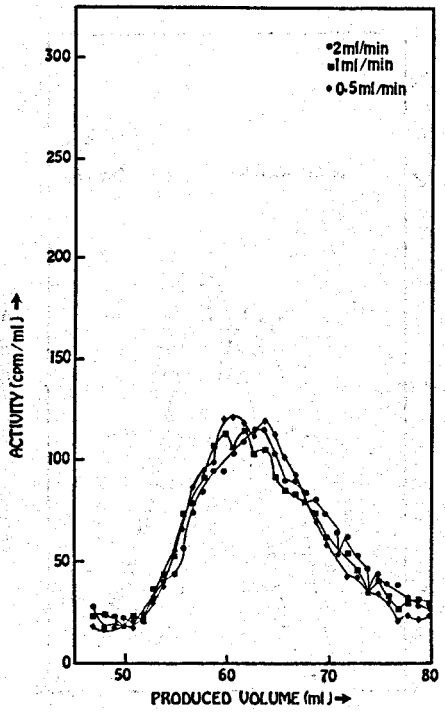

Fig. 44 Tritium Elutions from Ground-Up and Washed East Mesa Sandstone at Different Flowrates

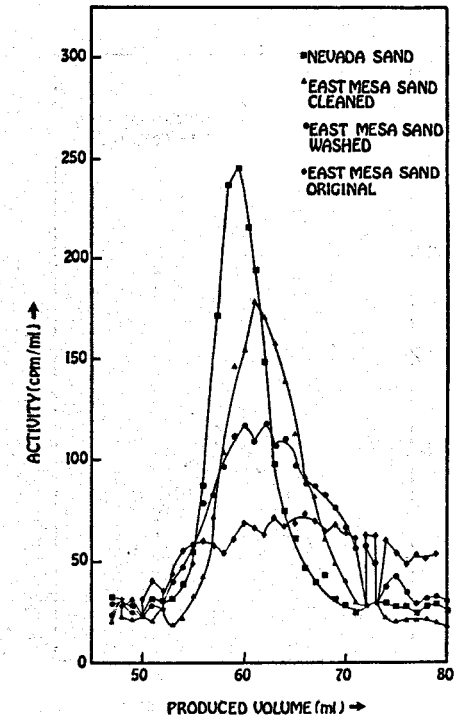

Fig. 46 Tritium Elutions Compared: Nevada Sand and East Mesa Sandstone (from Fig. 43, 44, 45). Flow Rate is 1 ml./min

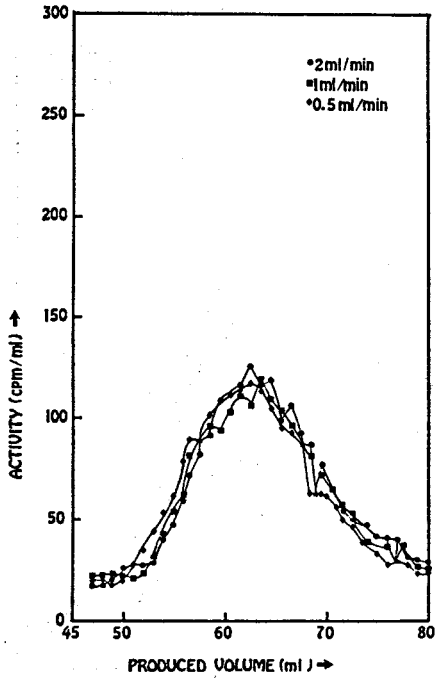

Fig. 47 Tritium Elutions as in Fig. 44, Repeat with Different Sandpack

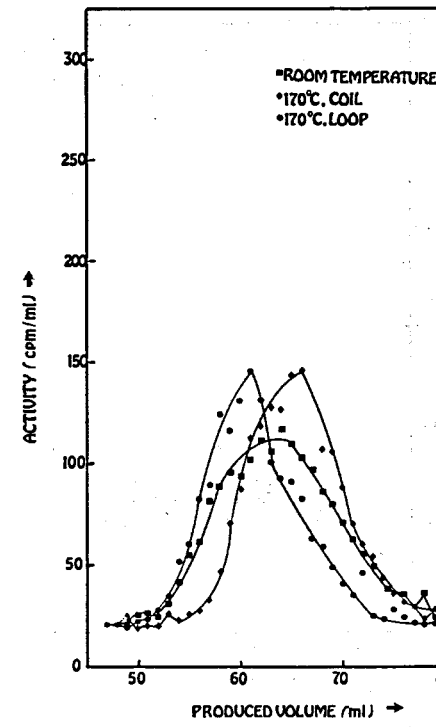

Fig. 49 Tritium Elutions: Influence of Temperature

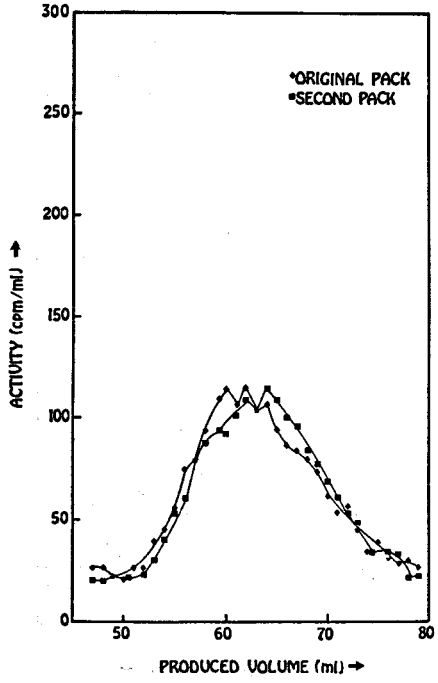

Fig. 48 Tritium Elutions from Different Sandpacks Compared (From Fig. 44, 45, each at 1 ml/min)

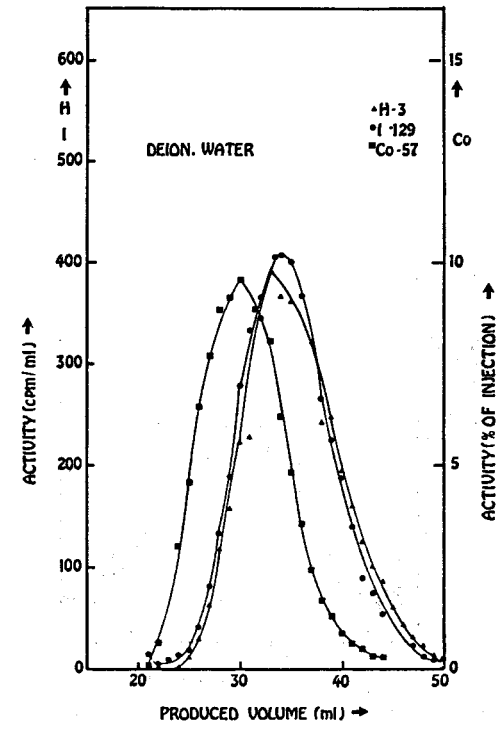

Fig. 50 Tracer Elutions From East Mesa Sandpack in Deionized Water

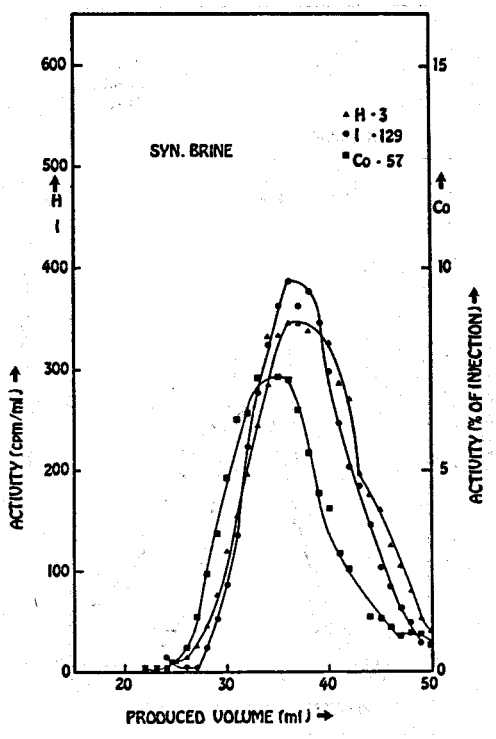

Fig. 51 Tracer Elutions from East Mesa Sandpack in Synthetic Brine

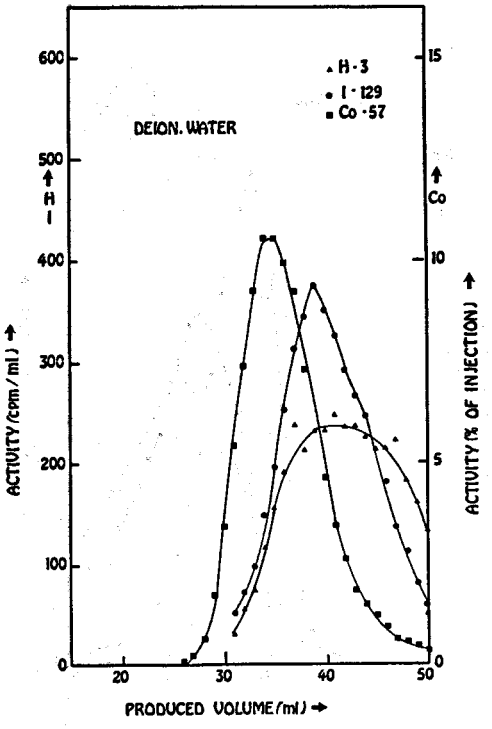

Fig. 53 Tracer Elutions from Desert Peak Sandpack in Deionized Water

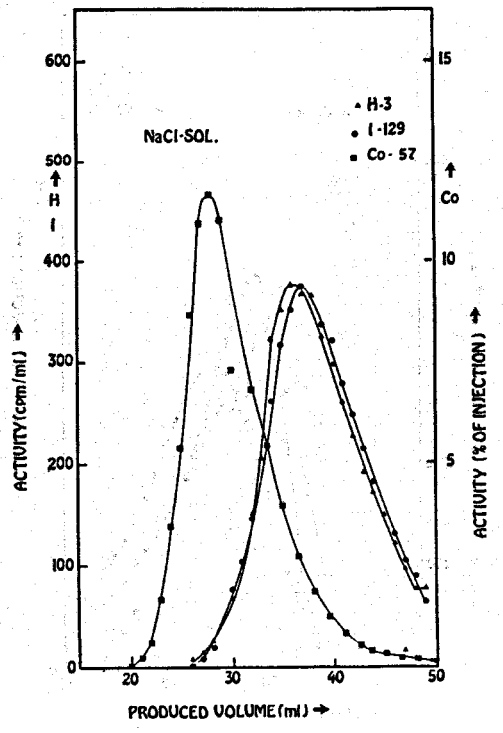

Fig. 52 Tracer Elution from East Mesa Sandpack in NaCl Solution

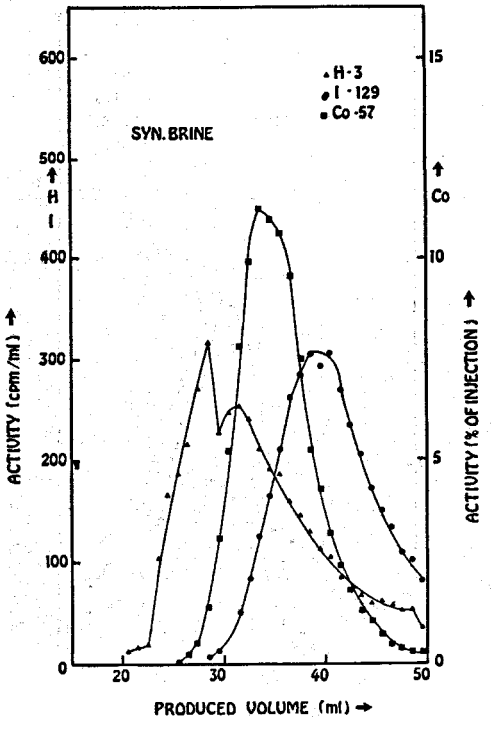

Fig. 54 Tracer Elutions from Desert Peak Sandpack in Synthetic Brine

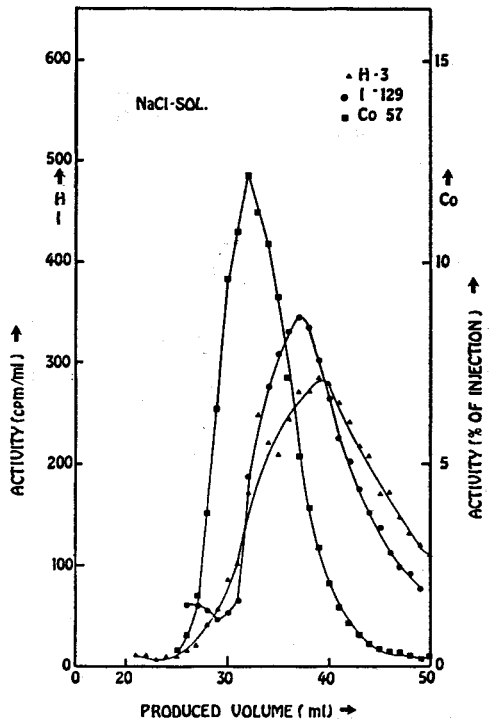

Fig. 55 Tracer Elutions from Desert Peak Sandpack in NaCl Solution

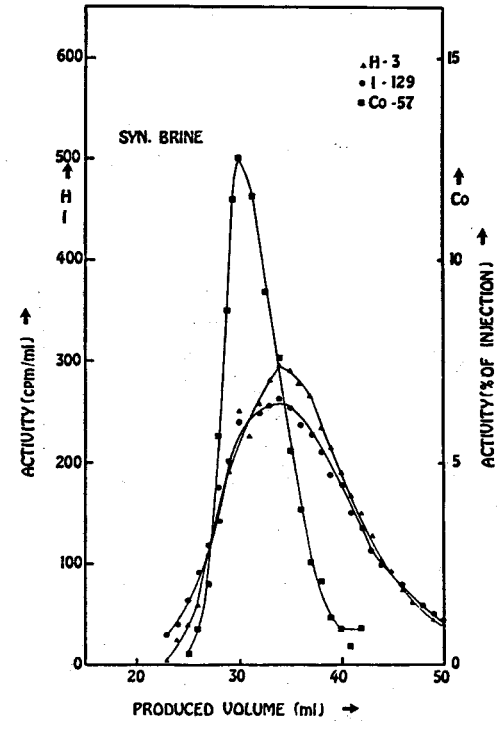

Fig. 57 Tracer Elutions from Quartz Sandpack in Synthetic Brine

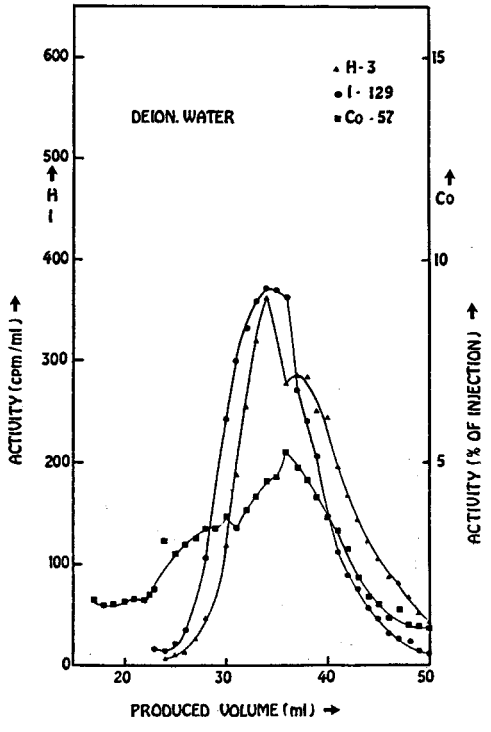

Fig. 56 Tracer Elutions from Quartz Sandpack in Deionized Water

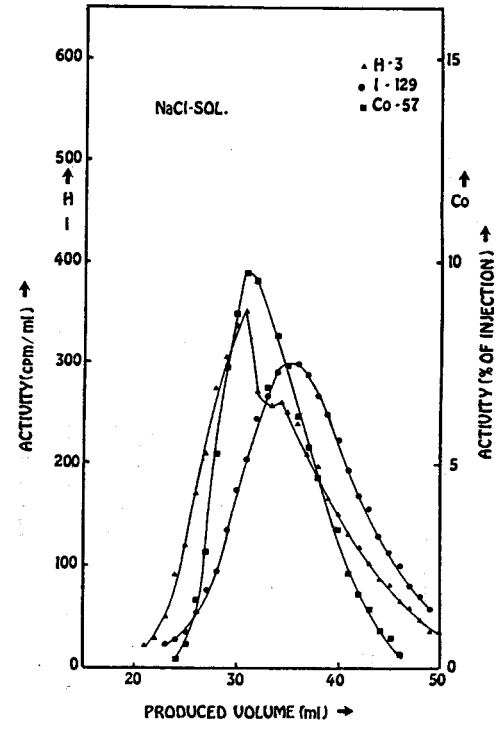

Fig. 58 Tracer Elutions from Quartz Sandpack in NaCl Solution

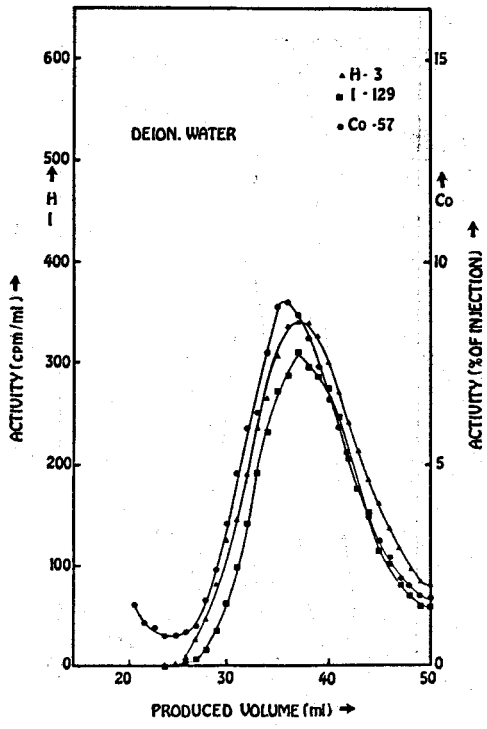

Fig. 59 Tracer Elutions from Thermal Power Sandpack in Deionized Water

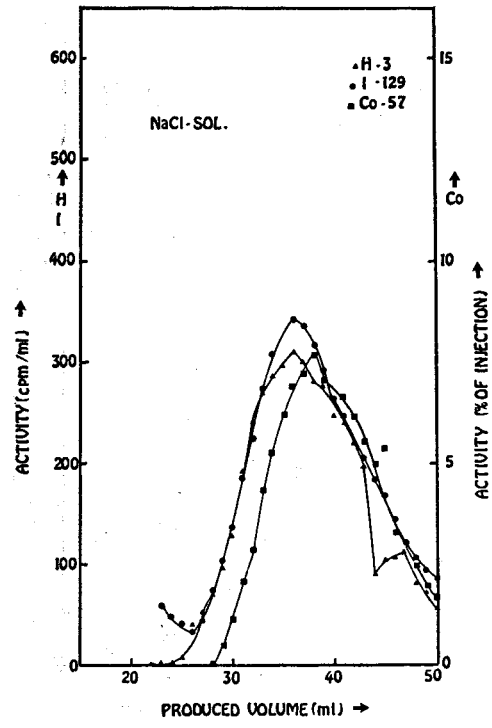

Fig. 61 Tracer Elutions from Thermal Power Sandpack in NaCl Solution

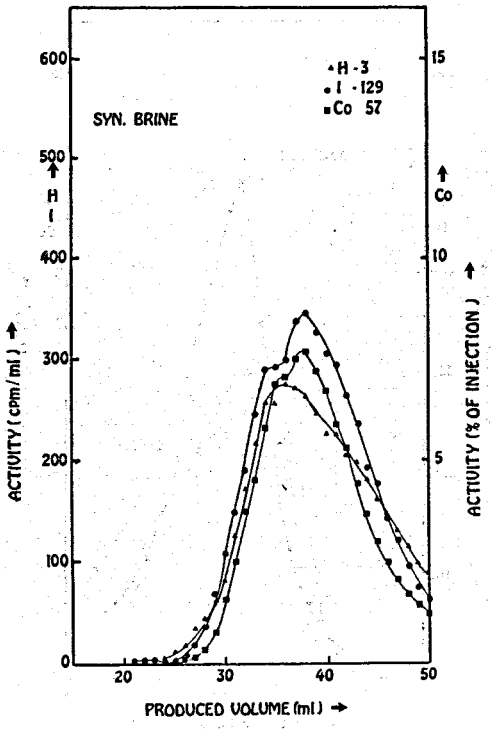

Fig. 60 Tracer Elutions from Thermal Power Sandpack in Synthetic Brine

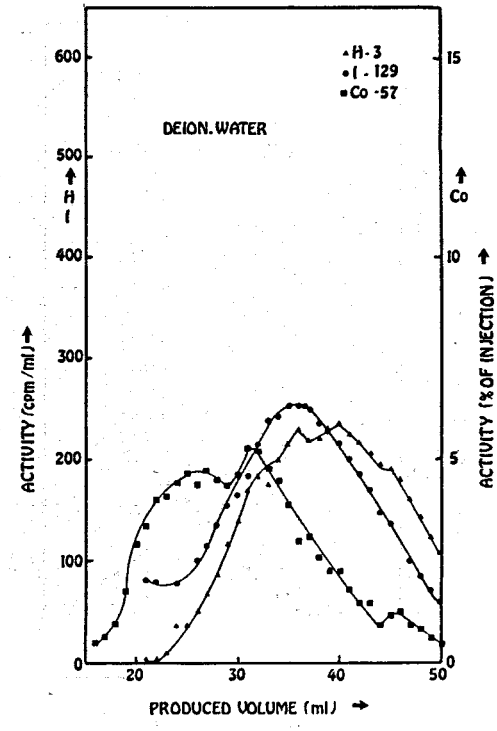

Fig. 62 Tracer Elutions from Calcite Sandpack in Deionized Water

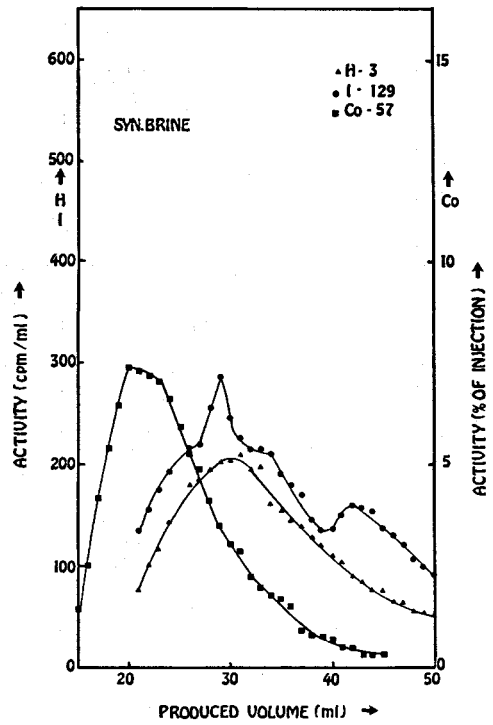

Fig. 63 Tracer Elutions from Calcite Sandpack in Synthetic Brine

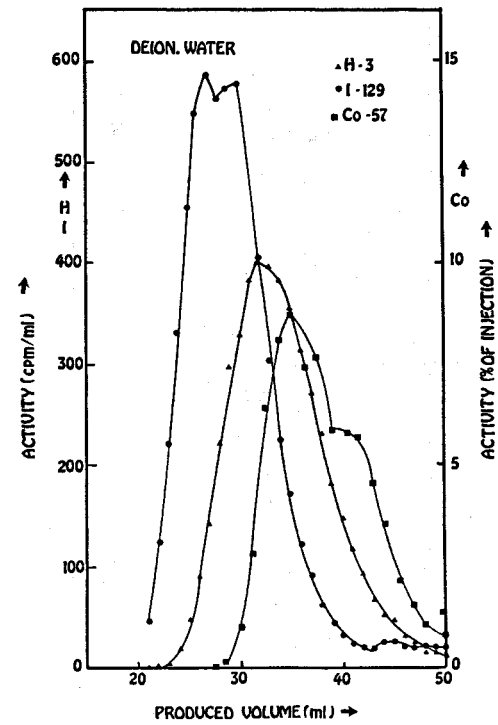

Fig. 65 Tracer Elutions from Berea Sandpack in Deionized Water

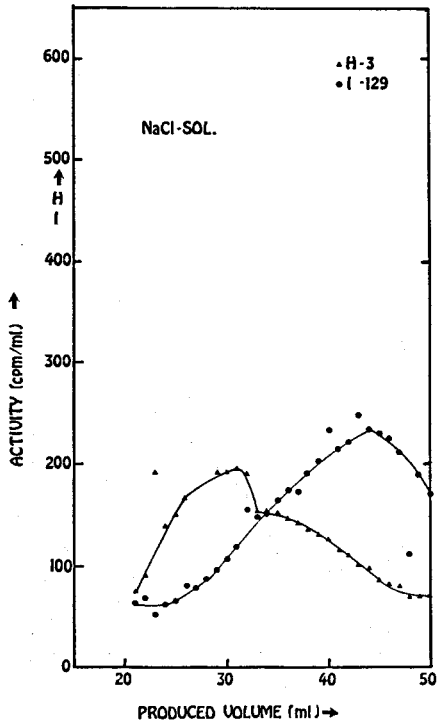

Fig. 64 Tracer Elutions from Calcite Sandpack in NaCl Solution

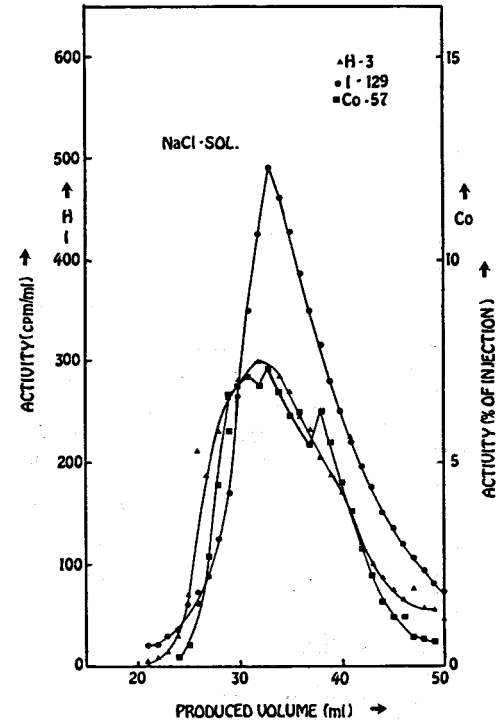

Fig. 66 Tracer Elutions from Berea Sandpack in NaCl Solution

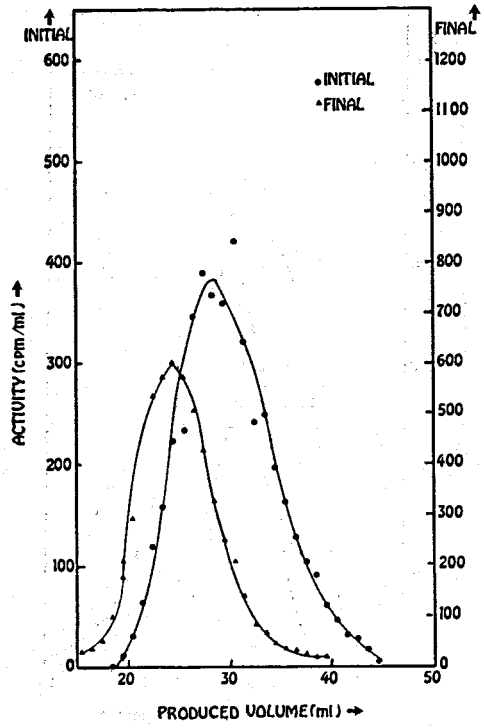

Fig. 67 Initial and Final Tritium Elution from East Mesa Sandpack in Deionized Water

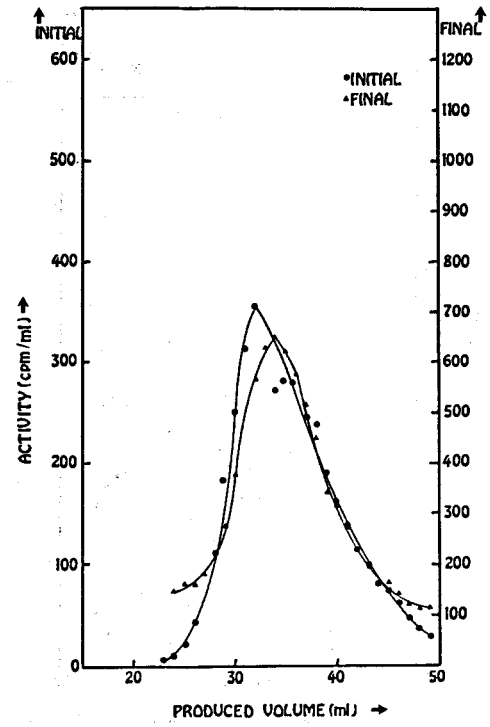

Fig. 69 Initial and Final Tritium Elution from Quartz Sandpack in Deionized Water

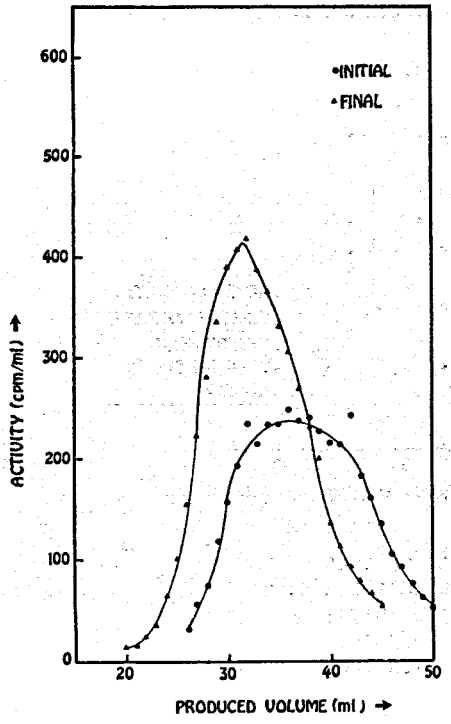

Fig. 68 Initial and Final Tritium Elution from Desert Peak Sandpack in Deionized Water

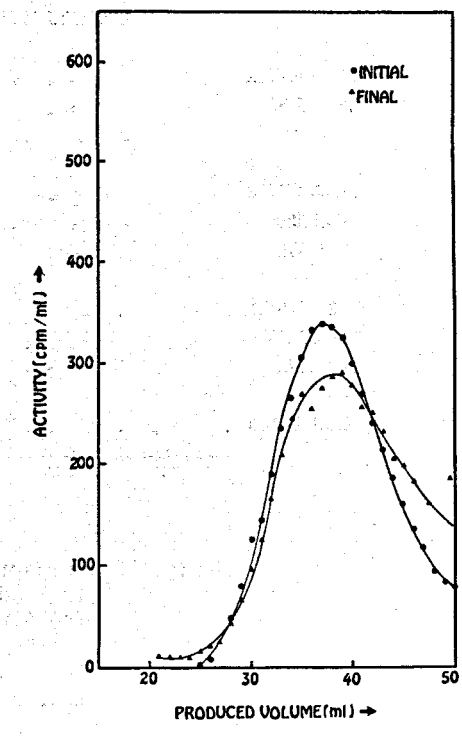

Fig. 70 Initial and Final Tritium Elution from Thermal Power Sandpack in Deionized Water

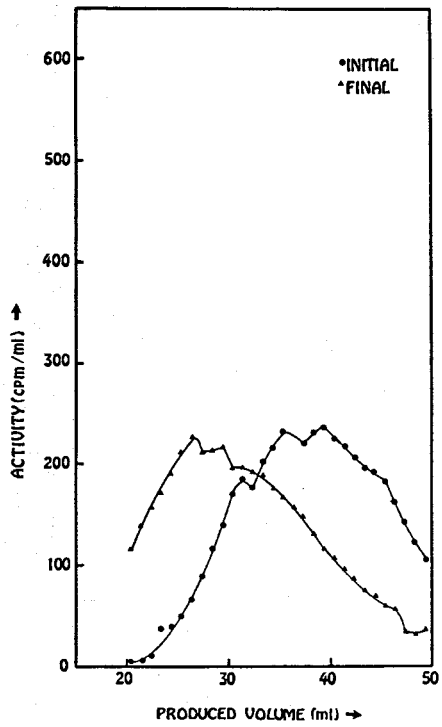

Fig. 71 Inital and Final Tritium Elutions from Calcite Sandpack in Deionized Water

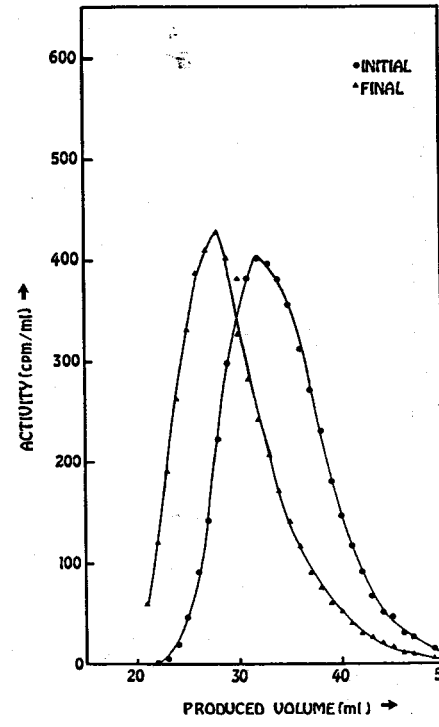

Fig. 72 Initial and Final Tritium Elution from Berea Sandpack in Deionized Water

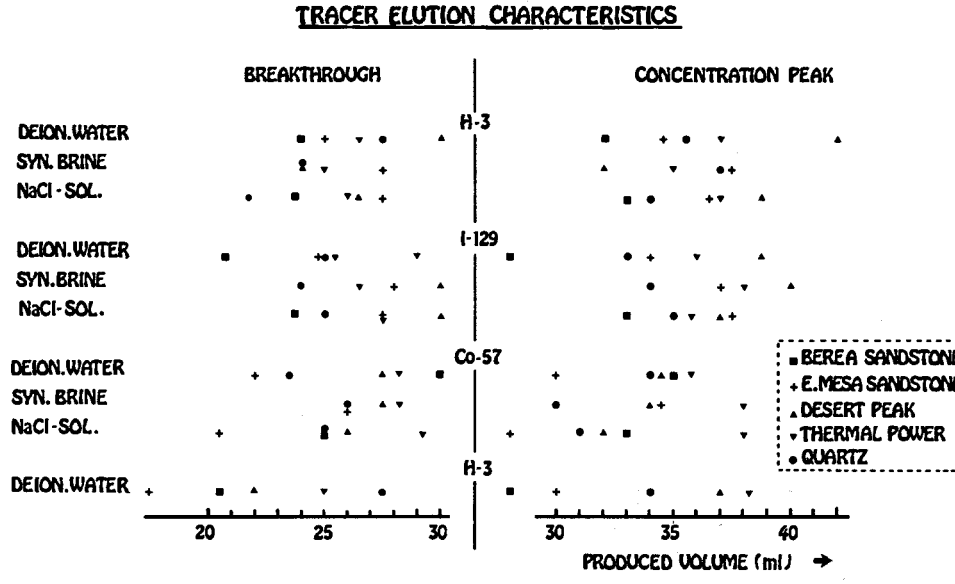

Fig. 73 Comparison of Tracer Retention Times in Sandpacks of Various Rock Materials. The first line represents the initial tritium elution from each sandpack, the last line the final elution from that same sandpack